From Department of Clinical Science, Intervention and Technology,
Division of Obstetrics and Gynecology
Karolinska Institutet, Stockholm, Sweden

DEVELOPMENTAL INSIGHTS AND BIOMEDICAL POTENTIAL OF HUMAN EMBRYONIC STEM CELLS

Modelling Trophoblast Differentiation and Establishing Novel Cell Therapies for Age-related Macular Degeneration

Álvaro Plaza Reyes

Stockholm 2020

All previously published papers were reproduced with permission from the publisher.
Published by Karolinska Institutet.
Printed by Universitetsservice US AB 2020
Cover: **[Left side]**: Human embryonic stem cell-derived trophoblast cells expressing cytokeratin 19 (red) and GATA3 (green). **[Right side]**: Human embryonic stem cell-derived retinal pigment epithelium cells expressing BEST1 (green) and having its DNA stained (blue). Image was created using own microscopy pictures and objects from Biorender.com

ISBN 978-91-7831-806-3

Department of Clinical Science, Intervention and Technology.
Division for Obstetrics and Gynecology

DEVELOPMENTAL INSIGHTS AND BIOMEDICAL POTENTIAL OF HUMAN EMBRYONIC STEM CELLS

Modelling Trophoblast Differentiation and Establishing Novel Cell Therapies for Age-related Macular Degeneration

THESIS FOR DOCTORAL DEGREE (Ph.D.)
which will be defended in public at Karolinska Institutet, Erna Möllersalen, Neo building, Blickagången 16, Campus Flemingsberg, Stockholm

Wednesday, May 27th, 2020 at 9:30 AM

by

Álvaro Plaza Reyes

Principal Supervisor:
Dr. Fredrik Lanner
Karolinska Institutet
Department of Clinical Science,
Intervention and Technology
Division of Obstetrics and Gynecology

Co-supervisor(s):
Professor Anders Kvanta
Karolinska Institutet
Department of Clinical Neuroscience
Division of Ophthalmology and Vision

Professor Kenneth R. Chien
Karolinska Institutet
Department of Medicine, Huddinge
Integrated Cardio Metabolic Centre (ICMC)

Opponent:
Professor Anna Veiga Lluch
Universitat Pompeu Fabra
Facultat de Ciències de la Salut i de la Vida

Examination Board:
Dr. Ola Hermanson
Karolinska Institutet
Department of Neuroscience

Dr. Sergey Rodin
Uppsala Universitet
Department of Surgical Sciences

Dr. Cecilia Götherström
Karolinska Institutet
Department of Clinical Science,
Intervention and Technology
Division of Obstetrics and Gynecology

Stockholm 2020

To my family, for supporting my enthusiasm to become a scientist, and to my fiancé, for keeping me sane on the long way there.

ABSTRACT

Understanding the molecular pathways responsible for lineage segregation in the preimplantation human embryo is critical in order to fully elucidate the mechanisms involved in pluripotency and differentiation of embryonic stem cells. A significant increase in our comprehension of such processes will lead to an improvement in the quality and efficiency of these cells for applications requiring stem cell maintenance and differentiation, such as regenerative medicine. Through responsible and ethical research, such new knowledge can then be translated effectively and efficiently into future advancements in health and medical practices. This thesis focuses on two different applications of human embryonic stem cells (hESC): first, as an in-vitro model to investigate the genetic requirements for human trophoblast formation and second, as a cell replacement therapy for age-related macular degeneration (AMD) through the establishment of efficient, scalable, and clinically compliant protocols for their differentiation into retinal pigment epithelium cells (RPE).

In paper I, we used human embryonic stem cells to model trophoblast establishment and differentiation in order to better understand the mechanisms governing trophectoderm segregation in the embryo. Combining this in-vitro model with the use of pharmacological inhibitors and CRISPR/Cas9 genome editing, we demonstrated that blockade of the YAP1/WWTR1-TEAD complex impairs not only trophoblast differentiation, but also survival of undifferentiated stem cells. Furthermore, through systematic targeting of the different components of the complex, we described a dominant role for YAP1 in these processes and a striking genetic and functional redundancy of the function of TEAD proteins. Altogether, the findings indicate a role for the Hippo signaling pathway, both in human trophectoderm segregation and in maintaining human pluripotency.

In papers II and III, we developed xeno-free and defined methodologies for the differentiation of human embryonic stem cells into RPE with the potential for use in replacement therapies for common retinal degenerative diseases, such as age-related macular degeneration. These in-vitro derived cells exhibited specific morphological and molecular features and functional properties that are typical of native RPE. In addition, upon subretinal transplantation into a large-eyed animal model, hESC-derived RPE cells were able to integrate and survive for extensive periods of time and rescued the neuroretina from the damage induced at the moment of injection. Finally, we identified a set of unique cell surface markers that were able to distinguish the RPE from other potential contaminating cell types or undifferentiated remnants and demonstrated their utility in monitoring differentiation efficiency and in increasing the purity and homogeneity of the final cell product.

Through this work, we demonstrate that human embryonic stem cells hold enormous potential for modeling specific aspects of human development, which can help to elucidate the complex mechanisms governing lineage segregation and support the production of bona fide differentiated cell types to serve in future replacement therapies.

.

RESUMEN EN ESPAÑOL

Dilucidar las vías moleculares implicadas en la segregación de los distintos linajes celulares presentes en el embrión humano previo a la implantación es de crucial importancia para comprender plenamente los mecanismos responsables de la pluripotencia y diferenciación de las células madre embrionarias. El aumento significativo en nuestra comprensión de tales procesos conducirá a una mejora en la calidad y eficiencia de estas células para aplicaciones que requieren el mantenimiento y diferenciación de células madre, tales como la medicina regenerativa. Sólo a través de una investigación responsable y ética, ese nuevo conocimiento se podrá traducir de manera efectiva y eficiente en futuros avances de las prácticas médicas. Esta tesis se centra en dos aplicaciones diferentes de las células madre embrionarias humanas (hESC): su uso como modelo para esclarecer los requisitos genéticos necesarios para la formación de trofoblasto humano y su uso traslacional como terapia de reemplazo para la Degeneración Macular asociada con la Edad (DMAE), a través del establecimiento de metodologías eficientes, escalables y clínicamente compatibles para su diferenciación en células de epitelio pigmentario de la retina (EPR).

En el artículo I, utilizamos células madre embrionarias humanas para modelar el establecimiento y la diferenciación de trofoblasto a fin de comprender mejor los mecanismos que rigen la segregación del trofectodermo en el embrión. Combinando este modelo in-vitro con el uso de inhibidores farmacológicos y la edición del genoma mediante la técnica CRISPR/Cas9, demostramos que el bloqueo del complejo YAP1/WWTR1-TEAD perjudica no solo la diferenciación del trofoblasto, sino también la supervivencia de las células madre indiferenciadas. Además, a través de la disrupción funcional sistemática de los diferentes componentes del complejo, describimos el papel dominante de la proteína YAP1 en estos procesos y la inesperada redundancia genética y funcional de las proteínas TEAD. Lo cual, en conjunto, indica un papel esencial de la vía de señalización Hippo tanto en la segregación del trofectodermo humano como en el mantenimiento de la pluripotencia humana.

En los artículos II y III, desarrollamos metodologías definidas y libres de xeno-componentes para la diferenciación de células madre embrionarias humanas en EPR con potencial para usarse como terapias de reemplazo celular en enfermedades degenerativas comunes de la retina, como la DMAE. Confirmamos que estas células derivadas in-vitro exhiben características morfológicas y moleculares específicas, así como propiedades funcionales típicas del EPR nativo. Además, mostramos que, tras el trasplante subretiniano en nuestro modelo animal, las células EPR derivadas de hESC pueden integrarse y sobrevivir durante largos períodos de tiempo, al mismo tiempo que son capaces de rescatar la neuroretina del daño inducido durante el proceso de inyección. Finalmente, identificamos un conjunto de marcadores de superficie celular únicos que permiten distinguir el EPR de otros tipos de células potencialmente contaminantes, así como de remanentes indiferenciados, y demostramos la utilidad de los mismos a la hora de monitorear la eficiencia de diferenciación y aumentar la pureza y homogeneidad del producto celular final.

En conjunto, el trabajo presentado en esta tesis demuestra el enorme potencial que poseen las células madre embrionarias humanas a la hora de modelar aspectos específicos del desarrollo humano, permitiendo estudiar en profundidad los complejos mecanismos que rigen la segregación de los distintos linajes celulares, además de servir como una fuente ilimitada de células indiferenciadas para la producción de diferentes tejidos con futuras aplicaciones en medicina regenerativa.

SCIENTIFIC PAPERS INCLUDED IN THE THESIS

I. **Alvaro Plaza Reyes**, Nicolas Ortega, Theresa M. Sommer, Philipp Schenk, Ainhoa Larreategui, Fredrik Lanner[3]
Role of Hippo Signaling Pathway in Human Trophoblast Differentiation
Manuscript

II. **Alvaro Plaza Reyes**[1], Sandra Petrus-Reurer[1], Liselotte Antonsson, Sonya Stenfelt, Hammurabi Bartuma, Sarita Panula, Theresa Mader, Iyadh Douagi, Helder André, Outi Hovatta[2], Fredrik Lanner[2,3] and Anders Kvanta[2]
Xeno-free and defined human embryonic stem cell-derived retinal pigment epithelial cells functionally integrate in a large-eyed preclinical model
Stem Cell Reports. 2016; 6, p.9-17
https://doi.org/10.1016/j.stemcr.2015.11.008

III. **Alvaro Plaza Reyes**[1], Sandra Petrus-Reurer[1], Sara Padrell Sánchez, Pankaj Kumar, Iyadh Douagi, Hammurabi Bartuma, Monica Aronsson, Sofie Westman, Emma Lardner, Helder André, Anna Falk, Emeline F. Nandrot, Anders Kvanta, Fredrik Lanner[3]
Identification of cell surface markers and establishment of monolayer differentiation to retinal pigment epithelial cells
Nature Communications. 2020; 11, 1609.
https://doi.org/10.1038/s41467-020-15326-5

SCIENTIFIC PAPERS NOT INCLUDED IN THE THESIS

I. Sandra Petrus-Reurer[1], Pankaj Kumar[1], Sara Padrell Sanchez[1], Monica Aronsson, Helder André, Hammurabi Bartuma, **Alvaro Plaza Reyes**, Emeline F. Nandrot, Anders Kvanta[2], Fredrik Lanner[3]
Preclinical safety studies of human embryonic stem cell-derived retinal pigment epithelial cells for the treatment of age-related macular degeneration
Stem Cells Translational Medicine. 2020
https://doi.org/10.1002/sctm.19-0396

II. Sandra Petrus-Reurer[1], Nerges Winblad[1], Pankaj Kumar, Laia Gorchs, Michael Chrobok, Arnika Kathleen Wagner, Hammurabi Bartuma, Emma Lardner, Monica Aronsson, **Alvaro Plaza Reyes**, Helder André, Evren Alici, Helen Kaipe, Anders Kvanta[2], Fredrik Lanner[3]
Generation of retinal pigment epithelial cells derived from human embryonic stem cells lacking human leukocyte antigen class I and II
Stem Cell Reports. 2020; 14, p1-15
https://doi.org/10.1016/j.stemcr.2020.02.006

III. Collier AJ[1], Panula SP[1], Schell JP, Chovanec P, **Plaza Reyes A**, Petropoulos S, Corcoran AE, Walker R, Douagi I, Lanner F[3], Rugg-Gunn PJ[3]
Comprehensive Cell Surface Protein Profiling Identifies Specific Markers of Human Naive and Primed Pluripotent States.
Cell Stem Cell. 2017, 20(6), p.874–890.
https://doi.org/10.1016/j.stem.2017.02.014

IV. Sophie Petropoulos[1], Daniel Edsgard[1], Bjorn Reinius[1], Qiaolin Deng, Sarita Pauliina Panula, Simone Codeluppi, **Alvaro Plaza Reyes**, Sten Linnarsson, Rickard Sandberg[3], Fredrik Lanner[3]
Single-Cell RNA-Seq Reveals Lineage and X Chromosome Dynamics in Human Preimplantation Embryos
Cell. 2016, 165(4), p.1012-1026.
https://doi.org/10.1016/j.cell.2016.03.023

V. Eeva-Mari Jouhilahti[1], Elo Madissoon[1], Liselotte Vesterlund, Virpi Töhönen, Kaarel Krjutškov, **Alvaro Plaza Reyes**, Sophie Petropoulos, Robert Månsson, Sten Linnarsson, Thomas Bürglin, Fredrik Lanner, Outi Hovatta, Shintaro Katayama, Juha Kere[3]
The human PRD-like homeobox gene LEUTX has a central role in embryo genome activation
Development. 2016, 143, p.3459-3469;
https://doi.org/10.1242/dev.134510

[1]Co-first author

[2]Co-senior author

[3]Corresponding author

CONTENTS

LIST OF ABBREVIATIONS

AMD	Age-related Macular Degeneration
ANOVA	Analysis of Variance
ANPEP	Membrane Alanyl Aminopeptidase
aPKC	Atypical Protein Kinase C
BAF	Blue-Light Fundus Autofluorescence
BAP	In-vitro Trophoblast Differentiation Media Containing BMP4, A83-01 and PD173074
BEST1	Bestrophin 1
bFGF/FGF2	Basic Fibroblast Growth Factor
BM	Bruch's Membrane
BMP4	Bone Morphogenetic Protein 4
BSA	Bovine Serum Albumin
BSS	Balanced Salt Solution
CaCo-2	Human Epithelial Colorectal Adenocarcinoma Cell Line
Cas9	CRISPR-associated protein 9
cCaspase3	Cleaved Caspase-3
cDNA	Complementary Deoxyribonucleic Acid
CDX2	Caudal Type Homeobox 2
CFSE	Carboxyfluorescein Succinimidyl Ester
CGB3	Chorionic Gonadotropin Subunit Beta 3
CMV	Cytomegalovirus
CNV	Choroidal Neovascularization
CO_2	Carbon Dioxide
CRALBP	Cellular Retinaldehyde Binding Protein
CRISPR	Clustered Regularly Interspaced Short Palindromic Repeats
CXCR4	C-X-C Chemokine Receptor Type 4
DAPI	4',6-diamidino-2-phenylendole
dH_2O	Distilled Water
DMEM/F12	Dulbecco's Modified Eagle Medium: Nutrient Mixture F-12
DNA	Deoxyribonucleic Acid

DPBS	Dulbecco's Phosphate-Buffered Saline
Dpf	Days Post Fertilization
E1-7	Embryonic Day 1-7
EB	Embryoid Body
EDTA	Ethylenediaminetetraacetic Acid
ELISA	Enzyme-Linked ImmunoSorbent Assay
EOMES	Eomesodermin
EPI	Epiblast
FACS	Fluorescence-Activated Cell Sorting
FBS	Fetal Bovine Serum
FGF	Fibroblast Growth Factor
FITC	Fluorescein Isothiocyanate
FMO	Fluorescence Minus One
FOXA2	Forkhead Box A2
GA	Geographic Atrophy
GAPDH	Glyceraldehyde-3-Phosphate Dehydrogenase
GATA3	GATA Binding Protein 3
GD2	Disialoganglioside GD2
gDNA	Genomic Deoxyribonucleic Acid
GMP	Good Manufacturing Practice
hCG	Human Chorionic Gonadotropin
HE	Hematoxylin Eosin
hESC	Human Embryonic Stem Cells
hiPSC	Human Induced Pluripotent Stem Cells
HLA-G	Human Leukocyte Antigen G
Hoechst	2'-[4-ethoxyphenyl]-5-[4-methyl-1-piperazinyl]-2,5'-bi-1H-benzimidazole trihydrochloride trihydrate)
hPSC	Human Pluripotent Stem Cell
hPSC-RPE	Human Pluripotent Stem Cells-Derived Retinal Pigment Epithelial
hrLN	Human Recombinant Laminin

IF	Immunofluorescence
ICE	Inference of CRISPR Edits
ICM	Inner Cell Mass
INL	Inner Nuclear Layer
IR-cSLO	Infrared-confocal Scanning Laser Ophthalmoscopy
KDR	Kinase Insert Domain Receptor
KO	Knock Out
KRT7	Cytokeratin 7
KRT19	Cytokeratin 19
LIN28A	Lin-28 Homolog A
LPA	Lysophosphatidic acid
MAP2	Microtubule-associated protein 2
MEF	Mouse Embryonic Fibroblasts
MITF	Microphthalmia-Associated Transcription Factor
MYOD1	Myogenic Differentiation 1
$NaIO_3$	Sodium Iodate
Na+/K+	Sodium/Potassium
NCAM1	Neural Cell Adhesion Molecule 1
NEAA	Non-Essential Amino Acids
NES	Nestin
O_2	Oxygen
OCT3/4	Octamer-Binding Transcription Factor
ONL	Outer Nuclear Layer
ORT	Outer Retinal Thickness
OTX2	Orthodenticle Homeobox 2
OV	Optic Vesicle
PAM	Protospacer Adjacent Motif
PARD6B	Par-6 Family Cell Polarity Regulator Beta
PAX6	Paired Box Protein Pax-6
PCA	Principal Component Analysis
PCR	Polymerase Chain Reaction

PE	Primitive Endoderm
PEDF	Pigment Epithelium-Derived Factor
PDGFRB	Platelet-derived growth factor receptor beta
PGC	Primordial Germ Cell
PGF	Placental Growth Factor
PMEL	Premelanosome Protein
POS	Photoreceptor Outer Segments
POU5F1	POU Class 5 Homeobox 1
PR	Photoreceptor
PVDF	Polyvinylidene Difluoride
qPCR	Quantitative Polymerase Chain Reaction
RIPA	Radioimmunoprecipitation Assay Buffer
RNA	Ribonucleic Acid
RNA-seq	Ribonucleic Acid Sequencing
ROCK	Rho-associated coiled-coil kinase
RP	Retinitis Pigmentosa
RPE	Retinal Pigment Epithelium
RPE65	Retinal Pigment Epithelium-Specific Protein 65kDa
SALL4	Sal-like protein 4
scRNA-seq	Single Cell Ribonucleic Acid Sequencing
SD	Stargardt's Disease
SD-OCT	Spectral-Domain Optical Coherence Tomography
SDS-PAGE	Sodium Dodecyl Sulfate–Polyacrylamide Gel Electrophoresis
SEM	Scanning Electron Microscopy
sgRNA	Single Guide Ribonucleic Acid
shRNA	Short Hairpin RNA
siRNA	Short Interference RNA
SOX1	Sex Determining Region Y-box 1
SOX2	Sex Determining Region Y-box 2
SOX9	Sex Determining Region Y-box 9
SOX17	Sex Determining Region Y-box 17

T	Brachyury
TB	Trophoblast
TBS	Tris-Buffered Saline
TE	Trophectoderm
TEAD1	Transcriptional Enhancer Activator Domain 1
TEAD2	Transcriptional Enhancer Activator Domain 2
TEAD3	Transcriptional Enhancer Activator Domain 3
TEAD4	Transcriptional Enhancer Activator Domain 4
TEER	Transepithelial Resistance
TEM	Transmission Electron Microscopy
TGFβ	Transforming Growth Factor-Beta
TIDE	Tracking of Indels by Decomposition
t-SNE	t-distributed stochastic neighbor embedding
TUBB3	Tubulin Beta 3 Class III
TX	Transplantation
TYR	Tyrosinase
UMI	Unique Molecular Identifier
VEGF	Vascular Endothelial Growth Factor
VP	Verteporfin
WB	Western Blot
WT	Wild Type
WWTR1	WW Domain Containing Transcription Regulator 1
XF	Xeno-free
YAP1	Yes-associated Protein 1
ZO-1	Zona Occludens-1

1 INTRODUCTION

1.1 IN-VITRO MODELLING OF HUMAN TROPHOBLAST DIFFERENTIATION

1.1.1 Human Embryo Preimplantation Development

Embryo preimplantation is the developmental period that spans from the one-celled embryo (or zygote), after fertilization, until the implantation of the multicellular blastocyst into the uterine wall (Figure 1). When an oocyte is fertilized with a spermatozoid, it completes the division of its second meiosis making the female pronucleus haploid while releasing the second polar body. The pronuclei then migrate towards each other, replicating their DNA as they approach. At this point, the male and female pronuclei fuse together and begin a series of mitotic divisions, known as cleavage divisions, that will sequentially divide the zygote into two, four, eight and 16 daughter cells (or blastomeres) without increasing the total size. During that time, and more specifically during the transition from four to eight cells occurring after developmental day 2 (E2), a process known as embryonic genome activation (EGA) takes place. When EGA occurs, the embryo ceases to rely on maternally inherited transcripts and proteins from the oocyte and initiates its own genetic program. Following that, in the 16-celled embryo, or morula, the blastomeres start to develop gap and tight junctions and undergo a process known as compaction, in which the blastomeres reduce their intercellular space to the point of becoming nearly indistinguishable while still dividing. The embryo continues developing through a process designated as blastulation in which the outer blastomeres differentiate into the trophectoderm (TE), a layer of epithelial cells that will later facilitate embryo implantation and will form the fetal placenta[1,2]. The trophectoderm then surrounds a less-differentiated group of cells, the inner cell mass (ICM), formed by epiblast cells, which will give rise to the embryo itself, and primitive endoderm cells, which will be the major constituent of the yolk sack[3–5]. Polarized transport of ions and water through the trophectoderm helps in creating an inner cavity, the blastocoel, which supports the already formed blastocyst to increase its volume and hatch through the zona pellucida, a protective glycoprotein layer surrounding the embryo. Once the blastocyst has hatched, it can implant in the endometrial lining of the uterus, where it resumes development until the formation of the fetus.

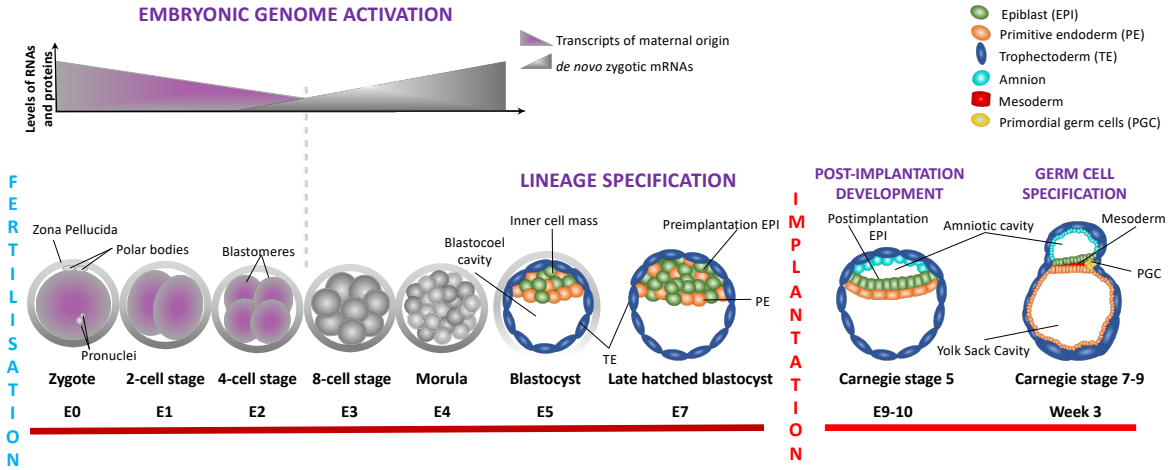

Figure 1. Schematic overview of human early embryonic development. The totipotent zygote undergoes several rounds of cell divisions before becoming a multicellular morula, around day 5. During such process, maternal transcripts are gradually degraded and gets replaced by the embryo's own transcripts in a process known as embryonic genome activation. Once it reaches the morula stage, the embryo undergoes compaction and initiates the formation of a blastocoel activity that will continue its expansion until the formation of a blastocyst, around day 7. By that time the embryo is known to be configurated by three different cell types: TE, EPI and PE, and it is ready to initiate implantation in the endometrium. After implantation, the embryo continues developing and start forming dedicated structures, such as the amniotic and yolk sack cavities, and specialized tissues, such as mesoderm and primordial germ cells. Image was adapted from ref.[6], with permission from Elsevier.

1.1.2 Animal Models for Studying Early Embryogenesis

Studies of human preimplantation development have historically focused solely on the morphological examination of embryos through the different developmental stages[7–9]. While these studies have informed the optimization of assisted reproductive techniques and in-vitro embryo culture conditions, they have failed to foster a comprehensive understanding of the molecular and cellular processes that occur during that time. Basic research on mammalian preimplantation using animal models, especially the mouse, was traditionally the only manner of gaining insights into the different molecular and cellular mechanisms governing embryo preimplantation development. While human and mouse preimplantation developments are morphologically very similar, recent findings of species-specific differences have raised the question of whether the same molecular and cellular mechanisms controlling such processes in the mouse are conserved in humans. While most of these known differences are structural, especially during postimplantation development, some refer to the signaling pathways and downstream gene regulatory mechanisms that regulate the major lineage specifications occurring before implantation (Figure 2)[10–14].

During mouse preimplantation development, two major differentiation events take place: the first event separates the trophectoderm and the inner cell mass, and the second event separates the epiblast and the primitive endoderm within the inner cell mass. In mice, the first cell differentiation event occurs as early as the morula stage and is primarily driven by the Hippo signaling pathway, which senses the positional and polarity information of the blastomeres and regulates the transcription of the trophectoderm and inner cell mass determinants[15–21]. By the end of this process, the polarized outer cells of the morula are committed to become trophectoderm, while the inner cells will remain as inner cell mass. Afterwards, during blastocyst formation, the cells in the inner cell mass undergo a second lineage specification

process, now controlled by the fibroblast growth factor/mitogen-activated protein kinases (FGF/MAPK) signaling pathways. Throughout this differentiation event, cells with a higher expression of *Fgfr2* that are thereby more sensitive to FGF4 will form the primitive endoderm, while the other cells will remain as the epiblast[22,23].

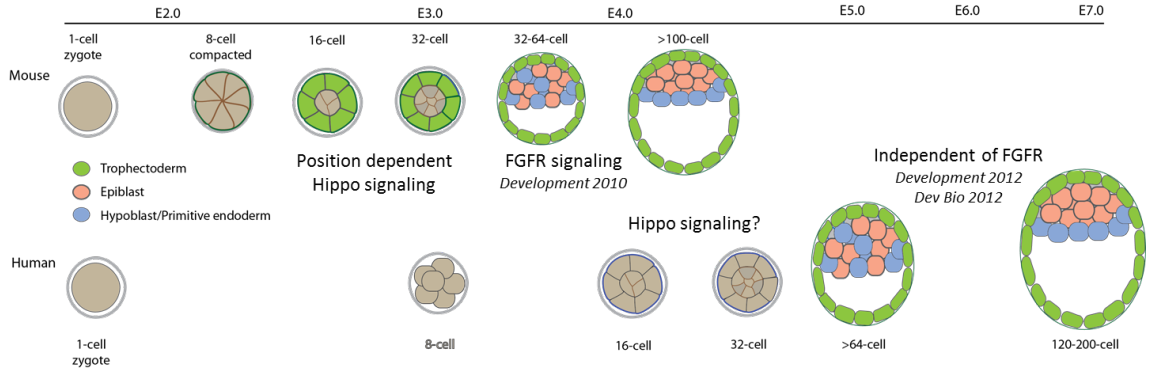

Figure 2. Comparative scheme of mouse and human preimplantation development. While human and mouse embryos are morphologically very similar, several differences have been described between these two species. Image was adapted from ref.[24], with permission from Elsevier.

Mouse and human preimplantation development demonstrate significant differences, especially in the timing of the events and the expression pattern of lineage specific markers. Compared to the 4.5 days in mice, in humans it takes seven days to form a mature blastocyst that is ready to implant in the uterine wall[3,25–27]. At this point, there are three distinct cell lineages that express the same key lineage-specific transcription factors as those displayed in the late blastocyst of mice. However, the timing of expression and the pathways controlling such defining factors are not similar between mice and humans. Probably one of the first clues that made us aware of the developmental differences between these two species was the significant disparities in the timing of the expression of *Cdx2*, a determinant factor in mice for trophectoderm identity and maintenance. In mice, *Cdx2* expression can be observed as early as the eight-cell morula stage prior to trophectoderm formation, whereas in the human embryo, its expression is not evident until the late blastocyst, suggesting a less critical role of this factor in human trophectoderm specification[12,28].

Another important difference between mouse and human development is the independence from FGF signaling observed during human primitive endoderm formation. In contrast to the findings in mice, *FGFR2* expression is not present in E6 human embryos when primitive endoderm and epiblast lineages are well segregated. Furthermore, the inhibition of FGF/MAPK signaling pathways in humans does not interfere with primitive endoderm formation, which still expresses lineage-specific markers such as *GATA6* and *GATA4* even under the complete absence of FGF signaling[11,13]. Moreover, in addition to differences in the timing and expression patterns, recent studies using single-cell high-throughput transcriptomics have demonstrated that, in contrast to findings in mice, the segregation of the three cell lineages occurs almost simultaneously in humans[29]. This observation aligns with the late expression of *CDX2* and delayed morula compaction that is perceived in humans compared to mice.

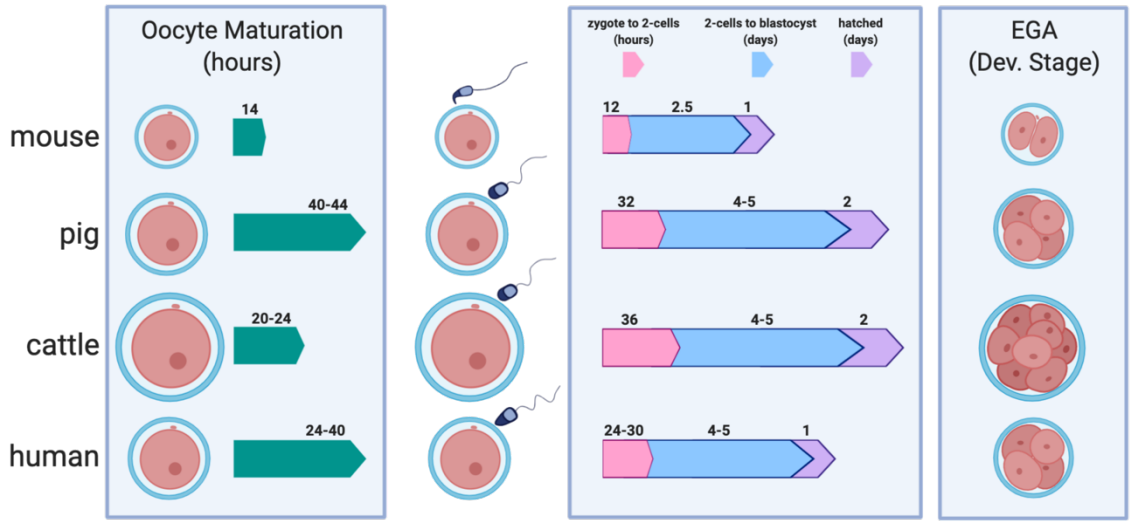

Figure 3. Main known differences between mouse, pig, bovine and human oocyte and early embryo development. Differences in the object sizes correlate with the proportional differences in mean size of oocytes and embryos among the different species. Time differences in oocyte maturation (green arrows) and embryo development (pink, blue and purple arrows) are also depicted. Likewise, the different developmental stages at which EGA takes places in these different species are illustrated in the right panel. Image was adapted from ref.[30], with permission from Springer Nature and using Biorender.com.

While the use of animal models, such as mice, has proven to be advantageous for uncovering many shared fundamental molecular mechanisms with humans, the many differences across species, such as the ones discussed above, make it difficult to accurately infer developmental events in human embryos from any other animal model system (Figure 3). Recent studies of bovine, porcine, and rabbit embryos revealed that important aspects of development in these species resemble human embryo development better than the mouse does[10,11,31–35]. These aspects include the coexpression of *OCT4* and *CDX2* observed in the TE and the independence of FGF/MEK signaling for the regulation of the second lineage differentiation. While these alternative animal models may still prove to be very helpful to our understanding of mammalian development, certain species-specific features can only be determined by performing functional studies directly in human embryos. Improved understanding of the processes involved in human development (e.g., fertilization, embryo genome activation, X-chromosome dosage compensation, cell lineage development, pluripotency regulation and implantation) will have practical consequences for the development of improved IVF technologies and the derivation of better stem cells for disease modeling and application in regenerative medicine.

1.1.3 Hippo Signaling Pathway

As described in the previous section, the Hippo signaling pathway plays the main role in separating the trophectoderm and inner cell mass during morula formation in mice. This pathway was first described in Drosophila as a tumor suppressor pathway and it was later found to be conserved in mammals, where it has been extensively studied for its function as a regulator of organ size in mice and humans[36]. In all of its different functions, the Hippo pathway always translates information from extracellular stimuli, such as cell position and polarization, into gene regulation of several downstream effectors. When the Hippo signaling pathway is active, the paralogous transcriptional coactivator molecules termed YAP1 and WWTR1

(commonly named TAZ) are phosphorylated by a set of Hippo-inherent kinases termed LATS1/2. YAP1/WWTR1 normally interacts with several transcription factors, such as the TEA domain transcription factor family (TEAD1-4), which are localized in the nucleus and, once activated, drive the expression of their target genes. However, in the event of phosphorylation by LATS1/2 kinases, YAP1/WWTR1 is retained in the cytoplasm, where it is prevented from interacting with any transcription factors and eventually is degraded by the proteasome (Figure 4)[37–39].

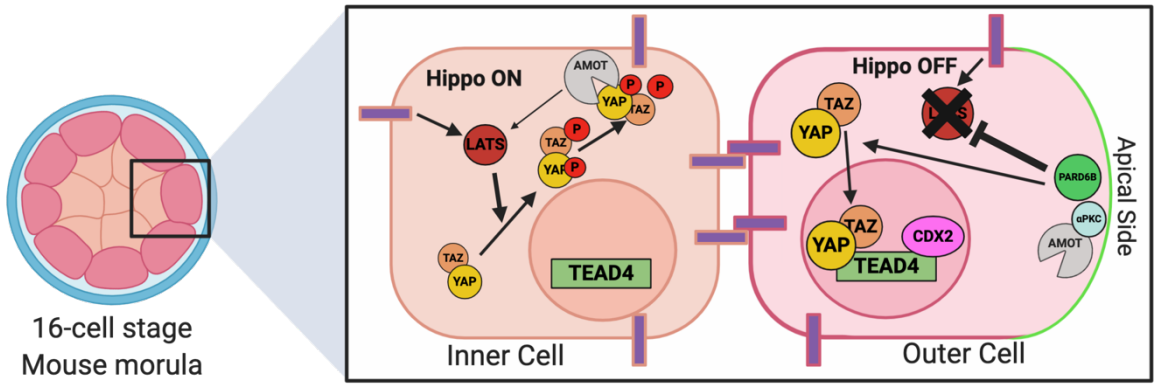

Figure 4. Function of the Hippo signaling pathway during mouse embryo development. The right panel illustrates the transcriptional regulation of trophectoderm-specific markers, such as CDX2, in inner and outer cells of the mouse morula. In outer cells apical and polarity factors like PARD6B and αPKC inhibit the activity of the Hippo pathway kinases LATS and allow the migration of coactivator factors YAP and TAZ to the nucleus, where they bind to TEAD4 and initiate the transcription of TE genes. Contrary, in inner cells, Hippo pathway remains active and LATS kinases phosphorylate YAP and TAZ, forcing their retainment in the cytoplasm by factors such as AMOT and impeding the activation of TEAD4 and posterior transcription of TE genes. Image was created with Biorender.com.

The role of the Hippo pathway signaling pathway in cell specification during early development in mice was recently uncovered. The first clue that led to this discovery came from the analysis of *Tead4* mutants mouse embryos. It was found that *Tead4* null embryos downregulated trophectoderm specific genes such as *Cdx2* and *Gata3*, which made all of the cells acquire an inner cell mass constitution and consequently impaired the development of these embryos into blastocysts. This finding indicates an essential role of *Tead4* for the activation of trophectoderm-specific genes[15,17,20]. Furthermore, subsequent studies have demonstrated that phosphorylated YAP1 can only be found in the cytoplasm of inner cells at the 16-cell-stage morula, which are already committed to become inner cell mass[21]. This differential activation of the Hippo pathway observed in the mice embryos suggests a novel mechanism through which activated Hippo inhibits the expression of trophectoderm-specific genes by phosphorylating YAP1 and preventing its interaction with TEAD4. However, the processes that correlate cell position with Hippo pathway activation remain unknown.

The aim to understand the mechanisms that control lineage segregation during preimplantation development attracted interest even before discovery of the involvement of the Hippo pathway. Two major models have traditionally been proposed: the positional model and the polarity model. According to the first model, the cell fate is determined by the position of each cell within the embryo; outer cells in the morula become trophectoderm, while inner cells give rise to inner cell mass[40,41]. The second model, which is more accepted today, focuses more on the polarization status of the blastomeres conforming the morula. According to the polarity model,

polar cells situated in the outer part become TE, while apolar cells inside the embryo turn into ICM[2,42].

Following the idea that polarity may play a central role in regulating cell fate during the first lineage segregation, different authors have sought to understand the connection between polarity and Hippo pathway activation. In mouse embryos, the Par-aPKC system is responsible for regulating cell polarity. Previous experiments with embryos in which polarity had been disrupted, by targeting the Par-aPKC system demonstrated that Hippo differential activation between the outer and inner compartments of the morula is highly dependent not only on the polarity status of each individual cell, but also on the presence of cell-to-cell adhesions[16,43,44]. Loosing apical-basal polarity results in the Hippo pathway being active in all cells (inner and outer). Meanwhile, losing cell-to-cell adhesions, by dissociating the blastomeres, causes a complete loss of Hippo activation. In further support of this model, later studies have demonstrated that the link between the Hippo pathway and cell polarity may be operated by a family of junction-associated proteins known as angiomotins. Two of the three angiomotins present in mice (AMOT and AMOTL2) were found to be expressed in mouse embryos. Blocking AMOT and AMOTL2 in mouse embryos resulted in an accumulation of nuclear YAP1 in all cells and differentiation into TE, highlighting the essential role of these proteins in Hippo activation. In addition, AMOT proteins were found to be differentially distributed in the outer and inner cells of the 16-cell mouse embryo. In the inner cells, AMOT is found in adherent junctions (AJ) throughout the entire cell membrane, where it interacts with LATS1/2 kinases and activates the Hippo pathway. In contrast, in outer cells, AMOT is sequestered to the apical part by the Par-aPKC system, where it binds to F-actin and is kept away from AJs; therefore being unable to activate Hippo through interaction with LATS1/2 (Figure 4)[16,19,45,46].

Despite recent progress, our knowledge about the role of the Hippo pathway in the mouse embryo preimplantation remains incomplete. Questions on how cell polarity is regulated, and which mechanisms are involved in the Par-aPKC-mediated subcellular distribution of Amot remain to be answered. Furthermore, the possibility of having an equally important role in TE-ICM specification in humans remains unexplored. Although, the differences in the timing of lineage specification and in the expression of appropriate transcription factors make this possibility unlikely, thorough experimental evaluation is still necessary.

1.1.4 Early Stages of Human Placenta Development

The placenta, which derives from the preimplantation trophectoderm, constitutes the first fetal organ to develop during pregnancy. Among its primary functions are the exchange of nutrients, gases, and excretory material between the mother and the fetus; the anchoring of the conceptus to the wall of the reproductive tract; the secretion of necessary hormones; and the protection of the fetus against the maternal immune system. Proper formation of the placenta is essential for normal in-utero development in mammals, as defects in placentation are known causes of common pregnancy-related complications such as pre-eclampsia, fetal growth restriction and miscarriage[47,48]. Despite the importance of the placenta, cellular and molecular mechanisms governing the early stages of human placentation are poorly understood, largely due to the

obvious ethical and practical obstacles impeding direct investigations of early human pregnancy and to the historical lack of appropriate cellular model systems. Most of the knowledge that we have to date on the first weeks of human placental development comes from morphological observations and experimentation on samples from early pregnant hysterectomies, as well as from studies in relevant animal models, such as higher primates[26,49,50]. According to those studies, human placental development until the end of the first trimester can be divided into five different phases: pre-lacunar stage, lacunar stage, primary villous stage, secondary villous stage, and tertiary villous stage.

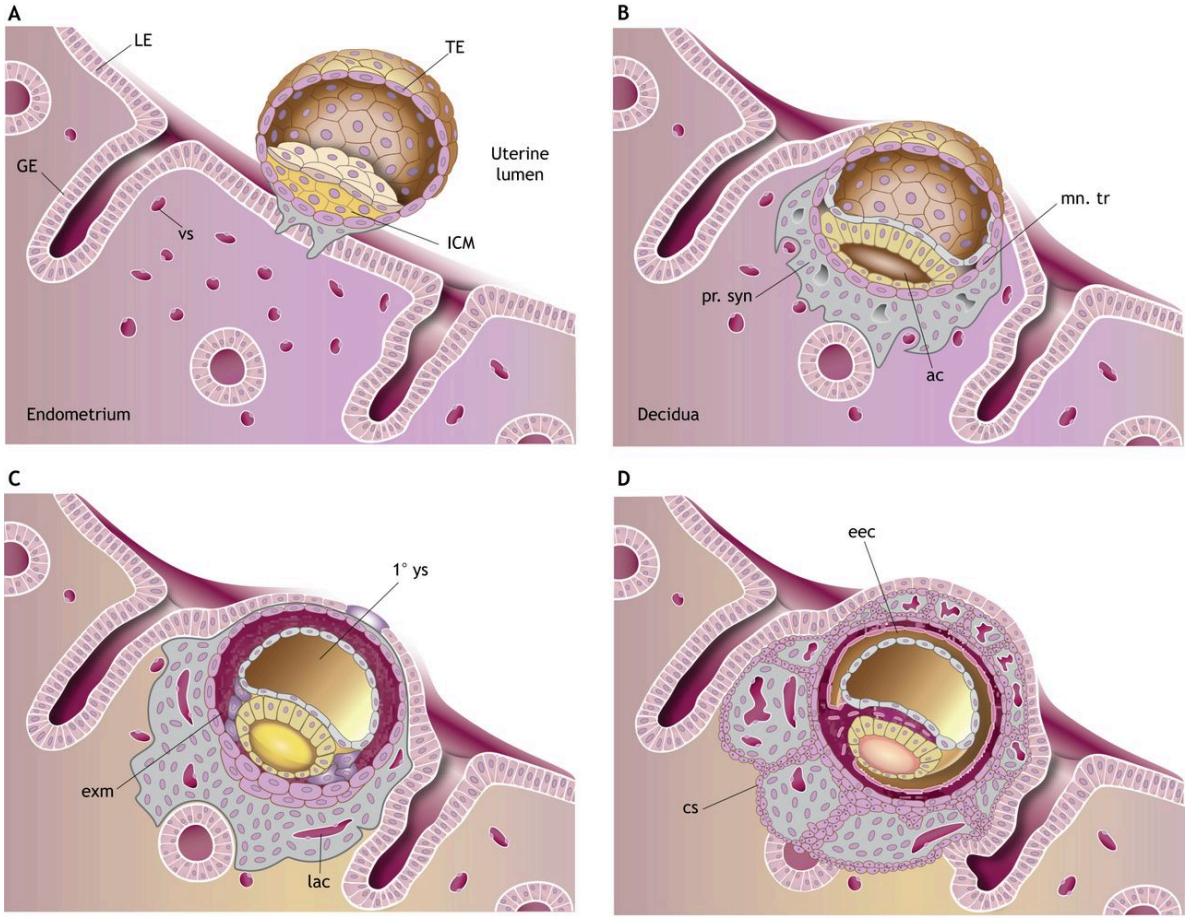

Figure 5. Early stages of human placental development. Illustration portraying the early phases of placenta formation, right after blastocyst implantation. (A, B) The implantation and pre-lacunar stages. (C) The lacunar stage. (D) The primary villous stage. 1° ys, primary yolk sac; ac, amniotic cavity; cs, cytotrophoblastic shell; eec, extra-embryonic coelom; exm, extra-embryonic mesoderm; GE, glandular epithelium; ICM, inner cell mass; lac, lacunae; LE, luminal epithelium; mn. tr, mononuclear trophoblast; pr. syn, primary syncytium; TE, trophectoderm; vs, blood vessels. Image was adapted from ref.[51], with permission from The Company of Biologists.

1.1.4.1 Implantation and Pre-lacunar stage

Right before implantation, at 6-7 days post fertilization (dpf), the area of the trophectoderm that is contiguous to the underlying inner cell mass differentiates into what is known as the polar trophectoderm. Polar trophectoderm cells are morphologically and transcriptionally different from the remaining trophectoderm which sits distal to the inner cell mass (termed the mural trophectoderm) and mediates the attachment of the embryo to the uterine surface epithelium in a process called implantation[29]. Upon implantation, trophectoderm cells fuse, forming a primary syncytium that will continue invading the surface epithelium during the

following days, until it reaches the underlying endometrium, which at this point should have transformed into decidua (Figure 5A-B)[52,53].

1.1.4.2 Lacunar stage

By 14 dpf, the blastocyst is completely implanted into the decidua and surrounded by the surface epithelium. Vacuoles begin forming inside the primary syncytium and continue expanding until they become lacunae. The fluid-filled lacunae become then become surrounded by a network of structures called trabeculae, comprised by the remaining cells (Figure 5C)[51].

1.1.4.3 Primary villous stage

Cytotrophoblast cells sitting underneath the syncytium push through the primary syncytium, forming projections that are composed of a cytotrophoblast core and a syncytiotrophoblast (SCT) outer layer, known as primary villi[54]. Up to 17 dpf, villous trees are formed by the continuous branching and proliferation of the primary villi. Meanwhile, the neighboring lacunae become the intervillous space. At the end of the primary villous stage, the cytotrophoblast eventually breaks through the primary syncytium and forms a shell surrounding the embryo, which is now covered by three layers: the inner chorionic plate, the villi with their intervillous space, and the cytotrophoblast shell (Figure 5D).

1.1.4.4 Secondary villous stage

Around 17-18 dpf, primary mesodermal cells known as extraembryonic mesoderm, which are believed to be derived from the hypoblast, invade the primary villi and transform them into secondary villi.

1.1.4.5 Tertiary villous stage

After extraembryonic mesoderm invasion at 18 dpf, fetal capillaries derived from umbilical vessels appear within the mesodermal core of the villi to form tertiary villi (Figure 6)[55]. From that moment until the end of the first trimester, villous trees continue branching and proliferating, forming a network called the labyrinth structure. During that time, individual cytotrophoblast cells leave the embryonic shell and the tip of the villi to invade the decidua as extravillous trophoblast (EVT).

1.1.5 Cell Types of the Human Placenta

During the course of placenta formation, many different cell types emerge and cooperate to ensure its correct functioning, which is essential in reproductive success. While the vast majority of these cells belong to various trophoblast cell subtypes - such as cytotrophoblast, syncytiotrophoblast and extravillous trophoblast – additional placental cell types not derived from the TE also provide important functions, such as endothelial, immune, and fibroblast cells (Figure 6).

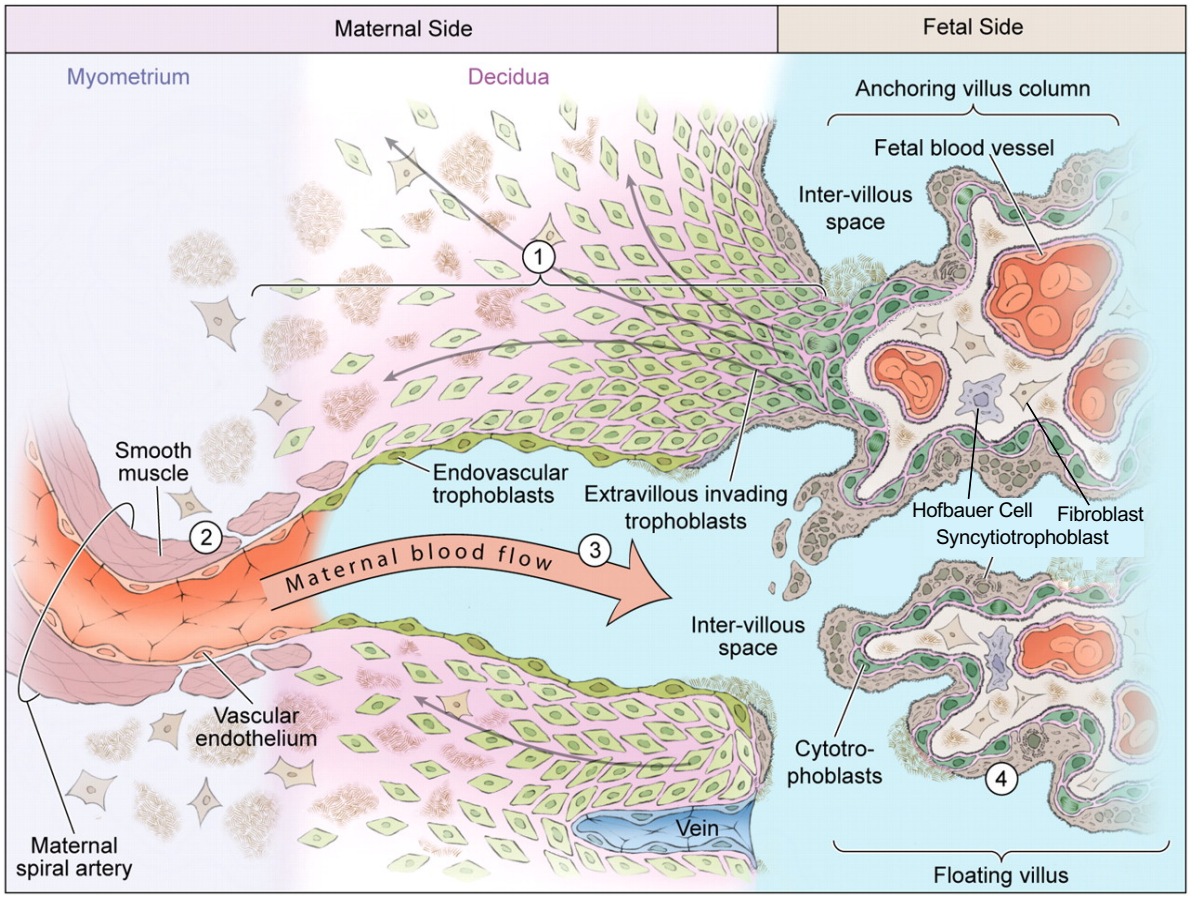

Figure 6. Cell types present in the human placenta. Diagram depicting the main cell types present in the maternal and fetal sides of the placenta by the end of the first trimester. Extravillous cytotrophoblasts proliferate in anchoring columns and invade the maternal side through the decidua (1) where they reach the distal spiral arteries and initiate their transformation (2). These transformations facilitate the necessary increase in volume flow at low pressure into the intervillous space (3). On the fetal side, placental villi are enclosed by the syncytiotrophoblast and the underlaying proliferative cytotrophoblast (4). Image was adapted from ref.[56], with permission from The American Society of Hematology.

1.1.5.1 Cytotrophoblast (CTB)

Cytotrophoblasts are historically considered to be bipotent progenitor cells, capable of differentiating towards syncytiotrophoblast and extravillous cytotrophoblast. They are regarded as the germinative layer due not only to their differentiative potential but also to their preserved proliferative capacity. Transcriptionally, they are typically characterized for expressing markers such as TEAD4, p63, GATA2/3, TFAP2C, ELF5, and TCF1[57].

1.1.5.2 Syncytiotrophoblast (SCT)

Syncytiotrophoblasts are a multinucleated layer of cells formed after the fusion of villous cytotrophoblast cells. They are the majority cell type in the placenta and sits in direct contact with maternal glandular secretions and maternal blood flowing through the intervillous space[54]. SCT have a major endocrine function: secreting necessary hormones and proteins for successful pregnancy – such as human chorionic gonadotropin (hCG), human placental lactogen (hPL) and human placental growth hormone (PGH) – into the maternal circulation[58]. Furthermore, SCT lacks expression of HLA molecules, which allows it to function as a protective barrier against maternal immune cells[59].

1.1.5.3 Extravillous cytotrophoblast (EVT)

EVT originate from the cytotrophoblasts present in the embryonic shell and in the tip of the villi, which undergo a process closely resembling epithelial-mesenchymal transition (EMT) and invades the adjacent decidua. Once EVT cells invade the decidua, they reach the maternal spiral arteries and replace smooth muscle and endothelial cells[60]. In this manner, EVT are able to remodel these arteries into vessels capable of high conductance at low pressure: a feature that is essential for successful pregnancy (Figure 6). EVT expresses HLA-Ib molecules, such as HLA-G and HLA-E, which have immunomodulatory functions and play an important role in avoiding rejection from maternal immune cells, especially NK cells[61–63].

1.1.5.4 Other placental cells

Apart from the different trophoblast cells, several other cell types play important roles in placental function and homeostasis. These non-trophoblastic cells include fibroblasts, which may be involved in vascular development; Hofbauer cells, which protect the fetus from infections and also assists in trophoblast and vascular development as the only immune cells in the placenta; and vascular cells comprising the vascular system, which, by the end of the first trimester, connects to the fetus through the umbilical cord[64,65]. All of these cells are believed to be derived from the extraembryonic mesoderm, which in humans is thought to arise from the embryonic epiblast[66].

1.1.6 In-vitro Models for Trophoblast Differentiation

Given the inherent ethical and logistical barriers for the direct study of human early pregnancy, and the lack of physiologically relevant animal models, consequence of the diversity of strategies followed by eutherian mammals for placental formation, in-vitro models are devised as invaluable research tools for gaining insights into the mechanisms that govern the early stages of human placental development[67].

1.1.6.1 Primary trophoblast cultures

Primary trophoblast, which is primarily derived from term placentas, have been deemed as useful for studies on placental hormone secretion, and the transcellular transportation of nutrients, drugs, and pathogens across the placental syncytium[68]. When maintained in culture, these isolated trophoblast cells spontaneously differentiate into SCT and display phenotypic characteristics of third-trimester placentas, which makes them a weak model for the study of placental early development. In addition, these primary cultures display a limited expansion potential and face the inherent risk of contamination by maternal epithelium and fetal mesenchymal cells that can eventually outgrow the trophoblast cells.

1.1.6.2 Immortalized trophoblast cell lines

In addition to the use of primary trophoblast cell cultures, many previous studies have benefited from the use of immortalized trophoblast cell lines derived from choriocarcinoma (e.g. BeWo line) or normal placentas (e.g. HRP-1 line). While these cells also display typical features of

third-trimester placentas, unlike their primary counterparts, they are mostly unable to differentiate in culture. Their capacity to indefinitely expand and to form polarized monolayers, however, makes them a useful placental model to investigate asymmetric transcellular transportation[68]. Nevertheless, the lack of consensus on defining the essential markers and phenotypic characteristics necessary to define the trophoblastic nature of immortalized cell lines, have elicited the use of cell lines not representative of bona fide trophoblast cells in-vivo. Therefore, caution is warranted when interpreting the conclusion of the many published studies using this particular in-vitro model system[69,70].

1.1.6.3 Trophoblast stem cells (hTSC)

The derivation of trophoblast stem cells was previously only possible from mouse embryos[71]. However, recent advances in organoid culture along with systematic screening of essential growth factors has allowed the isolation of these cells from human first-trimester placentas and human blastocysts[72]. The propagation and long-term expansion of these cells requires the simultaneous stimulation of EGF and WNT, together with inhibition of Activin A, HDAC, and Rho kinase. Slight modification of these culture conditions allows hTSC to differentiate into EVT and SCT, demonstrating the bipotentiality of these progenitor cells. Contrary to primary and immortalized cell lines, the developmental origin of hTSC renders them a valuable model system to study early placental development. However, up to now, no other groups have reported successful replication of these results.

1.1.6.4 3D organoids

Although hTSC represent a promising resource for understanding the mechanisms that control the differentiation mechanisms of the different trophoblast subpopulations, hTSC grow as a monolayer and therefore cannot recapitulate the formation of complex 3D placental structures that occur in-vivo. For that reason, recently developed 3D cultures of human trophoblast organoids represent a better alternative to understand complex events in placental early development, such as cytotrophoblast column formation[73,74]. Initial studies using hTSC-derived organoids have described the self-organization of the cells, with progenitor CTBs sitting on the outside and differentiated subtypes emerging on the inside. Moreover, the possibility of combining hESC and hTSC opens the door for the creation of embryoid-like structures that could become helpful in understanding the crosstalk between embryonic and extraembryonic lineages. In that line, recent studies using similar embryoid-like constructions in mice, found that NODAL and BMP signals secreted by the epiblast are essential for trophoblast maturation and embryo cavitation[75,76].

1.1.6.5 Human embryonic stem cell-derived trophoblast cells

Due to their phenotypic features and growth requirements, hESC have been traditionally considered to resemble the postimplantation epiblast of the embryo and are therefore believed to be “primed” for differentiation into the different embryonic lineages exclusively. However, several researchers have found that, when exposed to high concentrations of BMP2/4, these cells are able to change their morphology and exhibit molecular characteristics of trophoblasts,

such as bipotential differentiation into SCT and EVT, secretion of hCG and progesterone, or expression of specific markers, such as TFAP2A/C, GATA2/3, CDX2, TEAD4, KRT7, and p63[77–79]. While some studies have speculated that BMP4 acts by reverting hESC to a totipotent-like state that is able to differentiate into extraembryonic tissues, the fact that these cells originated from hESC together with their expression of several markers that are shared between trophoblast and mesoendoderm lineages has elicited some controverted opinions in the field[80]. While some researchers believe in the mesodermal or extraembryonic mesodermal nature of these cells, others have defended the possibility of hESC-derived trophoblasts representing an early-post-implantation trophoblast population[80–82]. Subsequent publications have demonstrated that inhibiting FGF2 and Activin A signaling during BMP4 treatment (termed BAP-TB differentiation), avoids any potential mesoderm diversion and have provided solid evidence through the combination of RNAseq, microarray, ELISA, WB and flow-cytometry techniques that hESC can efficiently differentiate into trophoblasts[83]. Moreover, studies combining transcriptome and chromatin occupancy analysis on BAP-TB have concluded that GATA2/3 and TFAP2A/C coordinately mediate the downregulation of pluripotency genes and simultaneous initiation of trophoblast differentiation in these cells[84]. Supporting the theory that BMP4 enables the differentiation of hESC by reverting them to more totipotent state, a couple of recent publications have reported the enhanced potential of naive stem cells to differentiate towards trophoblast, which proved to be able to do so even in the absence of BMP4[82,85].

1.1.7 CRISPR/Cas9 Genome Editing

The CRISPR/Cas9 system has elicited a revolution since its first appearance as an effective genome editing tool in eukaryotes[86–88]. This system was first described by Francisco Mojica, who found a curious arrangement of interspaced repeats in the genome of an archaeal microbe isolated from Alicante's marshes, which he would later name clustered regularly interspaced palindromic repeats (CRISPR)[89,90]. In archaea and bacteria, this system acts as a primitive immune system that protects the microbes against possible viral infections[91]. In the event of a viral infection, special endonucleases known as CRISPR-associated (Cas) nucleases recognize the foreign DNA and cleave it into pieces. A piece of the viral DNA will then be stored in a dedicated region of the bacterial genome, the CRISPR array, which serves as a memory of all previous viral infections. Upon a second infection with the same type of virus, the microbe will transcribe this CRIPSR array into a long RNA molecule known as pre-CRISPR RNA, which will be further processed into many short CRISPR RNAs (crRNAs). The crRNA corresponding to the invading type of virus will then guide a Cas nuclease through sequence complementarity to the invading viral DNA, where it will generate double strand breaks (DSBs) and promote its degradation.

The ability of the CRISPR/Cas9 complex to generate such DSBs is what makes it an interesting as a genome editing tool in other cell systems. In contrast to what occurs in viral genomes, when a DSB is introduced in an eukaryotic genome, the intrinsic DNA repair machinery of the cell will try to fix it, and it is actually this DNA repair that ultimately elicits the edition of the genome. DNA repair after a DSB can occur in two different ways: via the non-homologous

end-joining (NHEJ) pathway, which fixes the DSB through the addition or deletion of a few nucleotides; or via the homology-dependent repair (HDR), which repairs broken strands of DNA through utilizing a homologous template[92,93]. While NHEJ repair often results in a deleterious frame-shift mutation, the HDR mechanism, which occurs at a much lower frequency, is assumed to be error free as long as there is an available template. Both of these mechanisms have demonstrated to be equally interesting from the gene-editing perspective. On the one hand, frame-shift mutations caused by the NHEJ repair have been exploited to create genetic knockouts with the aim of studying the function and importance of certain genes in different biological settings[94]. On the other hand, homologous recombination resulting from HDR repair has allowed the inclusion of reporter genes in various loci, as well as the insertion or correction of point mutations of known importance for certain health conditions[95].

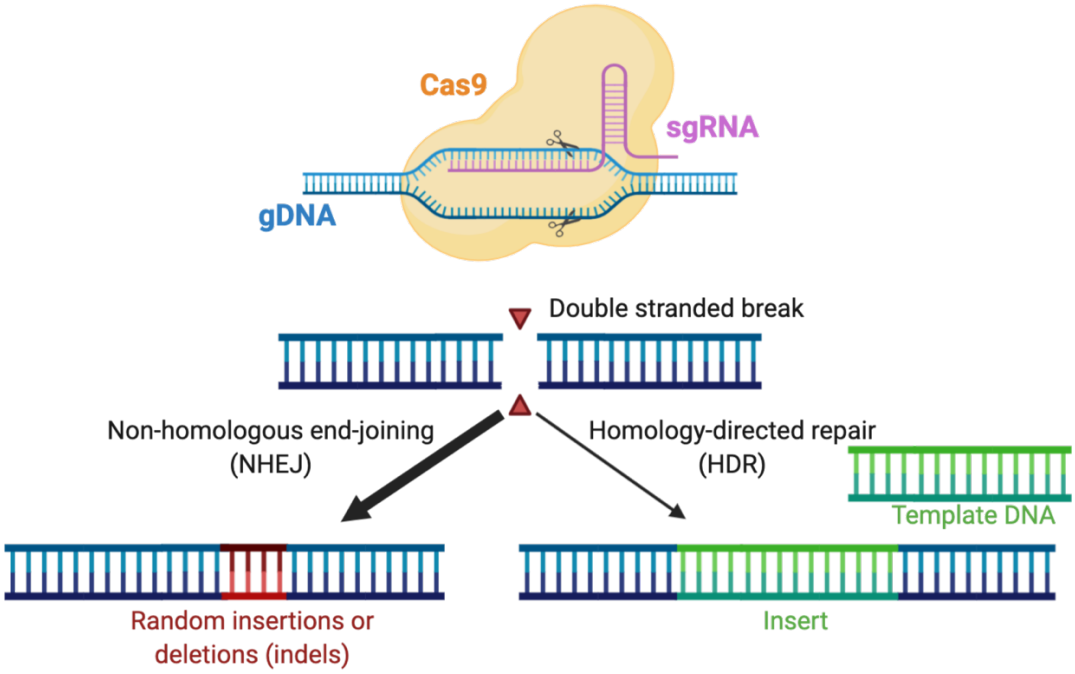

Figure 7. CRISPR/Cas9 Genome Editing. The programmable nuclease Cas9, directed by a sgRNA, introduces a target-specific double-stranded break (DSB) in genomic DNA. In the absence of a repair template, the cell will process the DSB mostly by NHEJ, resulting in indels at the site of editing. In the presence of a separate DNA template containing sequences homologous to the regions flanking the DSB, HDR can result in the incorporation of the repair template into the genomic DNA. Image was created with Biorender.com.

Although genome editing has been in use for many decades, none of the techniques available until the appearance of CRISPR/Cas9 reached its level of efficiency and simplicity. Genome editing using CRISPR/Cas9 only requires two components: a Cas endonuclease, which is responsible for creating the DSB, and a chimeric single-guide RNA (sgRNA) containing a target sequence that can be tailored to guide the Cas protein to the desired locus in the genome[96,97]. The simplicity of this system and its relative ease of use had expanded the applications of genome editing to new frontiers, such as the human embryo.

The possibility of using CRISPR/Cas9 in human embryos has triggered an enormous debate around the ethics of this application, especially regarding the possible clinical use of the technique as a way to correct disease-causing mutations or enhance some features in embryos

that could eventually give rise to individuals. Such concerns ended up embodied in two different publications, in which renowned scientists and ethicists called for a moratorium on all research involving genome modification of the human germline, or more specifically on the clinical applications of such technologies[98,99]. However, despite the growing consensus among scientists, several groups adventured to demonstrate the potential of CRISPR/Cas9 embryo editing for clinical applications, igniting a firestorm of controversy worldwide that resulted in the creation of a committee through the joint efforts of the National Academy of Science and the National Academy of Medicine[100,101]. The Committee on Human Gene Editing was convened to analyze the benefits, risks, regulatory frameworks, ethical issues, and societal implications of this new technology. The resolution of the study was published in a report in which the committee permitted the clinical application of heritable germline editing on the condition that a solid regulatory framework is in place, limiting its use to the treatment of serious diseases or conditions, and only in those cases where there is an absence of reasonable alternatives. Furthermore, the committee expressed its opposition to the use of genome editing in any other clinical setting beyond the treatment or prevention of a disease or disability, while it supported the use in basic laboratory research under existing ethical norms and regulatory frameworks at the local, state, and federal levels[102]. These recommendations from the Committee on Human Gene Editing were, however, not able to avert the polemical announcement of the world's first genome-edited babies using CRISPR technology, a notice that was severely criticized by the scientific community and that resulted in the incarceration of the main responsible, who was convicted for illegal medical practice[103].

The availability of transcriptomic data on the early human embryo and the emergence of new tools to help in the downstream analysis of gene disruption and gain- or loss-of-function experiments, create the perfect environment for genome editing techniques, such as CRISPR-Cas9, to increase our understanding of the genes and processes involved in normal embryo development and reproductive health[29,104–108]. Such investigations, in addition to providing important insights into human developmental biology, may shed some light on the causes of miscarriage, optimize assisted reproduction techniques, and provide potential benefits in enhancing fertility and in regenerative medicine.

1.2 HUMAN EMBRYONIC STEM CELLS FOR THE TREATMENT OF AGE-RELATED MACULAR DEGENERATION

1.2.1 Age-related Macular Degeneration

Age related macular degeneration (AMD) is a degenerative retinal disease characterized by a progressive loss of vision in the center of the visual field (Figure 8). As the name indicates, the region of the eye affected in this condition is the macula, a relatively small area situated near the center of the retina in humans and in some other mammals (Figure 9).

The retina has two types of photosensitive cells (a.k.a. photoreceptors): cones and rods. In the human retina, there are three types of cones, which are responsible for color vision and function best in bright light. Rod cells cannot discriminate colors, but exhibit a higher sensitivity than

cones and work better under dim light conditions, which makes them responsible for our night vision. The macula is the region of the retina with the highest density of cones, which explains its role in central, high-resolution color vision under bright light circumstances[109]. This type of vision is the one impaired under medical conditions that damage the macula, such as AMD.

AMD is the main cause of vision loss in the Western world, accounting for 54% of blindness among the white population in the US and 42% of the blindness in UK. Its incidence is higher in individuals over 50 years-old, especially in those with Caucasian ethnicity[110,111]. The disease is normally characterized by an impairment in the retinal pigment epithelium (RPE) cell layer, which leads to death and loss of the photoreceptors in that area[112]. Although the etiology of AMD is not well understood, it is known to be a multifactorial disease in which both genetic and environmental factors are involved[113].

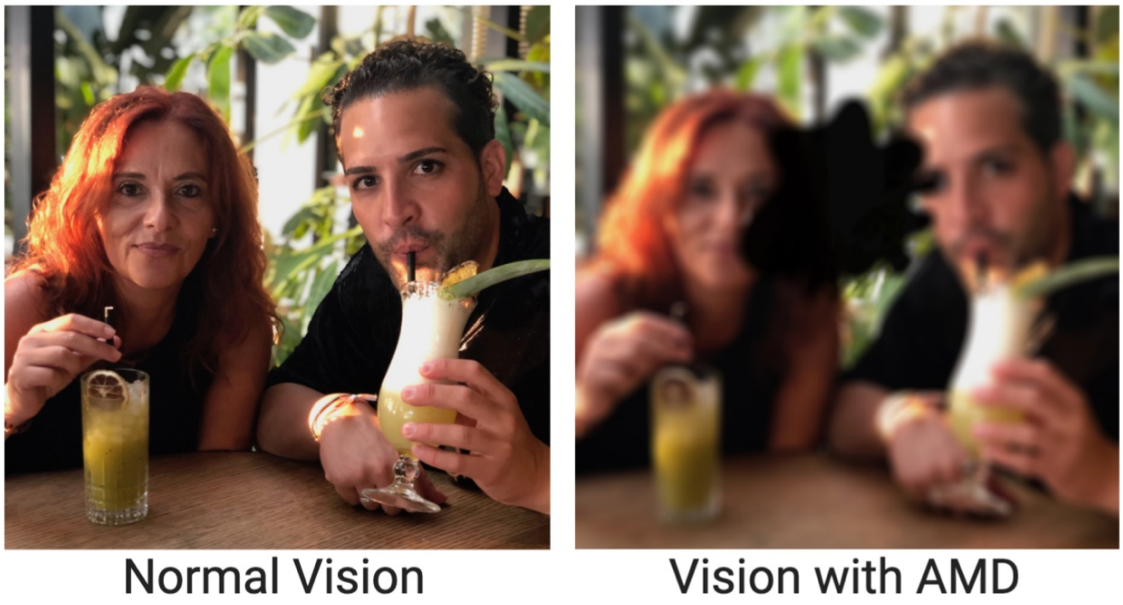

Figure 8. Age-related Macular Degeneration. A scene as it might be viewed by someone with normal vision and by someone affected by AMD.

AMD generally starts with the progressive accumulation of yellow deposits, known as drusen, between the RPE layer and the underlying choroid. However, the appearance of drusen is not always regarded as a synonym for AMD, and many people above the age of 60 exhibit drusen deposits without reporting an impairment in their vision[114]. The early and intermediate forms of AMD are usually asymptomatic, although abnormalities in the RPE layer may be found already this stage, especially in the intermediate forms. In the late forms of AMD, there is enough retinal damage, in addition to drusen, that subjects begin to suffer from symptomatic loss of central vision[115]. Depending on the nature of the retinal damage, late AMD is further divided into two subtypes: wet AMD and geographic atrophy (GA). Wet AMD, also known as exudative or neovascular AMD, is characterized by an abnormal growth of blood vessels from the choroid into the subretinal space, causing edema and hemorrhages that are eventually responsible for damage in the RPE and photoreceptors and lead to vision loss. In contrast, in GA, also known as advanced dry AMD or non-exudative AMD, there is no neovascularization

involved and the loss of photoreceptors results from an atrophy and progressive degeneration of the RPE layer at well-demarcated areas in the macula. Dry AMD, including early and intermediate states besides GA, accounts for 90% of AMD cases. Of all patients with some type of dry AMD, it is known that 10-20% will progress to the wet type[116,117].

There are currently treatments for the wet form of AMD, including those targeting the vascular endothelial factor (VEGF), which is crucial for the neovascularization process[118]. However, there are no efficient treatments to date for the dry forms of AMD, and current strategies focus only on slowing down the progression of the disease by delivering supplements such as lutein and zeaxanthin or by trying to restore the damaged areas through the transplantation of healthy RPE[119–121].

1.2.2 Retinal Pigment Epithelium

The retinal pigment epithelium, or RPE, is a cell layer of polarized, hexagonal, and heavily pigmented cells that are found in the retina. It is positioned between the photoreceptors and the Bruch's membrane (BM), a basement membrane that separates the choriocapillaris from the neural retina (Figure 9)[122].

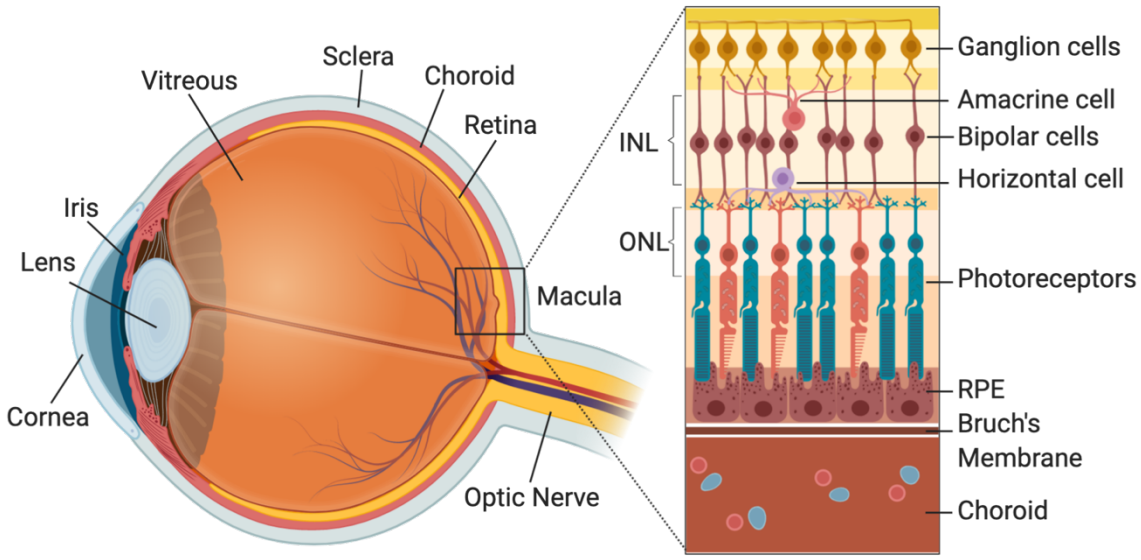

Figure 9. Retinal structure. Schematic view of the eye displaying the location of the macula and the main retinal layers and cell types. Image was created with Biorender.com

The RPE is formed by a single layer of densely packed cells that are attached to each other by strong tight junctions creating - together with the BM - what is known as the blood-retina barrier[123]. RPE cells are polarized, which means that their apical and basal membranes have specific and distinct functions. On the apical membrane, which is the membrane facing the neural retina, the RPE displays long microvilli that surrounds the photoreceptors' outer segments and establishes a complex interaction that is essential for maintaining the homeostasis of the retinal tissue. On the basal membrane, which faces the BM and the choroid, the RPE secretes ions, water, and metabolic end-products from the subretinal space into the blood. This

polarization also allows the RPE to secrete distinct growth factors that are needed by the photoreceptors (e.g. PEDF) and by the choroid (e.g. VEGF), as wells as immunosuppressive cytokines that contribute to the immune-privileged status of the eye[122,124,125].

The pigment present in the RPE cells enables the absorption of the light energy focused by the lens on the retina, which has an important role in preventing photo-oxidative damage and maintaining visual function. In addition to preventing photo-oxidative damage and providing essential nutrients, the RPE layer has other important functions for the maintenance and function of photoreceptors. For example, RPE cells help to maintain the excitability of photoreceptors through the phagocytosis of their outer segments, which are saturated with radicals and photo-damaged proteins and lipids. They also contribute to the visual cycle by regenerating all-trans-retinal into 11-cis-retinal, which is used by photoreceptors to transduce light energy into electrical impulses[126].

These complex different functions make the RPE an essential retinal component for visual function. As such, dysfunction of the RPE, which occurs in medical conditions such as AMD, will inevitably leads to degeneration of the retina, loss of visual function, and blindness.

1.2.3 Development of the RPE

Human eye formation begins in week five post conception and continues until postnatal month 18. During this time, many different signaling pathways coordinate to form the specific structures and cell types present in the adult human eye (Figure 10). The development process begins with the establishment of the neuroectodermal plate during gastrulation (at around 18 dpf) through the combined activities of FGF signaling; Notch signaling; time-dependent canonical WNT activation and inhibition; and inhibition of BMP signaling by Noggin, Chordin, and Follistatin[127]. Soon after, an area of the early forebrain is specified as the eye field due to the joint expression of eye-field transcription factors (including RX1, PAX6, SIX3, and OPTX2), which is believed to be regulated by Notch signaling[128,129]. At week four of development, optic vesicles arise from the early forebrain due to the action of Sonic Hedgehog (Shh), which also specifies the proximal and ventral region of the optic vesicles that will give rise to the optic stalk and neuroretina, respectively[127]. During optic vesicle expansion, extracellular signals from the surface ectoderm segregate the vesicle into three regions: the optic stalk, neuroretina, and RPE. Release of BMP and TGFβ family members (such as Activin A) from the surface ectoderm initiates MITF expression in the proximal mesenchyme, making it differentiate into retinal pigment epithelium[130]. FGF induction of VSX2 and SOX2 transcription factors by the surface ectoderm subsequently initiates the neuroretina specification of the distal wall of the optic vesicle. Finally, after optic vesicle protrusion, the combined actions of WNT and Shh result in the evagination and formation of the optic cup, where the RPE becomes pigmented and retinal progenitors will resume their maturation until eventually configuring the different specialized subtypes present in the human eye.

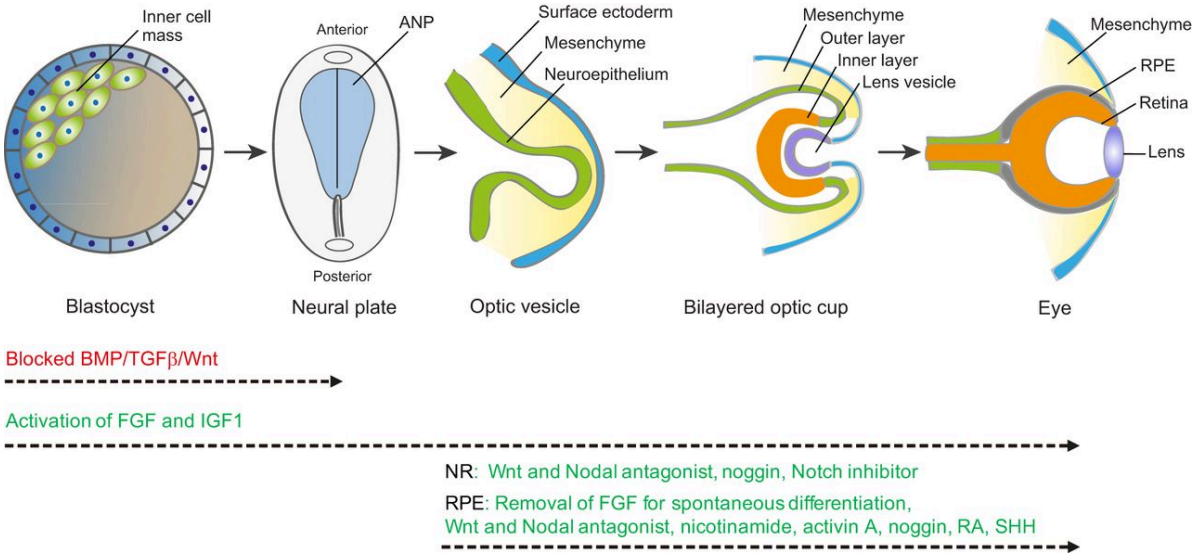

Figure 10. Development of the Retinal Pigment Epithelium. Diagram representing key stages of retina development. Once the blastocyst implants and initiates gastrulation and neurulation, the neural plate is formed. Blockage of BMP, TGFB and Wnt activity at the anterior neural plate (ANP) enables the emergence of the early eye field, which subsequently continues developing and forms the optic vesicles. Invagination of the optic vesicle leads to establishment of the bilayered optic cup. Coordinated activities of Wnt, FGF, BMP, Notch, SHH, RA and activin A signaling pathways enable then the specification of the RPE and NR from the outer and inner layers of the optic cup, respectively. Image was adapted from ref.[131], with permission from The Company of Biologists.

1.2.4 RPE Replacement as a Treatment for AMD

The important role of the RPE in maintaining retinal homeostasis and its implication in the degenerative forms of AMD has drawn the attention into the potential of transplanting healthy RPE cells to prevent the secondary loss of photoreceptors and potentially to preserve or restore vision.

Different studies have examined RPE cell transplantation as a therapy for AMD using several cells sources: autologous RPE, established RPE cell lines, fetal RPE or cadaveric donors[120,121,132–136]. Each of these sources demonstrates unique strengths and weaknesses. Autologous RPE, which is normally derived from the periphery of the same eye affected by AMD, has the advantage of being non-immunogenic. However, among the disadvantages of these cells are the risk of transplanting cells that are affected by the disease and will therefore have an already impaired function, and the limited availability of these cells. Conversely, established RPE cell lines represent an unlimited source for transplantation, but they exhibit a high level of batch-to-batch variability and lack of some of the properties from functionally mature RPE cells. Finally, fetal RPE cells may overcome most of the problems of the other cell sources; however, they are a limited source and their use involve significant ethical concerns.

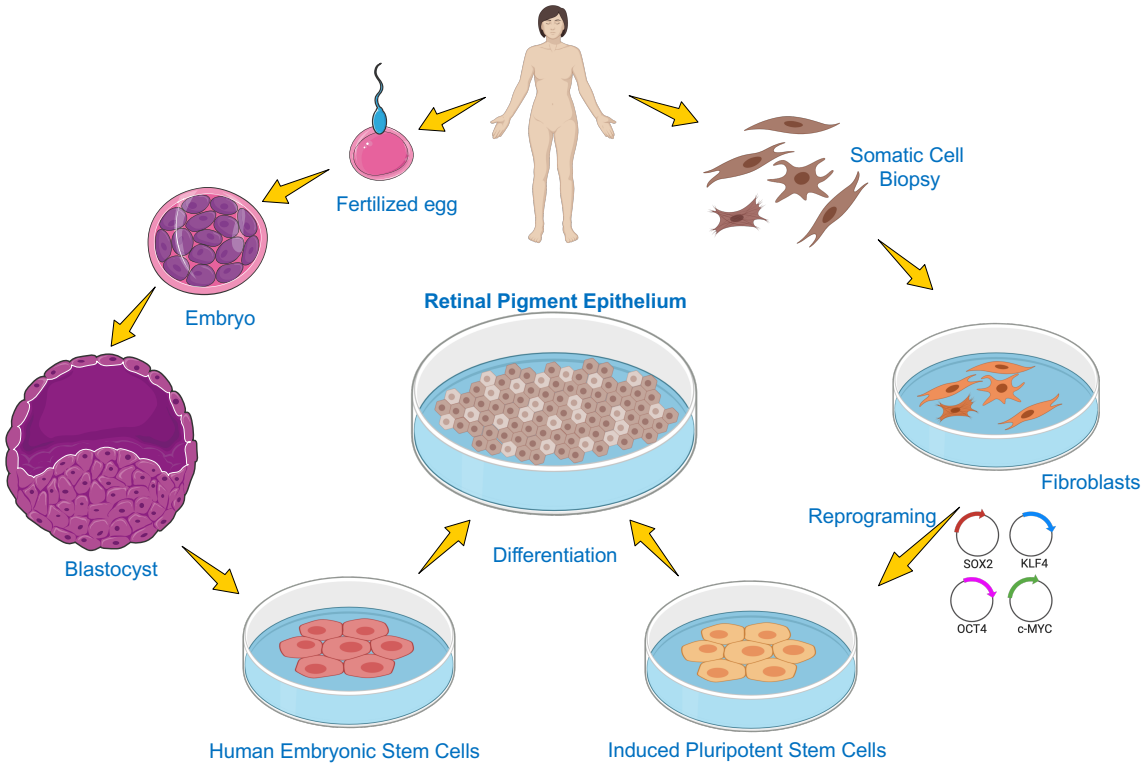

Figure 11. Human pluripotent stem cells as a source of RPE. Visual representing the derivation of human embryonic stem cells and the reprograming of human induced pluripotent stem cells, as well as their differentiation into retinal pigment epithelium with potential application in cell replacement therapies. Image was created with Biorender.com using objects from Servier Medical Art.

Aiming to find a better source of RPE cells for transplantation, some authors have recently begun to explore the possibility of generating RPE from human pluripotent stem cells (hPSC). Two types of hPSC are currently being used for differentiation into RPE: human embryonic stem cells (hESC), which are derived from the undifferentiated inner cell mass of human embryos, and induced pluripotent stem cells (hiPSC), which are derived from adult somatic cells via chemical or genetic reprogramming. Both cell types present an attractive source of replacement cells for RPE tissue engineering, as they are readily available in limitless supply and can be differentiated into any tissue in the body[137,138], which allows for the production of an unlimited number of healthy, young, and well-characterized clinical grade cells (Figure 11)[139].

1.2.5 Production of hPSC-RPE

Since the emergence of hESC cultures, many authors have described the differentiation of these cells into RPE. Many of these protocols rely on the spontaneous differentiation into RPE after the removal of basic fibroblast growth factor (bFGF) from the hPSC culture media[140–143]. Despite being simple and inexpensive, these protocols normally involve long differentiation processes and fail to render a homogeneous population of RPE cells, which is a critical aspect for their clinical application. For these reasons, many authors have proposed different strategies to increase the efficiency of the differentiations and the purity degree of the final cell product. These strategies include the use of several retinal-inducing factors and inhibitors to direct the

differentiation of hPSC solely towards RPE, as well as the use of biologically relevant culture substrates (Figure 12)[141,143–151].

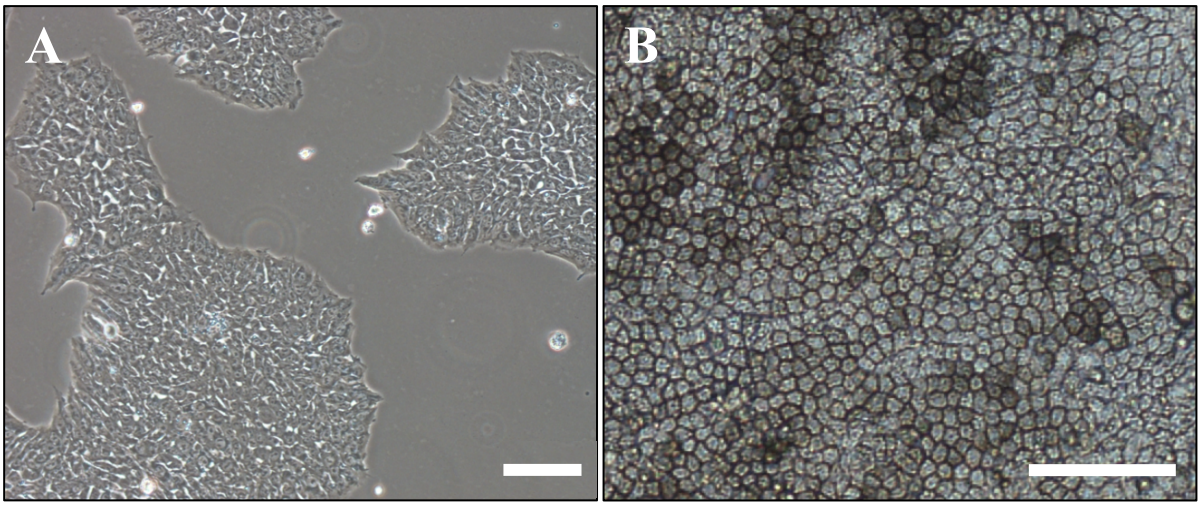

Figure 12. Differentiation of human embryonic stem cells into RPE. Representative phase contrast pictures of hESC (A) and hESC-RPE cells (B) both growing on human recombinant laminin 521. Scale bar = 100µm

In addition to their classification into spontaneous or directed protocols, differentiation protocols can also be subclassified into suspension and adherent protocols. Suspension protocols rely on the aggregation of hPSC into embryoid bodies (EBs), which are maintained in ultra-low attachment culture plates and, after some time in culture, typically display differentiated structures known as optic vesicles (OVs) that contain the RPE cells. Meanwhile, in adherent protocols, the differentiation process does not include an EB stage; instead, cells are maintained in 2D cultures until colonies of RPE cells begin to emerge. In both cases, the initial differentiated product is significantly heterogeneous and requires subsequent purification processes: manual dissection and enzymatic dissociation of OVs followed by replating and culturing of the obtained cells in 2D cultures after suspension protocols, or manual selection and dissociation of pigmented RPE colonies and their posterior expansion in culture after adherent protocols.

1.2.6 cGMP and Large-scale Manufacturing of hPSC-RPE

In light of the enormous potential that hPSC-RPE cells hold as a cell replacement treatment for AMD, efforts have recently been made toward the establishment of cleaner and defined differentiation protocols capable of rendering a more clinically compliant cell product. Examples include the establishment of xeno-free protocols, which could avoid the risk of rejection or microbial contamination upon transplantation created by the presence of non-human components in the final cell product (such as MEFs, animal-derived growth factors and matrices), and the use of chemically defined culture conditions, which eliminates the batch-to-batch variability associated with the use of serum, as well as the risk of having contaminants in the final product[147–150,152]. Furthermore, in order to meet the requirements demanded by the regulatory agencies to ensure patient safety, there is an increasing trend of establishing clinical good manufacturing practice (cGMP) routines for the production and quality control of the hPSC-RPE cells that are intended for transplantation (Figure 13).

In addition to the application of xeno-free and defined conditions, the potential clinical application of any cell-based product also requires its scalability. The identification of cell-specific surface markers can facilitate access to highly enriched populations of differentiated cell types derived from hESCs and hiPSCs, such as hPSC-RPE, and can enable greater control of the differentiation process, as previously demonstrated for other differentiated cell types[153–156]. Implementation of these surface markers in techniques such as FACS or MACS would facilitate the isolation of hPSC-RPE in an automated manner and support its large-scale manufacturing. Moreover, the application of these specific cell-surface markers as in-process quality-control assays could warrant the detailed and quantitative phenotypic evaluation of the cells and the generation of defined and safer cell products for transplantation.

To ensure the identity and functionality of hPSC-RPE cells, the final cell product obtained after differentiation must be characterized. The features of these cells that are normally investigated include: morphology (hexagonal shape and grade of pigmentation); expression of molecular markers, such as BEST1, MITF, RPE65, and CRALBP at the RNA and protein levels; polarized secretion of growth factors, typically PEDF and VEGF on the apical and basal sides, respectively; their ability to phagocyte photoreceptor outer segments, and their integrity as an epithelial barrier measured by transepithelial electric resistance (TEER). In addition, when considering the use of these cells in replacement therapies, their safety upon transplantation would also need to be analyzed. Safety tests include discarding the presence of other contaminant cells (e.g., undifferentiated cells) in the final product by flow-cytometry, immunostaining or qPCR analysis, as well as ensuring the stability of the cells through whole-genome sequencing, or tumorigenicity and biodistribution studies in animals. Finally, before their use in human patients, the function and efficacy of hPSC-RPE cells in rescuing retinal structure and visual function must be demonstrated in relevant animal models such as the Royal College of Surgeons (RCS) rat, which mimics photoreceptor degeneration associated with dry AMD, or in large-eyed animal models like pigs, rabbits, or primates, which resemble more faithfully the real scenario in terms of diagnostic and surgical procedures[157–162].

1.2.7 RPE Transplantation

Despite of the increasing number of studies that report the functionality of hPSC-RPE transplants in different animal models and the extensive efforts being made to generate these cells at the highest standards of purity and safety, the best method to deliver the cells into the subretinal space of patient eyes remains unclear (Figure 13). In cell replacement studies performed with animal models, RPE cells have traditionally been delivered to rats and mice via subretinal injections of cell suspensions in saline[142,144,163]. While many of these studies have reported partial restoration of visual function, in most, the histology demonstrated limited cell survival and an abnormal or poor integration of the cells in the subretinal space, with cells normally clustering together into a large clump rather than integrating into a monolayer between the photoreceptors and the choroid. Such weak results have led many authors to argue that delivering the cells in suspension is not the right approach and that giving the cells a supporting material will enhance not only cell survival, but also cell integration, as cells will

no longer have to rely on the native basement membrane, the Bruch's membrane, which may be damaged in the advanced stages of the disease[164–168]. The implantation of hPSC-RPE growing on bioscaffolds was foreseen by many as a better approach to cell suspension delivery, as the cells will exhibit improved stability and maintain cell polarization.

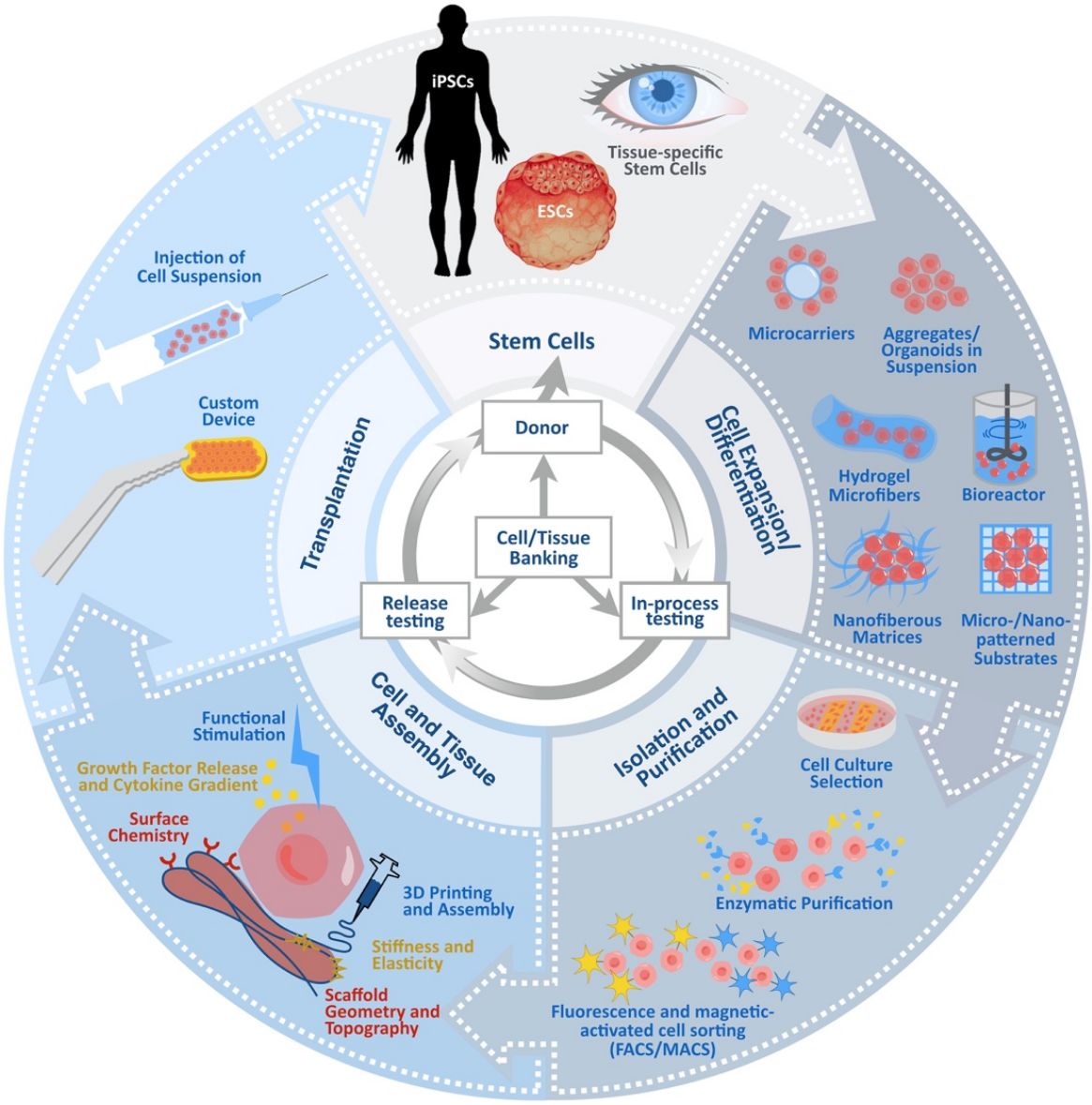

Figure 13. Cell and tissue engineering for the treatment of retinal diseases. Graphic representation of the key stages and main challenges surrounding the manufacturing and clinical translation of cell therapies. Image was adapted from ref.[169], with permission from Elsevier.

Although the theoretical approach seemed rational, the first studies in animal models demonstrated that this new approach created more complications than advantages. First, the transplantation of patches of cells implied a more severe surgery than the necessary for a subretinal injection. In addition, the lack of flexibility of the scaffolds made the subretinal delivery across the damaged retina difficult, often resulting in impairment of the retinal microstructure during transplantation, which negatively impacted the outcome of the procedure[164,166]. Finally, the restraints on the size of the cell patches made this approach a very limited solution for advanced stages of the disease where retinal damage is presumed to be extensive. In parallel to these discouraging experiments with 2D cell sheets, the first clinical

trial with hPSC-RPE cells delivered in cell suspension occurred in the US[170]. The results derived from this trial were very promising, in contrast to the previously noted studies in animals. The cells integrated and formed a monolayer of cells that survived for at least two years and partially improved visual function in patients with AMD[170,171].

In view of the promising results of the cell suspension approach reported in that first clinical trial, many authors attempted to further improve the methodology through the use of biodegradable hydrogels as an injectable scaffold to improve cell survival during the subretinal delivery. However, the first studies using hyaluronic acid-based gels for the delivery of hPSC-RPE cells reported failure in cell integration due to the relatively slow degradation of the scaffold (more than three weeks), which likely exceeded the migration time window of hPSC-RPE cells[172]. This limitation has fortunately been overcome through the use of hyaluronan-methylcellulose (HAMC) hydrogels, which degraded within one week after transplantation[173,174]. In addition to the use of biodegradable hydrogels, significant efforts have been exerted toward developing specialized devices for the delivery of hPSC-RPE on a scaffold that allows the insertion of larger patches while reducing the size of the retinotomy, which translates into a reduction of related surgical complications (Figure 13).

Given the advantages and disadvantages of both transplantation strategies described in these preliminary studies, it is still unclear which will prove to be the best in a clinical context. Only the result of the first pilot clinical trials for both transplantation strategies will provide insight to that question.

1.2.8 Clinical Trials using hPSC-RPE

hPSC-RPE transplantation holds immense potential as a replacement therapy not only for AMD, but also for other major ophthalmological conditions, such as Stargardt's disease, a less prevalent autosomal recessive form of macular degeneration that affects younger patients. The considerable progress made in establishing more efficient and safer hPSC-RPE differentiation protocols, together with the promising preclinical studies in animal models that have demonstrated the effectiveness of these cells in stopping retinal degeneration and rescuing vision, has prompted the emergence of several clinical trials around the globe aiming to bring this therapy closer to the bedside (Figure 14). The first early phase trial began in the US in 2012 (NCT01344993)[170,175,176], in which hPSC-RPE cell suspensions were injected into a small group of patients with the principal aim of demonstrating the safety of the cells and the delivery method. Similar studies were subsequently initiated in Japan[177], the UK (NCT01691261)[178], the US (NCT02590692)[179] and Israel (NCT02286089), where hPSC-RPE were transplanted into patients suffering from advanced forms of AMD. Although the finding of culture-acquired oncogenic mutations on the transplanted cells forced the termination of the Japanese clinical trial, this first attempt to use hiPSC in a clinical context served to increase awareness on the need to perform thorough safety testing of any hPSC-derived cell product, even when produced under a cGMP setting[180,181]. In addition to the safety of the final cell products, current concerns center around whether hPSC-RPE can achieve sufficient maturation levels upon transplantation or if they could remain stalled at an embryonic level, impeding their complete functional

performance[182]. Nevertheless, several studies on the transplantation of CNS derivatives suggest that delivering hPSC-RPE at an intermediate progenitor stage could be significantly more effective in engrafting and repairing than a terminally differentiated cell product, while also allowing for a reduction of manufacturing time and expenses[183].

While the eye has been historically considered to be immunoprivileged due to the presence of a blood-retina barrier and immunomodulatory cytokines, largely provided by the RPE, immunorejection can still occur[184,185]. Using autologous hPSC-RPE transplants will likely solve the problem; however, the impractically high manufacturing expenses necessary for the generation of a personalized cell product for each patient, limit their applicability[186]. For this reason, the majority of current strategies that seek to use hPSC-RPE as a therapeutic cell product still focus on the use of allogenic sources[175,176,178,179]. Ongoing clinical trials have demonstrated that limited immune suppression during the 3-12 months after transplantation is enough to avoid rejection of allogeneic donor cells, as it is thought that during this time, the blood-retina barrier can be reestablished and ocular immunoprivilege can be restored[169,185]. In the future, advancements in large-scale manufacturing of clinical-grade hPSC might hold the promise of individual-use hPSC-RPE from autologous hiPSC. Meanwhile, progress is also being made in the establishment of HLA-typed stem cell banks, both via banking hPSC covering the most-represented HLA subtypes in the population or by using genome editing strategies to create HLA-modified universal donor cells[187–190].

In short, hPSC-RPE replacement therapies offer great potential for decelerating the progression of macular dystrophies and protecting photoreceptors from further degeneration. However, photoreceptors are terminally differentiated neurons, and once lost, they cannot be regenerated. As such, several studies are exploring the possibility of transplanting cocultured hPSC-RPE and hPSC-derived photoreceptor explants, which may prove to be more effective in restoring retinal function, especially in more advanced stages of AMD and SD[191,192]. Still, several challenges must be overcome before this approach could be brought to the clinic, such as ensuring connectivity to the neuroretina and determining methods for enriching for cone photoreceptors to match the high concentration of cones present in the native macula.

Identifier	Title	Type	Conditions	Sponsors and Collaborators	Cell type
NCT02590692	Study of Subretinal Implantation of Human Embryonic Stem Cell-Derived RPE Cells in Advanced Dry AMD	Phase I/IIa	Dry Age Related Macular Degeneration, Geographic Atrophy	Regenerative Patch Technologies	hESC-RPE on a scaffold
NCT01691261	A Study Of Implantation Of Retinal Pigment Epithelium In Subjects With Acute Wet Age Related Macular Degeneration	Phase I	Age Related Macular Degeneration	•Moorfields Eye Hospital NHS Foundation Trust •University College, London •Pfizer	hESC-RPE on a scaffold
NCT01674829	A Phase I/IIa, Open-Label, Single-Center, Prospective Study to Determine the Safety and Tolerability of Sub-retinal Transplantation of Human Embryonic Stem Cell Derived Retinal Pigmented Epithelial(MA09-hRPE) Cells in Patients With Advanced Dry Age-related Macular Degeneration(AMD)	Phase I/IIa	Dry Age Related Macular Degeneration	CHABiotech	hESC-RPE in suspension
NCT01469832	Safety and Tolerability of Sub-retinal Transplantation of Human Embryonic Stem Cell Derived Retinal Pigmented Epithelial (hESC-RPE) Cells in Patients With Stargardt's Macular Dystrophy (SMD)	Phase I/II	Stargardt's Macular Dystrophy	Astellas Institute for Reg. Medicine	hESC-RPE in suspension
NCT01345006	Sub-retinal Transplantation of hESC Derived RPE(MA09- hRPE)Cells in Patients With Stargardt's Macular Dystrophy	Phase I/II	Stargardt's Macular Dystrophy	Astellas Institute for Reg. Medicine	hESC-RPE in suspension
NCT01344993	Safety and Tolerability of Sub-retinal Transplantation of hESC Derived RPE (MA09-hRPE) Cells in Patients With Advanced Dry Age Related Macular Degeneration	Phase I/II	Dry Age Related Macular Degeneration	Astellas Institute for Reg. Medicine	hESC-RPE in suspension
NCT02286089	Safety and Efficacy Study of OpRegen for Treatment of Advanced Dry-Form Age-Related Macular Degeneration	Phase I/IIa	Age Related Macular Degeneration	•Lineage Cell Therapeutics, Inc. •CellCure Neurosciences Ltd.	hESC-RPE in suspension

Figure 14. Clinical trials using hPSC-RPE. Table summarizing the clinical trials involving the use of hPSC-RPE for the treatment of common retinal diseases that are currently taking place. Table created with information from clinicaltrials.gov (updated in May 2020).

2 AIMS

The general aim of this thesis is to elucidate the genetic requirements for human trophoblast formation using human embryonic stem cells and to develop robust, scalable, and clinically compliant methodologies for the production of hESC-RPE that can be used in replacement therapies for patients suffering from non-exudative forms of AMD.

The specific aims of the three projects are as follows:

I. To examine to what degree the mechanisms regulating TE-ICM lineage segregation in mice are conserved in humans by studying the function of the Hippo signaling pathway during human trophoblast differentation

II. To establish a xeno-free, defined, and clinically compliant hESC-RPE differentiation protocol and to evaluate the in-vivo performance of these cells in a rabbit model of AMD

III. To identify and validate novel cell surface markers for hPSC-RPE and to develop more robust and scalable differentiation methodologies

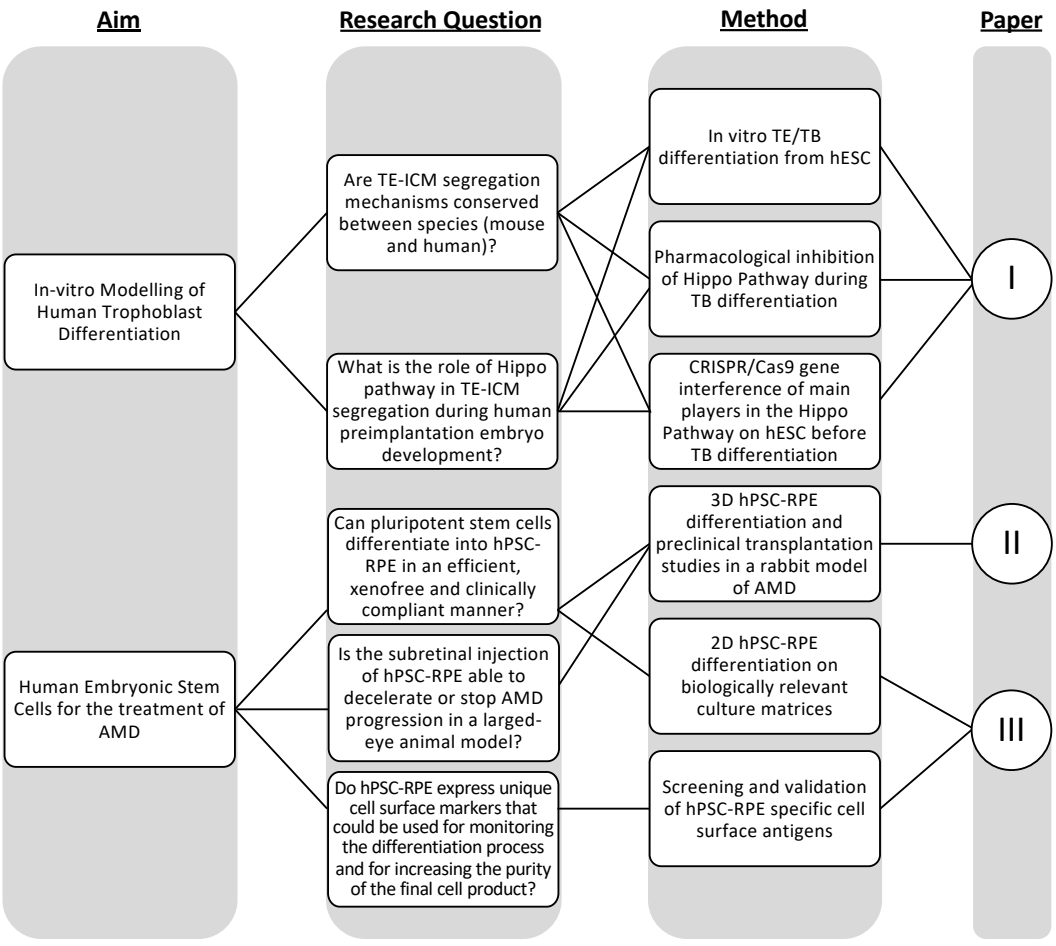

Figure 15.Thesis at a glance. Flowchart portraying an overview of the aims, research questions and methods covered by the present thesis work.

3 MATERIAL AND METHODS

3.1 ETHICS

3.1.1 Human Pluripotent Stem Cells

Human embryonic stem cell lines HS975, HS980 and HS983a were derived from supernumerary in-vitro fertilized human embryos that were kindly donated to us upon proper written consent from the donor couples and with approval from the Swedish Ethics Review Authority (Permit number: 2011/745:31/3).

Human induced pluripotent stem cell lines CTRL-7-II, CTRL-9-II, CTRL-12-I and CTRL-14-II were kindly provided by the Karolinska Institutet iPSC Core facility. Derivation and subsequent use of these cell lines was performed after adequate consent from donors and with approval from the Swedish Ethical Review Authority (Permit numbers: 2012/208-31/3 and 2010/1778-31/4).

3.1.2 Animals

For the studies included in the present thesis, a total of 27 female New Zealand albino rabbits were used. These animals were provided by Lidköpings rabbit farm (Lidköping, Sweden). All experiments were conducted after approval from the Northern Stockholm Animal Experimental Ethics Committee (Permit number: N25/14) and in accordance with the Statement for the Use of Animals in Ophthalmic and Vision Research.

3.2 CELL CULTURE

3.2.1 Human Pluripotent Stem Cells

Human embryonic stem cell lines HS975, HS980 and HS983a were derived and cultured in our laboratory as previously described, under xeno-free and defined conditions[193,194]. HS983a cell line was derived from a single blastomere biopsied from a supernumerary in-vitro fertilized 8-cell stage human embryo. The Wisconsin H9 (WA09) human embryonic stem cell (ESC) line was obtained from WiCell. For human pluripotent stem cell maintenance (hESC and hiPSC), cells were seeded onto plates previously coated overnight at 4°C with 10µg/mL hrLN521. Cells were kept at 5%CO_2/5%O_2 and fed daily with NutriStem hPSC XF media. Once they reached confluency, cells were enzymatically dissociated into single cells using TrypLE and passaged into new hrLN521 coated plates at a 1:10 ratio. When needed, cells were frozen using Stem Cell Banker freezing solution.

3.2.2 hPSC-RPE Differentiation

3.2.2.1 Paper II

Human embryonic stem cells were cultured until confluency on hrLN521 coated plates. At this stage, cells were washed and incubated at 37°C with DPBS (without Calcium and Magnesium) for 5 minutes. Then, using a pipette tip, the hESC monolayers were scraped and divided into

smaller clumps, these cell clumps were then transferred to ultra-low attachment plates containing 10μM Y-27632 in NutriStem hPSC XF media lacking bFGF and TGFβ (NutriStem -/-). From the day after plating until day 30, media was exchanged twice a week using fresh NutriStem -/- without Y-27632 and cultures were kept at 5%CO_2/21%O_2. During this time, cell clumps in the ultra-low attachment plates formed embryoid bodies that continue differentiating until they eventually produced optic vesicles (OV) containing hESC-RPE cells. These OVs were manually dissected using a scalpel and enzymatically dissociated into single cells using TrypLE followed by flushing through a 20G needle and syringe. The resultant cell suspension was then passed through a cell strainer (ø 40 μm) and plated onto tissue culture plates coated with 20μg/mL hrLN521 at a cell density of 0.6-1.2x10^4 cells/cm^2 and fed twice a week with NutriStem -/- medium for another 30 days until a homogenous pigmented hESC-RPE monolayer was obtained.

3.2.2.2 Paper III

hPSC (hESC or hiPSC) were plated at a cell density of 2.4x10^4 cells/cm^2 on tissue culture plates coated with 20μg/mL hrLN521 or hrLN111 and using NutriStem hPSC XF medium. 10μM Y-27632 was added during the first 24h, while cells were kept at 37°C, 5% CO_2/5% O_2. After 24h, medium was replaced with differentiation medium (NutriStem -/-) and cells were placed at 37°C, 5% CO_2/21%O_2. Cells were fed three times a week and kept for 30 days. From day 6 after plating until day 30, 100 ng/mL of Activin A (R&D Systems) was added to the media. Monolayers were then enzymatically dissociated into single cells using TrypLE Select. The resultant cell suspension was then passed through a cell strainer (ø 40 μm) and seeded on laminin coated dishes (hrLN521 at 20μg/mL) at different cell densities ranging from 1.4x10^6 to 1.4x10^4 cells/cm^2. Replated cells were fed three times a week with NutriStem hPSC XF medium without bFGF and TGFβ for another 30 days until a homogenous pigmented hESC-RPE monolayer was obtained.

3.2.3 In-vitro Trophoblast Differentiation

hESC growing on hrLN-521 and NutriStem hPSC XF were enzymatically dissociated into single cells and seeded onto new plates coated with 10μg/mL hrLN-521 at a cell density of 1,84x10^4 cells/cm^2. 24h after seeding, hESC were moved to a 5%CO_2/21%O_2 incubator and were differentiated into trophoblastic cells using NutriStem hPSC XF without bFGF and TGFβ that was supplemented with 10ng/mL BMP4, 1μM A83-01 and 0,1μM PD173074. The medium was changed every other day during the 9 days of culture.

3.2.4 Established Cell Lines

The human intestinal Caco-2 cell line was maintained on uncoated tissue culture plates with DMEM medium complemented with 4 mM glutamine, 100 u/mL penicillin, 100 u/mL streptomycin, 1% non-essential amino acids (NEEA), 10% heat inactivated FCS and sodium pyruvate at 37°C in 5%CO_2/21%O_2. For cell line maintenance, cells were kept in culture until they reached 50% confluency and were then enzymatically dissociated and seeded into new tissue culture plates at a cell density of 4.5x10^3 cells/cm^2. Medium was changed every two

days. For the verteporfin treatment experiments, cells were seeded on new tissue culture plates at a density of $3x10^5$ cell/cm^2 and maintained for 21 days in the above-mentioned medium; the medium was changed three times a week. At day 21, mature Caco-2 cells were then treated with different concentrations of verteporfin.

3.3 CRISPR/CAS9 GENOME EDITING

CRISPR/Cas9 genome editing system was used to knock out gene function of several genes related to the Hippo signaling pathway in Paper I.

Between 3 and 9 sgRNAs were designed for each target gene. Design and selection of the top candidates sgRNAs for each target was done using CRISPR-ERA (Xiaowo Wang lab, Tsinghua University) and E-CRISP (Boutros lab, German Cancer Research Center) online design tools.

For plasmid-based CRISPR/Cas9 delivery, the sgRNA target sequence was then cloned into a modified version of the bicistronic vector PX459 (Addgene #63988), where we had exchanged the CMV promoter for an EF1a promoter, which gave better results in hESC. For RNP-based CRISPR/cas9 delivery, chemically modified synthetic sgRNA containing the desired target sequences were ordered and right before transfection they were complexed with Cas9 protein through a 10 minutes incubation a room temperature.

Plasmids or RNP complexes containing the different sgRNAs for each target where then individually transfected in hESC using a Neon electroporation system (ThermoFisher Scientific). Following transfection with PX459 plasmids, the hESC cells were allowed to recover for 24h and then were subjected to antibiotic selection by treating them with 500ng/mL Puromycin for 48h. After antibiotic selection, transfected cells were grown until confluency and performance of the different sgRNAs was then assessed by targeted Sanger Sequencing of the target region, using TIDE or ICE sequence trace decomposition tools.

3.4 CLONAL ISOLATION OF KNOCK-OUT HESC LINES

For clonal isolation of CRISPR/Cas9-KO hESC lines, bulk transfected hESC cultures were enzymatically dissociated and suspended into limiting dilutions containing 20 cells/mL and 10μM Rock Inhibitor (Y-27632, Millipore). 100μL of these limiting dilutions were then plated per well into 96-well plates previously coated with 15μg/mL hrLN-521 and 1,7μg/mL E-cadherin. Individual cells were then allowed to grow until they formed confluent clonal colonies, which were then passaged and genotyped. Those clonal lines containing homozygous CRISPR/Cas9 frame-shift mutations were then analyzed for absence of the desired protein by Western Blot and/or immunofluorescence staining.

3.5 CELL COUNTS AND CELL SIZE MEASUREMENTS

In order to estimate cell survival and cell proliferation during BAP-TB differentiations in Paper I, cell density counts were performed at day 2, day 5 and day 9 of the differentiation using a Moxi Z Automated Cell Counter.

Cell size comparison between WT and CRISPR-KO hESC was achieved by measuring average cell diameter using a Moxi Z Automated Cell Counter of 70% confluent hESC cultures.

3.6 QUANTITATIVE PCR

For gene expression analysis, cells cultures were collected in RLT cell lysis buffer. Total RNA was isolated using the RNeasy Plus Mini Kit and treated with RNase-free. cDNA was synthesized using Superscript III reverse transcriptase, according to the manufacturer's instructions. Samples were subjected to real-time PCR amplification protocol using Taq-polymerase and specific Taqman probes for the genes of interest, on a StepOne™ real-time PCR System. Three independent experiments were performed for every condition and technical duplicates were carried for each reaction. Gene expression results are presented normalized to GAPDH expression and relative to a reference sample (ΔΔCt).

3.7 FLOW CYTOMETRY ANALYSIS

For extracellular protein detection by flow cytometry analysis, cells were enzymatically collected, incubated for 30min with conjugated antibodies for 30min, followed by washes and finally resuspended on FACS buffer (2%FBS, 1mM EDTA in DPBS) containing 7AAD or DRAQ7 live/dead stains.

For intracellular protein detection by flow cytometry analysis, cells were enzymatically collected, incubated for 30min with Violet Live/Dead fixable stain and fixed with BD Cytofix/Cytoperm™ kit. After fixation and permeabilization, cells were stained with a conjugated antibody for 30min or a primary antibody for 30min on ice, followed by washes and staining with secondary antibody for another 30min on ice. Finally, cells were resuspended on FACS buffer (2%FBS, 1mM EDTA in DPBS).

Fluorescence minus one (FMO) controls were included for each condition to identify and gate negative and positive cells. Stained cells were analyzed on a LSRFortessa equipped with 405 nm, 640 nm, 488 nm, 355 nm and 561 nm lasers or a CytoFLEX equipped with 405 nm, 638 nm, 488 nm and 561 nm lasers cell analyzers. Analysis of the data was carried out using FlowJo v.10 software.

3.8 FLUORESCENCE ACTIVATED CELL SORTING (FACS)

For cell sorting based on extracellular protein expression, cells were incubated with conjugated antibodies on ice for 30 min followed by washes and finally resuspended on FACS buffer (2% FBS, 1mM EDTA in DPBS) containing 7AAD or DRAQ7 live/dead stains. Fluorescence minus one (FMO) controls were included for each condition to identify and gate negative and positive cells. Stained cells were then sorted using a BD FACS Aria Fusion Cell Sorter (BD Biosciences) using FACSDiva Sofware v8.0.1. Sorted cells were collected on 15mL conical tubes containing cell culture medium with Penicillin/Streptomycin.

3.9 CYTOSPIN

For protein detection on cell suspensions after cell sorting, cells were resuspended to a concentration of $7x10^5$ cells/mL in FACS buffer (2% FBS, 1mM EDTA in DPBS). 100 µl of the cell suspensions were then loaded into the cytospin cuvettes and centrifuged for 5 minutes at 400 rpm onto glass slides. Slides were left to dry overnight at room temperature followed by fixation with 4% methanol-free formaldehyde at room temperature for 10 min and immunofluorescence staining.

3.10 WESTERN BLOT

Confluent cells cultures were collected after a brief 37°C incubation with Dulbecco's phosphate buffered saline buffer (DPBS). Whole cell extracts were lysed in RIPA buffer (Sigma-Aldrich), then fractionated by SDS-PAGE and transferred to a Nitrocellulose or polyvinylidene difluoride membrane using a Mini Trans-Blot® Cell apparatus, according to the manufacturer's protocol. After blocking with 5% nonfat milk in TBST (10 mM Tris, pH 8.0, 150 mM NaCl, 0.5% Tween 20) for 60 min, the membrane was washed once with TBST and incubated with primary antibodies. Membranes were washed three times for 10 min with TBST and incubated with Alexa Fluor 680 conjugated secondary antibodies for 1h. Blots were washed with TBST three times and imaged with an Oddysey NIR Western Imager system and images were analyzed on ImageJ software. Vinculin detection was used as a protein loading control.

3.11 IMMUNOFLUORESCENCE

Cell cultures and cytospin preparations were washed with DPBS and fixed with 4% methanol-free formaldehyde at room temperature for 10 minutes. After fixation, samples were permeabilized using 0.3% TritonX-100 in DPBS for another 10 minutes at room temperature, followed by a blocking step with 0.1% Tween 20 and 4% FBS in DPBS (Blocking Solution) for 1 hour at room temperature. Subsequently, samples were incubated overnight at 4°C with primary antibodies diluted in Blocking Solution. The following day, samples were washed 3 times for 5 minutes with Blocking Solution and incubated for 2 hours at room temperature with Alexa Fluor conjugated secondary antibodies diluted in Blocking Solution. Hoechst 33342 and sometimes rhodamine phalloidin were added to the secondary antibody mix for staining of nuclei and actin cytoskeleton, respectively. Finally, samples were washed 3 times for 5 minutes with Blocking Solution and imaged using an epifluorescence, laser scanning confocal or spinning disk confocal microscope, depending on the experimental requirements.

3.12 TIME-LAPSE MICROSCOPY

For the experiments part of Paper II, where we studied the behavior of hESC-RPE on the different substrates, cell migration and expansion was monitored using the Cell-IQ live imaging system (Chip-Man Technologies Ltd.), equipped with an automated stage, an integrated incubator (37°C, 5% CO_2) and a 10x phase contrast objective.

After OVs dissociation, hESC-RPE were seeded in triplicates on the different substrates tested in a 24-well plate format and kept with NutriStem -/- at 37°C in 5%CO_2/21%O_2 to allow their attachment to the substrate before initiating the imaging. The day after, plates were transferred to the time lapse imaging unit. For each well, images from several positions were acquired every hour over a total of 21 days.

Cell migration was assessed for each condition using NIS-Elements v.4.0 (Nikon). For each set of images 10 cells were randomly chosen and their position was manually tracked during the first 7 days of imaging. The length and path of the trajectories followed by the different cells was used to compare the migration potentials of hESC-RPE among the different substrates.

3.13 ENZYME-LINKED IMMUNOSORBENT ASSAY (ELISA)

In order to measure basal secretion of VEGF and apical secretion of PEDF by hPSC-RPE (Paper II and Paper III). Day 30 differentiations were seeded in triplicates on Transwell membranes (0.33 cm^2 pore size) that were previously coated with 20µg/mL hrLN521. Cells were grown on the transwells for at least 30 more days, changing media from both apical and basal compartments 3 times per week. On the day of the experiment, supernatants that have been for at least 48h in contact with the cells were collected. PEDF and VEGF secretion levels were measured in both apical and basal compartments for each condition and replicate using commercially available human PEDF and VEGF ELISA Kits (RD191114200R from BioVendor, and DVE00 from R&D Systems, respectively). The OD450 values were measured using SpectraMax 250 Microplate Reader and used for calculating protein concentrations in relation to a standard curve.

3.14 PHAGOCYTOSIS ASSAY

This assay is intended to assess the in-vitro functionality of hPSC-RPE by measuring the capacity of the cells to phagocyte photoreceptor outer segments (POS).

Day 30 hPSC-RPE were dissociated and seeded in triplicates onto Transwell membranes (0.33 cm^2 pore size) that were previously coated with 20µg/mL hrLN521. Cells were grown on the transwells for 30 more days, changing media from both apical and basal compartments 3 times per week. At day 60 of differentiation, cells were incubated at 37°C or 4°C overnight with $2.42x10^6$ FITC-labelled POS per Transwell diluted in DMEM or CO_2-independent media, respectively. Undifferentiated hESC treated in the same manner were used as a negative control. The day after, cultures were incubated with a solution containing 0.2% Trypan Blue for 10 minutes at room temperature in order to quench the fluorescence signal coming from the non-phagocyted POS. After that, cells were washed with DPBS and fixed with 4% methanol-free formaldehyde at room temperature for 10 minutes. Following fixation, samples were permeabilized using 0.3% TritonX-100 in DPBS for another 10 minutes at room temperature, before a final 20 minutes room temperature incubation with Hoechst 33342 and Rhodamine Phalloidin, used to visualize nuclei and cell boundaries, respectively.

Images were acquired with Zeiss LSM710-NLO point scanning confocal microscope and image analysis was performed using IMARIS (Bitplane). Automated quantification of total number of engulfed FITC-POS per condition was completed using CellProfiler software.

3.15 TRANSEPITHELIAL ELECTRICAL RESISTANCE (TEER)

Day 30 hPSC-RPE were dissociated and seeded in triplicates onto Transwell membranes (0.33 cm^2 pore size) that were previously coated with 20µg/mL hrLN521. Cells were grown on the transwells for 30 more days, changing media from both apical and basal compartments 3 times per week. At day 60 of differentiation, cultures were equilibrated outside the incubator at room temperature for at least 20 min before the experiment. Electrical resistance was measured using the Millicell Electrical Resistance System volt-ohm meter at three different positions on each well. Background electrical resistance measured in a well with no cells growing was subtracted from each measurement of the experimental wells. Measurements are reported as resistance in ohms times the area in square centimeters ($\Omega*cm^2$).

3.16 SCANNING ELECTRON MICROSCOPY (SEM)

hESC and day 60 hPSC-RPE cultures growing on transwell (as described above) were fixed by immersion in 2.5% glutaraldehyde in 0.1M phosphate buffer, pH7.4. The transwell membrane containing the cells was cut out and rinsed in dH_20 prior to stepwise ethanol dehydration and critical-point-drying using carbon dioxide. Inserts were mounted on specimen stubs using carbon adhesive tabs and sputter coated with a thin layer of platinum. SEM images were acquired using an Ultra 55 field emission scanning electron microscope (Zeiss, Oberkochen, Germany) at 3 kV and the SE2 detector.

3.17 TRANSMISSION ELECTRON MICROSCOPY (TEM)

hESC and day 60 hPSC-RPE cultures growing on transwell (as described above) were fixed by immersion in 2.5% glutaraldehyde in 0.1M phosphate buffer, pH7.4. The transwell membranes were ten cut out and into strips, rinsed in 0.1M phosphate buffer followed by a postfixation in 2% osmium tetroxide in 0.1M phosphate buffer, pH7.4 at 4°C for 2 hours. Following postfixation, membrane strips were dehydrated through stepwise ethanol exposure and finally flat embedded in LX-112. 50–60 nm sections were prepared using a Leica EM UC7 and contrasted with uranyl acetate followed by lead citrate. TEM imaging was performed on a Hitachi HT7700 transmission electron microscope (Hitachi High-Technologies) operated at 80 kV and using CCD camera.

3.18 HISTOLOGY

In Papers II and III characterization of transplanted hPSC-RPE in rabbit eyes as well as presence or absence of protein markers in rabbit and adult human retinas was assessed by histology and posterior immunohistochemistry and tissue immunofluorescence staining.

After euthanasia, rabbit eyes that were injected with hPSC-RPE or DPBS only were enucleated and fixed through intravitreal injection of 4% formaldehyde solution and posterior 24-48 hours incubation at 4°C. After that, eyes were embedded in paraffin and the injected retinal area was sectioned with a thickness of 4μm. Every fourth section of these retinas was stained with hematoxylin-eosin (HE).

3.19 IMMUNOHYSTOCHEMISTRY (IHC)

Cross sections of paraffin embedded tissue were deparaffinized in xylene and rehydrated by ethanol series followed by antigen retrieval through incubation in sodium citrate buffer (pH 6) at 96°C, followed by peroxidase and serum blocking. For immunohistochemistry, staining was performed in an automated manner in a Leica Biosystems Automated IHC stainer. For immunofluorescence staining, primary antibodies diluted in blocking buffer, were incubated overnight at 4°C, followed by washes and posterior incubation with Alexa Fluor conjugated secondary antibodies for 1 hour at room temperature. Finally, sections were mounted using mounting medium with DAPI under a 24x50 mm coverslip.

Images were acquired using an Olympus IX81 epifluorescence microscope or Zeiss LSM710-NLO point scanning confocal microscope. Image analysis was carried on with the help of ImageJ software.

3.20 SINGLE-CELL RNA SEQUENCING (SCRNA-SEQ)

In paper III, presence of potentially contaminating cells was analyzed through scRNA-Seq of day 60 hPSC-RPE 30 days after either replating or cell enrichment. Cell cultures were enzymatically dissociated into single cell suspensions using TrypLE and diluted to a concentration of $1x10^6$ cells/mL. Cell suspensions were then used to create 3' cDNA library for single cell RNA sequencing with the 10X Genomics platform available at the Eukaryotic Single Cell Genomics Facility in SciLife Lab, Stockholm.

Cell Ranger 2.1.1 pipeline was used to convert Illumina base call files to fastq format and STAR aligner was used to align sequencing reads to the hg19 transcriptome and generate feature-barcode matrices. Cell Ranger quality-control filtered cells were analyzed using Seurat suite version 2.3. Only hPSC-RPE cells with uniquely expressed genes ($\geq$ 2,000 to $\leq$ 5,000), UMIs ($\geq$ 10,000 to $\leq$ 30,000) and percentage of UMIs mapping to MT-genes ($\geq$ 0.025 to $\leq$ 0.10) were selected. Similarly, hESC cells with uniquely expressed genes ($\geq$ 2,000 to $\leq$ 8,000), UMIs ($\geq$ 10,000 to $\leq$ 80,000) and percentage of UMIs mapping to MT-genes ($\geq$ 0.025 to $\leq$ 0.10). Cell-cell variation in gene expression driven by UMIs, mitochondrial gene expression and cell-cycle stages were regressed out during data scaling process, followed by dimensionality reduction by principal-component analysis (PCA). For principal component (PC) selection, findings of PCHeatmap, jackStraw, PC standard deviations and Clustree analysis were assessed.

3.21 SUBRETINAL INJECTIONS IN THE RABBIT EYE

hPSC-RPE monolayers were washed with DPBS and enzymatically dissociated into a single cell suspension using TrypLE. Cell were counted on a hemocytometer using 0.4% trypan blue and aliquoted into 600µL units with a final concentration of $1x10^6$ cells/mL that were kept on ice until transplantation.

A day prior to the surgery, 2 mg (100µL) of intravitreal triamcinolone (Triescence 40 mg/mL) were administered to the rabbits (New Zealand Albino Rabbits). On the day of the surgical intervention, animals were anesthetized by intramuscular administration of 35 mg/kg ketamine and 5 mg/kg xylazine, the pupils were then dilated using a mix of 0.75% cyclopentolate and 2.5% phenylephrine. Microsurgeries were performed on both eyes using 3-port 25G transvitreal pars plana technique. The cell suspension was drawn into a 1 mL syringe connected to an extension tube and a 38G PolyTip cannula. Without infusion or prior vitrectomy, the cannula was inserted through the upper temporal trocar. After proper tip positioning, ascertained by a focal whitening of the retina, 50 µL of cell suspension (equivalent to 50.000 cells) were subretinally injected approximately 6 mm below the inferior margin of the optic nerve head, forming a clearly distinguishable and uniform bleb.

3.22 RETINAL IMAGING

In order to assess the integration of transplanted hPSC-RPE in the rabbit eyes in Paper II and Paper III, we used a combination of non-invasive ophthalmological techniques such as optical coherent tomography (OCT), infrared-confocal scanning laser ophthalmoscopy (IR-cSLO) and blue fundus autofluorescence (BAF).

Anesthetized rabbits were placed in an adjustable mount. A Spectralis HRA + OCT device was used to obtain at least 3 cross- sectional OCT scans were with concurrent IR-cSLO reflectance reference images representing the upper, central and lower portion of the transplanted area. Finally, equivalent BAF images were acquired using the Spectralis blue light-laser with an excitation wavelength of 488 nm and a barrier filter of 500 nm.

3.23 STATISTICS

In Paper I, unpaired 2-tailed Student's t-tests were performed to assess the effects the different knockouts on pluripotency gene expression. Same type of statistical tests was used to estimate the effect on cell density and on the proportion of cCaspase3 positive cells after treatment with LPA.

In Paper II, unpaired 2-tailed Student's t-test was performed comparing the relative outer retinal thickness between eyes with integrated and with non-integrated hESC-RPE after subretinal transplantation.

For the statistical analysis present in Paper III, two-way ANOVA and posthoc multiple comparisons using Tukey test correction were executed to assess the significance of changes

in gene expression and functionality performance of the different replating densities tested, as well as sorting versus replating experiments.

All quantifications were performed unblinded. In every case, statistical analysis was carried out on data from at least three independent experimental replicates. Comparisons between groups were planned before statistical testing and target effect sizes were not predetermined. Statistical analysis was carried out using Prism 7 software.

4 RESULTS AND DISCUSSION

4.1 ROLE OF HIPPO SIGNALING PATHWAY IN HUMAN TROPHOBLAST DIFFERENTIATION (PAPER I)

Hippo signaling plays an essential role in trophectoderm specification in mice. Inactivation of this pathway exclusively in the outer cells of the preimplantation embryo allows for the transcription of trophectoderm-specific genes through the activity of TEAD4 and its coactivator molecules, YAP1 and WWTR1. However, it remains unclear whether the same mechanisms govern trophectoderm establishment in humans. In an attempt to understand if the function of Hippo signaling is conserved in humans, we functionally examine the role of different downstream components of this pathway during in-vitro human trophoblast formation.

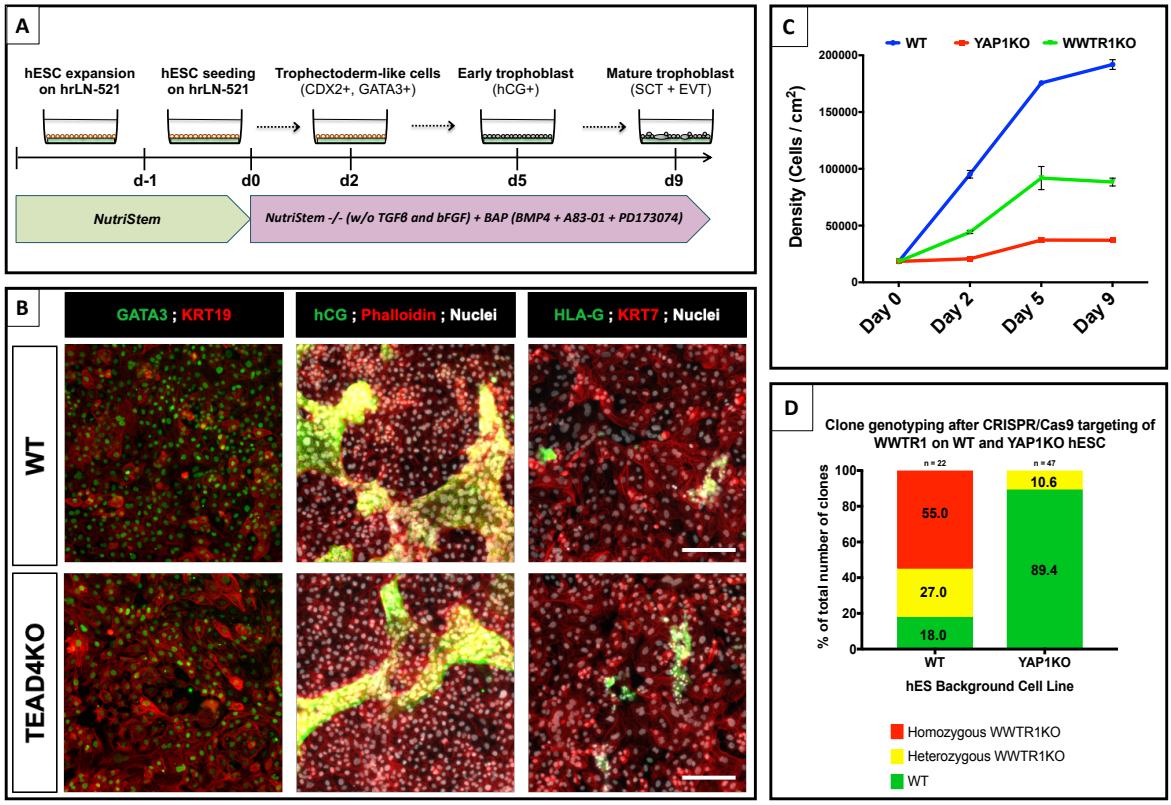

Figure 16. Role of Hippo Signaling Pathway in Human Trophoblast Differentiation. Summary of the main results presented in Paper I. (A) BAP-TB differentiation protocol scheme. (B) Immunofluorescence images confirming the presence of several TB markers (GATA3, KRT7, KRT19, hCG and HLA-G) at day 9 of BAP-TB differentiation in WT and TEAD4KO cells. (C) Graph displaying differences in cell density at day 0, day 2, day 5 and day 9 of BAP-TB differentiation in WT, YAP1KO and WWTR1KO cells. Each data point represents mean ± SEM from three independent experiments. (D) Bar graphs displaying the proportion of wild-type, heterozygous and homozygous clones obtained after targeting YAP1 or WWTR1 on WT hESC and WWTR1KO or YAP1KO hESC, respectively. Scale bars = 100 µm.

Study design

This study employed a combination of pharmacological and genetic targeting to examine the function of the Hippo pathway in human cells. Clonal knockout hESC lines were established for different effectors downstream from the Hippo pathway and were then subjected to in-vitro trophoblast differentiation (Figure 16A). We assessed the effect of ablation of the different

molecular players based on the outcome on cell survival and the impact on trophoblast marker expression, both at the transcriptional and protein levels.

Pharmacological inhibition of Hippo signaling impairs trophoblast differentiation and hESC survival

Previous studies have demonstrated that pharmacological inhibition of Hippo signaling using Verteporfin (VP), a drug that impedes YAP1-TEAD interaction, impairs trophectoderm formation during blastocyst formation in mice[195,196]. As the first 48h hours of our in-vitro trophoblast differentiation model recapitulates trophectoderm formation, we decided to treat these cultures with VP. We observed that pharmacological treatment induced extensive cell death not only on the in-vitro trophoblast, but also on hESC that were treated in parallel as a control, suggesting that YAP1-TEAD function was equally important for trophectoderm establishment and hESC maintenance. Because high concentrations of VP have been found to be toxic and in order to ensure that any effect derived from these treatments was due to the inhibition of YAP1-TEAD interaction and not to toxicity, we decided to test different concentrations of the drug in hESC and mature CaCo2 cells, which do not express YAP1. We found that the range of VP concentrations used in our previous experiment did not have a toxic effect on CaCo2 cells, indicating that the effect we observed on hESC and in-vitro trophoblast cultures was a consequence of the loss of YAP1-TEAD activity.

TEAD4 function is not essential for human trophoblast formation

Previous studies in mice have identified TEAD4 as an essential transcription factor for trophectoderm establishment. Based on these reports and our previous results, we sought to test if loss of function of TEAD4 could be responsible for the phenotypes we observed upon VP treatment. To do so, we established clonal TEAD4-knockout hESC lines using CRISPR/Cas9-mediated gene disruption. Immunostaining and transcriptional analysis by qPCR revealed preserved pluripotency marker expression and the absence of TEAD4 protein on TEAD4-KO hESC. We then exposed these cells to in-vitro trophoblast differentiation and found them to display comparable competence to differentiate as WT hESC, as assessed by morphology and phenotypic characterization using flow-cytometry, immunostaining, and qPCR (Figure 16B). Therefore, these results suggest that TEAD4 does not serve an indispensable function in trophectoderm and trophoblast differentiation.

YAP1 displays a leading role in trophoblast differentiation

Intrigued by the lack of effect observed on trophoblast differentiation after disruption of TEAD4 expression, we decided to examine the gene function of its coactivator molecules, YAP1 and WWTR1. Clonal YAP1-KO and WWTR1-KO hESC lines created following the same approach as previously described displayed no alterations of their pluripotent potential. However, when these lines were differentiated towards trophoblast, they exhibited a significant amount of cell death around the second day of differentiation, which was especially prominent on YAP1-KO hESC (Figure 16C). Despite the observed effect on cell survival, the few

remaining YAP1-KO and WWTR1-KO cells managed to resume differentiation and by day nine, demonstrated expression of typical markers of mature trophoblast, such as KRT7, KRT19, hCG, and HLA-G. These findings indicate that YAP1 and WWTR1 may have a function in trophectoderm formation, but not in its posterior maintenance and maturation towards trophoblast. Furthermore, treatment with LPA, a chemical inhibitor of LATS1/2 kinases, managed to rescue the phenotype in YAP1-KO, which then increased their survival to similar levels as observed in WT cells, indicating that YAP1 and WWTR1 can compensate one another. Despite the high editing efficiencies of our CRISPR/Cas9 sgRNA targeting YAP1 and WWTR1, all of our attempts to establish double-knockout YAP1/WWTR1-KO hESC clonal lines failed. None of the 79 clones generated in three separated events proved to be double-knockout, highlighting the presumptive role of YAP1/WWTR1 in hESC maintenance that was suggested by our VP experiments (Figure 16D).

YAP1/WWTR1 role in TE differentiation is mediated by the joint activities of TEAD proteins

Given these results, we sought to determine if the function of YAP1/WWTR1 in trophectoderm differentiation is mediated through their interaction with TEAD proteins or if their role can be explained by their interaction with other transcription factors. Although TEAD family members (TEAD1, TEAD2, TEAD3 and TEAD4) have historically been considered to play distinct roles during development, the fact that they exhibit a high amino acid identity (~70%) lead us to hypothesize that they could have homologous functions, which would explain why the loss of TEAD4 alone would not have a phenotypic effect on trophoblast differentiation. To test our hypothesis, we established single-knockout hESC lines, for which we ablated TEAD1 and TEAD2 separately, and a triple-knockout hESC line, for which we simultaneously disrupted TEAD1, TEAD2 and TEAD4, because these three TEADs are the only ones described to be present during early human embryo development. We found that, while TEAD1-KO and TEAD2-KO hESC lines exhibited unaltered pluripotency and trophoblast differentiation capacity, TEAD1/2/4-KO hESC exhibited reduced NANOG expression, which correlated with their ease of spontaneous differentiation in culture, and a high rate of cell death during the first two days of trophoblast differentiation, similar to the observations of YAP1-KO and WWTR1-KO lines. These findings suggest that the different TEADs can have interchangeable functions; therefore, as they can compensate one another, only the combined inactivation can cause a negative effect on trophoblast formation. Finally, these results also indicate that YAP1/WWTR1 regulate trophoblast differentiation through interaction with TEAD proteins and not any other alternative downstream target factors.

Discussion

In this study, we utilized hESC as a platform to study the function of the Hippo signaling pathway during trophoblast differentiation. Combining pharmacological and genetic targeting, we found that YAP1/WWTR1/TEAD downstream effectors of the Hippo pathway play an essential role in the establishment of human trophectoderm. Moreover, we observed that the function of YAP1/WWTR1 was also necessary for hESC maintenance, as simultaneous

disruption of these two coactivators resulted in hESC cell death. Finally, we found that members of the TEAD family perform homologous activities and that TEADs can functionally compensate for the loss of function of one of the members. This finding contradicts previous studies conducted in mice, in which the ablation of TEAD4 alone impeded trophectoderm formation.

Based on these results, we suggest that the function of Hippo signaling function in trophectoderm establishment may be conserved between mice and humans. Therefore, we propose that the mouse can still serve as a relevant model in the study of human early embryogenesis, as it demonstrates to recapitulate some of the key aspects related to the establishment of the TE. Moreover, we demonstrated the feasibility of in-vitro trophoblast differentiation models for the study of gene function. However, it is important to take into account that these types of models do not represent exact physiological conditions, as they fail to recreate important aspects such as intercellular signaling between the different compartments of the developing embryo (EPI, PE and TE). In line with previous studies, we demonstrated that the use of pharmacological inhibitors, such as verteporfin and LPA, can be very useful in the interrogation of the Hippo signaling pathway. Nevertheless, to exclude any potential confounding toxic or unspecific effects derived from the use of these inhibitors, it is always important to validate the obtained results using alternative approaches, such as the direct gene disruption by CRISPR/Cas9 genome editing. CRISPR/Cas9 genome editing also enables the examination of individual gene function, which is helpful in identifying the main effectors in a signaling pathway.

Increasing our knowledge around the processes involved in successful trophoblast differentiation will improve our understanding of the origin and prevention of common fertility and placental disorders, such as recurrent miscarriages or preeclampsia. At the same time, gaining insights into the molecular mechanisms that regulate the exiting and maintenance of pluripotency will likely translate into improved culture conditions that will yield better and more efficient stem cells for use in basic research and regenerative medicine.

4.2 XENO-FREE AND DEFINED HUMAN EMBRYONIC STEM CELL-DERIVED RETINAL PIGMENT EPITHELIAL CELLS FUNCTIONALLY INTEGRATE IN A LARGE-EYED PRECLINICAL MODEL (PAPER II)

Cell replacement using hESC-derived retinal pigment epithelium (hESC-RPE) is regarded as one of the most promising strategies in the treatment of retinal degenerative diseases such as age-related macular degeneration (AMD) and Stargardt´s disease (SD). Recent advancements in hESC derivation and maintenance have enabled the emergence of several strategies for the production of hESC-RPE. However, most of these methods still rely on the use of culture conditions that involve animal-derived components or the use of medium formulations that are either undefined or not xeno-free. In the present study, we describe a novel hESC-RPE differentiation protocol that relies on the spontaneous differentiation of the RPE in 3D cultures, using xeno-free and defined culture conditions. In addition, we validate the functional

integration of these cells upon subretinal transplantation into a large-eyed animal model and demonstrate their capacity for rescuing the retina from degeneration.

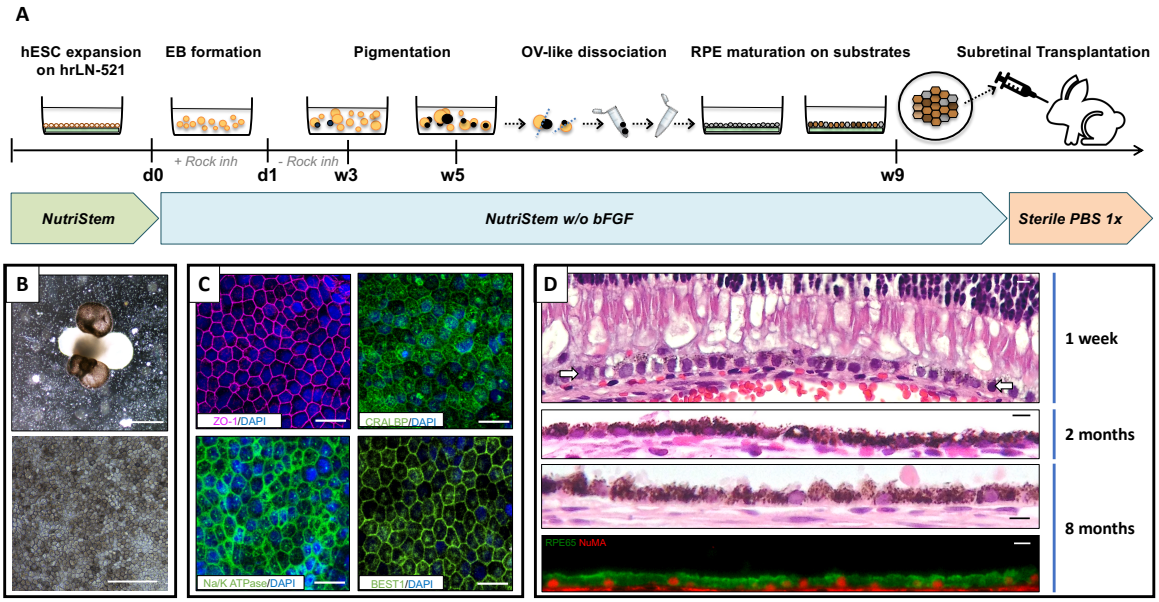

Figure 17. Xeno-Free and Defined Human Embryonic Stem Cell-Derived Retinal Pigment Epithelial Cells Functionally Integrate in a Large-Eyed Preclinical Model. Summary of the main results presented in Paper II. (A) 3D-based differentiation protocol scheme followed for the derivation of hESC-RPE. (B) Representative bright field images of an embryoid body containing optic vesicles (top) and mature hESC-RPE growing on hrLN-521 at the end of the differentiation protocol (bottom). (C) Immunofluorescence images demonstrating the presence of specific markers (ZO-1, CRALBP; Na/K ATPase and BEST1) in mature hESC-RPE. (D) H&E and immunofluorescence stained sections of the rabbit retinas after hESC-RPE transplantation. Transplanted hESC-RPE integrated in the subretinal space in a monolayered manner and survived up to 8 months, demonstrating sustained expression of RPE65 and the human specific antigen NuMA. Scale bars: (B-top) = 500 µm; (B-bottom) = 100 µm; (C) = 20 µm; (D) = 10 µm. Image was adapted from ref.[147], with permission from Elsevier.

Study design

hESC were aggregated into embryoid bodies (EB) and allowed to spontaneously differentiate until optic vesicles (OV) were formed. We performed morphological and molecular characterization and assessment of the functional performance of the cells to evaluate the most suitable substrate for hESC-RPE maintenance after OV dissociation (Figure 17A). hESC-RPE in suspension were then injected subretinally into albino rabbits in order to evaluate the stability, integration capacity, and in-vivo functionality of these cells upon transplantation.

3D xeno-free and defined hESC-RPE differentiation

The removal of bFGF and TGFβ from the stem cell culture medium, as previously described, sought to induce spontaneous differentiation towards retinal fate. Aiming to establish an RPE differentiation protocol that maintains the xeno-free and defined conditions of our hESC culture methodology, we used a modified version of our hESC culture medium (NutriStem hPSC XF) that lacks bFGF and TGFβ. We observed that hESC that were aggregated into EBs and cultured in suspension using the modified NutriStem medium started to generate optic vesicle-like (OV) structures by week three and continued producing them until week 10 of differentiation. At this point, the ratio of OV/EB reached 0.8, which was well in line with the efficiencies previously reported by other studies (Figure 17B).

Once the abundance of OVs in the EB cultures was adequate (around week five), they were dissociated into single cells and the resulting cells were plated onto different substrates with the intention of identifying the one that yielded the highest degree of expansion and maturation of the hESC-RPE. We compared the performance on four different laminin substrates that are normally present in human Bruch's membrane: hrLN-521, hrLN-511, hrLN-332, and hrLN-111, as well as gelatin, the substrate of choice in the majority of similar previous studies. While transcriptional analysis demonstrated that all tested substrates enabled the suppression of pluripotency and expression of typical RPE markers, further analysis demonstrated differences among the substrates. Flow-cytometry analysis of the percentage of MITF and BEST1 positive cells revealed that homogeneous expression of RPE markers was only achieved when hESC-RPE were cultured on laminins. Furthermore, time-lapse microscopy analysis revealed that cell expansion on gelatin was significantly reduced, while hrLN-521 and hrLN-511 enabled the best coverage and homogeneity, possible because hESC-RPE cells cultured onto these substrates displayed a more migratory phenotype. In addition, reduced levels of PEDF apical secretion and low TEER values indicated that cells grown on gelatin and hrLN-333 exhibited inferior functional performance. Finally, the molecular characterization of hESC-RPE cells growing on hr-LN521 revealed uniform cobblestone morphology; BEST1, CRALBP, and ZO-1 expression; and polarization of Na/K-ATPase, which is a typical feature of mature RPE (Figure 17B-C). Thus, all of the results indicated that hrLN-521 represent the most supportive and suitable matrix for the culture and expansion of hESC-RPE.

hESC-RPE transplantation into a large-eyed animal model

hESC-RPE cell suspensions were injected into the subretinal space of albino rabbits. These animals have an eye size that is approximately 70% the size of the human eye and possess unpigmented native RPE cells, allowing for the detection and tracking of the transplanted cells through the use of non-invasive techniques such as SD-OCT and IR-cSLO. The transplanted hESC-RPE could be detected only one week after injection by SD-OCT and histological analysis for detection of human cells in the rabbit retina (identified by their positive expression of NuMa). After eight weeks, the transplanted cells exhibited heavy pigmentation and were able to remain integrated in a monolayered structure for up to 34 weeks. At this point, the cells demonstrated specific RPE features such as basolateral expression of BEST1, detection of RPE65, and active phagocytosis of photoreceptor outer segments (POS) (Figure 17D).

As demonstrated in previous publications from our collaborators at Sankt Eriks Eye Hospital, subretinal injection of PBS in the rabbit eye, creates a GA-like phenotype that includes the loss of photoreceptors, represented by the thinning of the outer nuclear layer (ONL). In order to test whether subretinal injection of hESC-RPE can rescue the GA-like phenotype observed in our rabbit model, we compared the effect of injection of PBS only, injection of hESC-RPE, and injection of other cell types, such as hESC and fibroblasts. We observed that only those rabbit eyes that were injected with hESC-RPE suspensions and that displayed integrated RPE cells experienced preserved ONL and rescue of photoreceptors, further affirming the in-vivo functionality of these cells.

Discussion

In Paper II, we describe the establishment of an efficient xeno-free and defined hESC-RPE differentiation protocol. The protocol relies on the spontaneous differentiation of hESC after bFGF and TGFβ removal from the medium, followed by the manual selection and expansion of the putative hESC-RPE present in the OVs into hrLN-521, a substrate protein naturally present in the Bruch's membrane. We then validate the in-vitro morphological, molecular, and functional authenticity of the obtained hr-LN521-hESC-RPE cells and demonstrate their superior performance compared to four different substrates including gelatin, a non-defined and animal-derived substrate used in previous studies.

A xeno-free and defined differentiation protocol facilitates the clinical translation of the product cells for their use as potential medical treatments. Firstly, defined and xeno-free components can prevent possible immunoreactions and immunorejections initiated by the presence of non-human proteins or latent microbial contaminants, including virus or prions that have not yet been identified. Moreover, the use of biologically relevant substrates such as hrLN-521, which is naturally present in the Bruch's membrane, allows us to better recreate the natural cell niche of these cells, which is translated into more phenotypically stable cell cultures and reproducible protocols. However, there is still room for improvement in our protocol. As the initial steps depend on spontaneous EB-based differentiation followed by the manual dissection and digestion of the differentiated OVs, there is still significant batch-to-batch variability. Finding ways to translate our methodology into a fully 2D protocol, avoiding the necessity of generating EBs and manually selecting pigmented areas, will likely result in increased robustness and reproducibility, which are essential features for the clinical translation of any differentiation protocol.

This study also demonstrates the feasibility of our rabbit animal model for use in preclinical studies of future retinal therapies. Most of the previous animal studies in this field were performed using mice and rats, both of which have a very reduced eye size, forcing the researchers to use transplantation methodologies that differ substantially from the ones that would be used in future human subjects. The large size of the rabbit eye, almost comparable to the human eye, makes it possible to deliver the hESC-RPE cells subretinally through transvitreal injections and enables high resolution in-vivo tracking of the transplanted cells and monitoring of the rabbit retina using instrumentation identical to that used in a clinical setting. However, despite the fact that local immunosuppression was applied during the transplantation procedure, only half of the transplantation attempts resulted in successful integration of the hESC-RPE, while the other half demonstrated some indications of potential immunorejection. Although the eye is considered to be immunoprivileged, there is still an inherent risk in the surgical procedure of creating a damage in the basement membrane that separates the choroid from the RPE and neuroretina, which would cause the disruption of the blood-retina cell and enable the immunorejection of the xenotransplant by the rabbit's own immune system. Nonetheless, this inherent risk is probably lower when hESC-RPE are transplanted in suspension through the vitreous compared to transplantation of hESC-RPE sheets, which

generally requires more invasive surgical procedures that can increase the risk of rejection. For the prospective implementation of this procedure in humans, optimization of the immunosuppressive regime together with the use of an immunocompatible cell source (autologous or allogenic) will likely overcome this difficulty.

4.3 IDENTIFICATION OF CELL SURFACE MARKERS AND ESTABLISHMENT OF MONOLAYER DIFFERENTIATION TO RETINAL PIGMENT EPITHELIAL CELLS (PAPER III)

Over the past few years, several studies have reported the establishment of clinically compliant hPSC-RPE differentiation protocols for use in reparative therapies for common retinal disorders such as AMD and SD. Although these protocols employ xeno-free and defined components, most still rely on the manual selection and expansion of pigmented areas containing the putative hPSC-RPE from the bulk of cells emerging during the differentiation, which compromises their large-scale adaptability and substantially increases batch-to-batch variability. Furthermore, to date, there has been a lack of useful cell surface markers for the RPE lineage that could facilitate in-process monitoring of differentiation efficiency and enable automatization of hPSC-RPE cell enrichment and purification. In order to overcome such limitations, in the present study, we performed a comprehensive antibody screening that resulted in the identification of positive and negative markers for hPSC-RPE. The identified markers proved to be helpful not only in RPE cell enrichment, but also in tracking differentiation performance. Finally, with the aid of such cell surface markers, we established a more robust and scalable 2D-based xeno-free and defined hPSC-RPE differentiation.

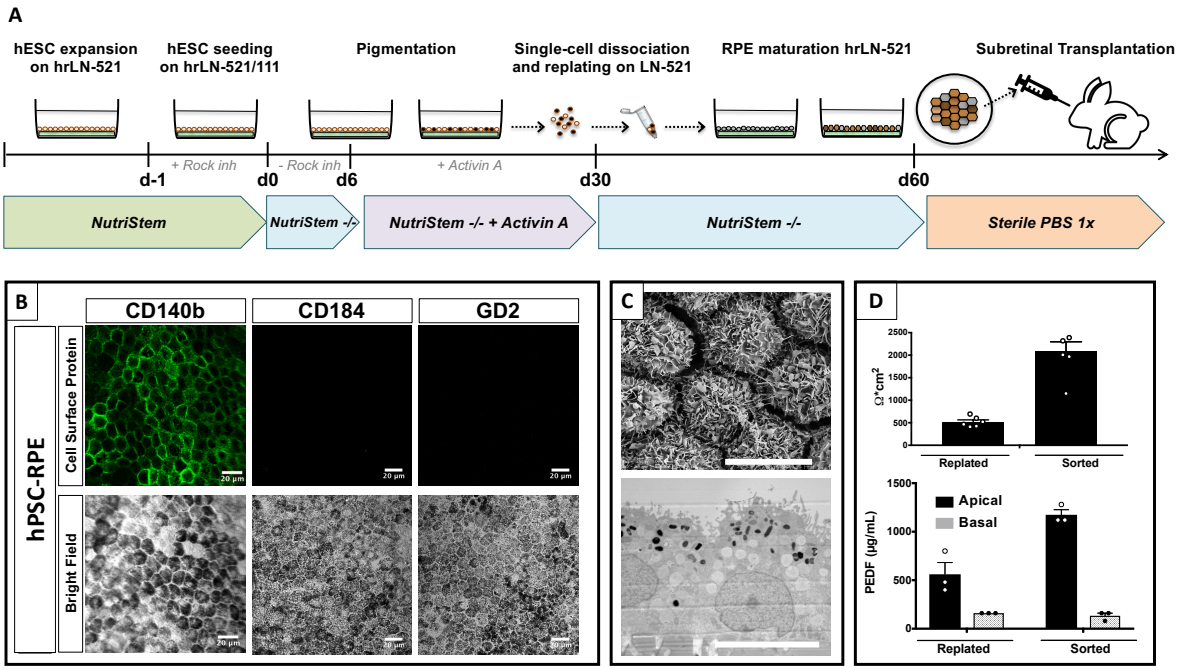

Figure 18. Identification of cell surface markers and establishment of monolayer differentiation to retinal pigment epithelial cells. Summary of the main results presented in Paper III. (A) Monolayer differentiation protocol scheme followed for the derivation of hPSC-RPE. (B) Representative immunofluorescence and bright field images demonstrating the presence of CD140b and the absence of CD184 and GD2 in day 60 hPSC-RPE. (C) SEM (top) and TEM (bottom) images of day 60 hPSC-RPE showing surface microvilli and polarized intracellular structures. (D) Functional assays demonstrating the increase in monolayer integrity measured by TEER (top), and in pigment epithelium-derived factor (PEDF) polarized secretion

measured by ELISA (bottom) in day 90 hPSC-RPE after sorting for CD140b+/CD184−. Bars represent means ± SEM from at least three independent experiments. Scale bars: (B) = 20 μm; (C) = 10 μm. Image was adapted from ref.[197], with permission from Springer Nature.

Study design

Dissociated OVs and mature hPSC-RPE were run against an antibody library recognizing 242 different CD antigens. Those markers present in both the OV and mature population were identified as positive RPE markers, while those present only in the OV were identified as negative RPE markers. The positive and negative candidates were then validated through immunofluorescence, flow-cytometry analysis, and FACS-sorting.

For the new 2D differentiation protocol, hESC or hiPSC were seeded onto new plates coated with hrLN-521 or hrLN-111 and cultured with NutriStem hPSC XF medium containing ROCK inhibitor. From the day after plating until day six of differentiation, medium was replaced with modified NutriStem without bFGF and TGFβ. From day six until day 30, differentiation towards retinal fate was enhanced by supplementing the media with Activin A. At day 30, differentiated cultures were replated or FACS-sorted using the identified markers into hrLN-521 coated plates, where they were allowed to expand and mature for 30 more days until homogeneous and pigmented hPSC-RPE monolayers formed (Figure 18A). The robustness of this new differentiation protocol was then assessed in three different hESC and four different hiPSC lines by comparing the expression levels of the positive and negative cell surface markers at day 30 and day 60 of the differentiation.

Identification of CD140b+, GD2-, and CD184- as surface markers of hPSC-RPE

In order to find novel extracellular markers for the RPE, dissociated optic vesicles and mature and expanded hPSC-RPE cultures were screened by flow cytometry using an antibody panel recognizing 242 different CD antigens. We found CD140b (PDGFRb) to be expressed in both the optic vesicles and mature hPSC-RPE, suggesting that it could be a good positive selection marker, as it was able to discriminate the RPE even during earlier phases of the differentiation. In addition, two additional markers, GD2 (disialoganglioside) and CD184 (CXCR4), that were detected in the OVs but were absent in mature hPSC-RPE were selected as potential negative selection markers under the assumption that they were probably detecting alternative lineages that emerged during RPE differentiation, but that were not present in the latest stages of the protocol. These three candidate surface markers were then validated by flow-cytometry of dissociated EB (at week five of differentiation) and by immunofluorescence staining of mature hPSC-RPE. We found that CD140b expression was restricted to the OV and homogeneously distributed in mature cultures, while GD2+ and CD184+ cells were primarily located in non-pigmented areas of the EBs and completely absent in mature hPSC-RPE (Figure 18B). Moreover, FACS-sorting for CD140b expression and posterior immunofluorescence of cytospinned positive and negative populations demonstrated that only CD140b+ cells were pigmented, co-stained positive for BEST1, and expressed high expression levels of RPE-specific markers. Finally, histological analysis confirmed the presence of CD140b in RPE of adult human retinas, as wells as in hPSC-RPE after subretinal transplantation into rabbit eyes.

Establishment of a novel 2D-based hPSC-RPE protocol

Seeking to develop a new protocol that does not rely on embryoid body formation, we used our recently validated surface markers to identify the best culture conditions for enabling 2D differentiation of hPSC into hPSC-RPE. We tested the performance of two different laminins present in Bruch's membrane (hrLN-111 and hrLN-521) as substrates, as well as the addition or exclusion of Activin A in the culture medium, which was previously reported to be a potent inducer of the retinal lineage on neuroectoderm cultures. The percentage of CD140b, GD2, and CD184 positive cells exhibited no difference in performance efficiency between the two tested laminins. However, we observed that the addition of Activin A from day six of differentiation resulted in a two-fold increase in differentiation efficiency, as denoted by the percentage of CD140b+ cells and the increase in RPE marker expression. We then compared the performance of this 2D hPSC-RPE induction with our previous EB-based protocol and found that our new approach yielded 10 times more CD140b+ cells over the time course of seven weeks of differentiation; a finding that was correlated with a comparable increase in RPE marker expression.

In order to refine our differentiation protocol further, we tested whether introducing a replating step after the initial 30 days of differentiation could remove potential CD140b- contaminant cells. hPSC-RPE cultures were replated at different densities and cultured for another 30 days before we analyzed their purity by flow-cytometry and qPCR and their functional performance in terms of PEDF secretion, phagocytosis, and TEER. We observed that all tested densities achieved a similar increase in the number of CD140b+ cells, which accounted for almost 100% of the total. However, the transcriptional analysis revealed a considerably higher expression of RPE markers on cultures that were replated at a 1:20 ratio, possibly indicating the presence of a more homogeneous and mature end product. This finding was supported by the fact that 1:20 replated hPSC-RPE functionally outperformed the other tested conditions, as demonstrated by TEER, PEDF ELISA, and phagocytosis assay. Moreover, hPSC-RPE that were replated 1:20 also displayed typical morphological features of mature RPE, such as the presence of surface microvilli and the polarized localization of subcellular organelles observed by SEM and TEM, respectively (Figure 18C). Finally, we also demonstrated that these replated hPSC-RPE were able to integrate and form a polarized monolayer upon subretinal transplantation in our rabbit model.

CD140b, GD2, and CD184 enable hPSC-RPE cell enrichment and evaluation of differentiation kinetics

We examined the robustness and reproducibility of our novel hPSC-RPE differentiation protocol by testing it with three different hESC lines and four other hiPSC lines. Differentiation efficiency was then assessed at day 30 and day 60 by flow-cytometry for our markers and qPCR for RPE-specific gene expression. Six out of the seven hPSC lines managed to differentiate efficiently, demonstrating robust expression of RPE markers at the transcriptional level and

fairly homogeneous pigmentation. These lines exhibited more than 60% of CD140b+ cells by day 30, which increased to nearly 100% by day 60, and reduced levels of GD2 and CD184, especially at the latter time point. In contrast, differentiation in the only non-responsive hPSC line, which exhibited no pigmentation and almost no expression of RPE markers, was characterized by CD140b+ levels below 20% by day 30 and high levels of GD2 and CD184 even at day 60.

To assess the potential of our surface markers for hPSC-RPE cell enrichment, we compared cultures that where either replated as described above or enriched with a combination of CD140b positive selection and negative selection using GD2 or CD184 at day 30. Replated and sorted populations were analyzed following an additional 30 days in culture on hrLN-521 using single-cell RNA sequencing. tSNE plotting of the scRNA-seq results indicated that the cells analyzed were distributed into three clusters with distinct gene signatures: an RPE cluster containing the majority of cells from all three samples, and eye field progenitor cluster, and a mesoderm cluster. We found that while replated cells harbored 11.3% of eye field progenitors and 1.2% mesoderm contaminant, these proportions were diminished to 3% and 0% when cultures were enriched for CD140b+/GD2- or CD140b+/CD184-, highlighting the potential of these surface markers for increasing the purity of the final RPE product. Furthermore, thorough characterization of FACS-sorted hPSC-RPE cultures demonstrated that cell enrichment for CD140b+/CD184- can improve pigmentation and maturation of hPSC-RPE, as well as their functional performance, especially during suboptimal hPSC-RPE differentiations (Figure 18D).

Discussion

In Paper III, we present the identification and validation of several cell surface markers, including CD140b, GD2, and CD184, which proved to be very helpful in the context of hPSC-RPE derivation for monitoring the efficiency of the differentiation process, as well as for generating a purer RPE cell product via positive and negative cell enrichment. The identified markers served to establish a more efficient and robust xeno-free and defined 2D-based differentiation protocol that circumvents the need for EB production and manual selection of the pigmented OVs.

From a safety perspective, in any cell manufacturing that is intended for its use in replacement therapies, it is critical to ensure a pure final cell product before transplantation. One must not only ensure that there are no undifferentiated remainders that could potentially give rise to tumors, but also eliminate contaminant cells from other lineages that could interfere later with the transplant normal function. For that reason, the establishment of efficient and reproducible protocols and the identification of extracellular markers that can discriminate the cell type of interest from alternative cell types becomes crucial.

We identified that CD140b and other markers that appeared later during differentiation (e.g., CD104), are expressed specifically by the RPE, as they emerged during hPSC-RPE in-vitro differentiation. Similar to most other CD antigens, CD140b is not solely expressed by RPE

cells; as it is also known to be expressed by other cell types including vascular cells, decidual cells, and fibroblasts. However, we found its expression to be specific to RPE in the context of hPSC-RPE differentiations. In addition, we demonstrated that this marker is also expressed by the endogenous RPE in the human retina, clearly suggesting that it plays a role in the natural retinal context. CD140b expression is related to diverse processes such as embryonic development, angiogenesis, cell proliferation and differentiation, yet its role in RPE and retinal function has not been previously described.

In addition to the identification of novel extracellular markers, we also established a more efficient and robust xeno-free and defined differentiation strategy for the production of clinically compliant hPSC-RPE. The primary advantage of this novel methodology is that it does not depend on free-floating EB-based differentiation and instead enables the entire differentiation process to occur in a 2D adherent culture, which makes the process more robust and reproducible, as demonstrated in our study. Furthermore, the elimination of EB differentiation, enables the selection and expansion of a purer hPSC-RPE by performing one bulk passage, eliminating the need to manually select and dissociate pigmented areas or OVs and making the protocol significantly more scalable and amenable to automatization. Finally, we leveraged the role of Activin A in boosting retinal differentiation to make our 2D protocol shorter and more efficient. These qualities are highly valued in protocols that are intended for the clinical production of cells, as they diminish the economic costs and the risk of introducing spontaneous genetic aberrations derived from the cell culture. Altogether, our adherent xeno-free and defined differentiation strategy, which combines the use of Activin A with the selection and expansion of hPSC-RPE by bulk passaging, renders a cell production yield that is ten-times superior to our previous suspension protocol, and allows the generation of up to 13,000 doses for their use in cell replacement therapies from a starting culture of only one million hPSC (assuming each patient is transplanted with 100,000-200,000 hPSC-RPE cells).

5 CONCLUSIONS

In this thesis, we evaluated the potential of hESC-derived trophoblast cells as an in-vitro model for the study of the molecular pathways involved in trophectoderm establishment and placental formation. We also established xeno-free and defined differentiation methodologies for the clinically compliant production of hPSC-RPE cells. Finally, we validated the morphological and molecular identity of these cells in-vitro and assessed their in-vivo functionality upon transplantation into a relevant large-eyed animal model.

The main findings of this thesis are as follows:

- Inhibition of YAP1/WWTR1-TEAD interaction through the use of verteporfin induced extensive cell death of hESC-derived trophoblasts and hESC, suggesting a role of the Hippo downstream effector complex integrated by YAP1/WWTR1/TEAD in trophoblast formation and hESC maintenance.

- CRISPR-Cas9-mediated disruption of YAP1 or WWTR1 gene function caused substantial cell death during the early stages of in-vitro trophoblast differentiation, indicating an important function of these two homologous coactivator molecules in trophectoderm establishment. Although YAP1 appeared to have a leading role, defined by the more severe phenotype observed in lines lacking this protein, the observation that LPA treatment was able to restore the normal function of the cells, indicated that YAP1 and WWTR1 can compensate for each other in this context. Moreover, the impossibility of deriving YAP1/WWTR1 double-knockout hESC clones indicated that their expression is also essential for hESC maintenance.

- Ablation of TEAD4 gene function did not have an effect on trophoblast differentiation, implying that, in contrast to what was described in the mouse, this transcription factor does not have an essential role in this process. Only simultaneous knockout of the three TEADs present during during early development (TEAD1, TEAD2, and TEAD4) was able to recapitulate the phenotype observed after disruption of YAP1 or WWTR1, also suggesting a redundant function of these paralogous factors.

- Efficient xeno-free and defined hPSC-RPE differentiation methodologies were established. Our intitial EB-based differentiation protocol proved to be effective in generating homogeneous and functional hESC-RPE cultures. Our novel 2D differentiation protocol demonstrated an increased reproducibility and efficiency by inducing differentiation directly in adherent cultures and using Activin A to enhance retinal differentiation. Finally, hrLN521 and hrLN111 were found to be very supportive culture substrates for the induction, expansion, and maturation of hPSC-RPE cells, outperforming other frequently used substrates such as gelatin.

- The identification of a set of cell surface markers – including CD140b, GD2, and CD184 – proved to be very helpful for monitoring differentiation efficiency as well as for hPSC-RPE cell enrichment in order to obtain a purer and more homogeneously mature cell product.

- hPSC-RPE subretinally that were injected into a large-eyed animal model integrated correctly in a monolayeric manner, exhibited preserved integrity and functionality, and succesfully decelerated retinal damage progression by rescuing photoreceptors from degeneration.

6 FUTURE PERSPECTIVES

A tremendous amount of knowledge has been generated since the discovery in 1998, of the methodologies necessary for the derivation and culture of human embryonic stem cells[79]. Only 22 years since those initial reports, hESC are used today for a myriad of different purposes, including their use in fundamental research for understanding complex events in human development, in drug testing and disease modeling, and as a source for many cell-based therapies. The work described in this thesis demonstrates that hESC can be very useful both in the establishment of in-vitro model systems for the study of early events in development, such as trophectoderm segregation and trophoblast differentiation, and as a renewable source for the clinical production of retinal cells to be employed in replacement therapies for diseases such as macular degeneration.

The use of hESC-derived trophoblast cells allowed us to examine some of the molecular mechanisms governing trophoblast differentiation. However, the questionable correlation of this model system with actual in-vivo development and its flaws in recapitulating the implications of intercellular signaling and embryonic architecture, requires the validation of these results through complementary approaches. Derivation of hTSC, or modification of in-vitro culture conditions to permit trophoblast differentiation of cells with expanded potential (e.g., naive stem cells) could likely help in the establishment of bona fide in-vitro models to better simulate the earliest events taking place during placental formation. Furthermore, the inclusion of these cell types in three-dimensional cultures, such as hTSC organoids or embryoids made by arranging different human stem cells and hTSCs would provide a much better idea of the biochemistry behind how this process occurs in the developing human body.

Apart from the improvement of the in-vitro models, the use of novel CRISPR-derived approaches, such as CRISPRi and CRISPRa, will facilitate precise dissection of dynamic and complex developmental processes by enabling interrogation of genes that are essential for hESC maintenance and embryo development with a temporal control[94]. Though in-vitro studies using hESC- or hTSC-derived systems will continue to be transformative to our comprehension of lineage segregation processes occurring during early mammalian development, certain developmental aspects can only be ascertained by performing functional studies directly in human embryos. The joint application of genome editing techniques to in-vitro models and human embryos will enable the study of gene function in developmental contexts that were previously inaccessible. The knowledge acquired in this field can be used in the establishment of better stem cell culture and derivation techniques, as well as to provide valuable insights for understanding common causes of infertility.

We described the establishment of xeno-free, defined, and clinically compliant methodologies to derive hPSC-RPE using hESC and hiPSC as a source. Both approaches described in this thesis were able to render a final cell product that is less prone to onset future complications when used clinically, as they are exempt from non-human proteins or other potential contaminants present in animal serum. However, clinical application of any cell product

requires further steps to ensure their safety and efficacy for future replacement therapies. First, the described methodologies would need to be adapted to comply with the evolving standards of Quality Assurance (QA) and Good Manufacturing Practice (GMP) imposed by the regional medical agency or administration[198]. Only then, and after fulfilling stringent in-process and batch release criteria, the resulting hPSC-RPE cell product could be authorized as an Advanced Therapy Medicinal Product (ATMP) for human application. Each batch of hPSC-RPE cells would then need to undergo extensive safety validations, including testing for potential culture-acquired mutations, biodistribution, and tumorigenicity assays to exclude the possibility of long-term or short-term complications in potential future patients.

In addition to ensuring the quality of the final cell product, future efforts should also focus on refining the transplantation techniques and improving the engraftment, survival, and functionality of the transplanted cells. Although our preliminary transplantation studies into a large-eyed animal model demonstrated the integration and long-term survival of our hPSC-RPE cells, successful engraftment was only achieved in half of the transplantation attempts, despite the use of local immunosuppression. Furthermore, previous publications from our collaborators have demonstrated that severe disturbance of the retinal microenvironment after sodium iodate-induced retinal degeneration impaired hPSC-RPE engraftment and photoreceptor rescue, suggesting that suspension transplantation will not be suitable when the underlying basement membrane is damaged[161]. Therefore, finding ways to enhance engrafting and transplant survival becomes crucial if we aim to treat patients with advanced stages of the disease. Potential solutions include the blending of hPSC-RPE with biomaterials such as hydrogels or biodegradable sheets, the delivery of biomolecules that favor cell survival, or combination with gene therapies that could potentiate the survival, integration and functionality of the graft[173,174,199,200]. In addition, as advanced stages of retinal degeneration are typically characterized by the irreversible loss of photoreceptors, future therapeutic strategies should consider the co-transplantation of hPSC-RPE with hPSC-derived photoreceptors and other supporting cell types[169]. Finally, as the degenerative microenvironment present in advanced stages of AMD and SD can compromise the blood-retina barrier, minimizing the immunoreactivity of the transplanted cells could also help in facilitating their long-term survival. Future strategies for minimizing the risk of immunorejection in hPSC-derived cell therapies would likely require the use of hypoimmunogenic hPSC, created through CRISPR-based human leukocyte antigen engineering or immunocompatible cell sources after the establishment of hPSC collections with HLA haplotypes that could match the vast majority of the population[187–190].

7 ETHICAL REFLECTION

The three studies included in the present thesis involved the culture and differentiation of human embryonic stem cells derived from surplus preimplantation embryos that were generously donated for research. While the regulations in Sweden are relatively permissive concerning research on human embryos, this type of research is regarded as controversial or non-ethical in many other countries. The regulations in place in Sweden ensure the responsible usage of these embryos, forbidding the use of research embryos for conception of human beings. These regulations also restrict the in-vitro culture of embryos to the first 14 days of development or until the appearance of the primitive streak, whichever comes first. The 14-day time limit, now broadly accepted, was first introduced in the UK in 1984 as part of the "Warnock Report" elaborated by the Committee on Human Fertilisation and Embryology known, which followed the world's first IVF birth in 1978. Those 14 days mark the last developmental time point when the embryo can split to give rise to twins, delimiting the moment an embryo becomes an "individual", as well as the time when gastrulation begins, which corresponds to the first tissue specifications.

There are two different categories of viable human embryos that can be used in research: surplus embryos donated with consent following in-vitro fertilization, and embryos created specifically for research. While most countries do not allow the creation of embryos specifically for research, many still allow the use of surplus viable embryos that can come from two main sources: embryos that have been cryopreserved over the legal limit, and embryos that have been discarded after preimplantation genetic diagnosis (PGD) because they are carriers of a disease-related mutation. Regardless of the source, the number of human embryos available is limited; therefore, it is crucial to promote an open access to any data derived from their use in order to avoid their misuse in repetitive experiments.

In addition to the use of human preimplantation embryos, our research also comprises the application of genome editing techniques, which is another ethically controversial subject, especially when it is used for gene edition of the human germline (embryos and germ cells). The potential clinical applications of CRISPR/Cas9 germline genome editing have been the central subject of many ethical and regulatory debates in the last four years, due to the highly controversial implications that germline genetic modification could have in society, including the potential for exploitation in nontherapeutic uses, and the existence of preimplantation genetic diagnosis (PGD) as a viable alternative. While CRISPR/Cas9 has not yet proved to be sufficiently safe and efficient to be employed therapeutically in the germ line, it still offers significant potential as a tool in basic research, which can help in examining early stages of human embryo development that were previously inaccessible.

8 ACKNOWLEDGEMENTS

It is unbelievable how fast can six years pass by. Although I would be lying if say I do not feel extremely happy to put an end to my PhD studies, I must recognize that I really enjoyed the way here. I would like to express my sincere gratitude to all the people that inspired, taught, supported and helped me during my PhD and throughout the rest of my life. Every one of you have contributed to shape me as the scientist and, most importantly, as the person I am today. Thank you!

First, I want to thank my main supervisor **Fredrik Lanner**, for offering me the opportunity of joining his team and allowing me to fulfil my dream of doing science in the embryology and stem cell research fields. I was very lucky to join your lab in its very beginning and thanks to that, I had the privilege of learning many of the technical aspects directly from you. Thank you for your patience and kindness during the extremely early mornings at the animal facility and the late evenings at the microscope and flow cytometer. Thank you also for showing me how to think and to work independently, to be critic with my own work and for never saying no to any course, conference or workshop that could allow me to grow as a scientist. A big hug to **Victoria and the girls** for always welcoming us to your house with a big smile. I wish you, your family, and the Lanner lab the best of lucks for the future.

Thanks to my co-supervisor **Anders Kvanta**, for bringing optimism, great energy and motivation to all the projects we shared. Thank you for always being super-efficient when I needed some feedback or even when I just needed a signature from you, regardless of how busy you were.

Thanks to my co-supervisor **Kenneth Chien**. Even if we did not get to meet very often, I am still grateful for the feedback and motivation you provided me with when we met after my halftime.

I would also like to express my gratitude to **Outi Hovatta**. You will always be an inspiration for the many of us who were lucky to work by your side. Thanks for initiating the RPE project together with Anders and for allowing me to be part of it. I am also indebted to you for putting me in contact with Fredrik when I was Master student pursuing to learn more about embryos and stem cells, who knew that e-mail would become the beginning of seven years of incredible science.

Thank you, **Sonya Stenfelt**, for being the supervisor of my master thesis and showing me how important is to plan experiments ahead, especially when they involved a two month-long differentiation.

Thanks to **Leander Blaas** for supervising me during my junior research project when I had no previous experience in cell culture and histology. I will always be grateful to you for making me a pro of tissue staining and confocal microscopy. I wish you the best with your newly started research team!

I also want to thank **Paco Gámez**, for being a patient and generous supervisor when I made my very first baby steps in the lab during my bachelor studies, and for being a good and fun friend!

I wish to show my gratitude to the head of CLINTEC, **Mats Blenow**, to the director and vice-director of doctoral studies, **Li Felländer Tsai** and **Olav Rooyackers**, and to the administrator of doctoral studies, **Agneta Wittlock**, for helping with the different administrative formalities and for solving each one of my questions and doubts.

To the head and former head of Obstetrics and Gynecology, **Ganesh Acharya** and **Magnus Westgren**, thank you both for supporting my PhD studies and for encouraging scientific research in our division.

Thanks to **Galina Lundberg**, the best administrator we could ever dream to have. Thanks for your patience with us and for being so efficient. You definitely made the increasing bureaucratic burden easier to digest. Congratulations on the child that is about to come, I know you'll be an excellent and caring mom.

I wish to thank all the former and present members of the **Lanner Lab**, whose assistance and moral support were a milestone in the completion of this thesis. **Liselotte**, thanks for transferring your extensive knowledge about human stem cells and sharing all your numerous tips and tricks to make the stem cells happier. **Sarita**, thanks for being an awesome lab mate and friend, and for trusting in me when you needed extra hands or just an opinion. **Sandra**, my partner in crime in the RPE project, thanks for being an excellent and hard-worker colleague, as well as good friend. I am convinced that you'll become a brilliant scientist. **JP**, thanks for sharing your motivation and passion for science and for spicing up our conferences and parties; I will not miss being your hotel roommate though…just kidding! :P. **Sophie**, you showed me that working hard is less painful when you also party hard; thanks for being a role model and for teaching me how to make a proper old fashioned; I wish you the best of lucks in your scientific career. Thanks **Sara**, for joining our Spanish retina gang, for the long experiments we shared and the awesome trips we enjoyed together. **Nerges**, you came when I was almost going crazy with CRISPR, thanks for teaming up with me in setting up the techniques and protocols necessary for gene editing, and foremost, for being a very good friend and a person I can rely on. **Nico**, you came to the lab like a hurricane, the lab was never the same after you arrived and I must admit that I enjoy it; thank you for that and for being my friend and a shoulder to lean upon when I needed. **Mona**, thanks for doing your best to keep the lab running smoothly, even during a pandemic, and for always caring about us. **Leni**, thanks for bringing some serenity to the office and also for providing helpful insights while discussing our projects; I wish you good luck in your coming PhD defence. Thank you, **Pankaj**, for your support analyzing complex scRNA-seq data. To **Siqin** and **Paschalis** for all the endless hours we shared in CCL1; I hope your amazing differentiation protocol can soon lead you to important publications. **Laura**, the latest addition to the retina project, thank you for the crazy parties and for your hard work; I wish you a very successful PhD. Thank you, **Heather**, for relying on me when you needed advice on RPE differentiation and characterization, and for sharing with me

your knowledge on the Notch pathway. To **Theresa Mader**, for sharing with me my early steps into the RPE project and for baking the best birthday cakes. Thanks **Sebastian**, for trusting in me when you wanted to learn about CRISPR and when you sought technical advice on embryo experiments. Thanks to **Geeta**, for always caring about us, for pushing me to go home before 8 PM and for always sharing some chocolates and candies when we most needed them. To **Jere**, for joining our lab and being willing to contribute to the Hippo project; I wish you a very successful postdoc.

I thank the students and interns who trusted in me as their supervisor. Thanks, **Philipp**, for your great contribution to the Hippo project by helping me establishing the numerous knockout lines; I wish you the best of lucks for your future PhD in Australia! To **Aggelos**, for never giving up on the naïve conversions; good look in your career as a medical doctor. Thanks also to **Theresa M. Sommer**, for coping with having me as supervisor in the distance during the coronavirus pandemic; I am sure you will produce a good master thesis and I wish you the best in your future steps.

Thanks to the former and present members of the **Damdimopoulou Lab,** for bringing a different perspective to our lab meetings and for teaching us how worrisome endocrine disruptors are. **Pauliina**, I saw you grow from postdoc to PI; thanks for your support and helpful feedback, also for the parties we shared during the various retreats and conferences we attended together. I wish you a great success in your search for better fertility preservation strategies and in your quest for minimizing the exposure to EDCs in our daily lives. Thank you, **Astrud**, for bringing joy to our lunches and for inviting us to your wonderful weeding. To **Richelle**, thanks for solving most of my statistical doubts, and for opening us your home for so many fun parties. Thanks to **Jie**, for the long evenings we shared in Forskningslab and for always trusting in my advice. To **Eri**, for the laughs we had together. **Jasmin and Tianyi**, I wish you good luck with your PhD studies. Thanks, **Delia**, for sharing your knowledge about bovine pluripotency and good luck with your postdoc.

To our collaborators in **Sankt Eriks Eye Hospital**, thanks for working hard to prove that our RPE cells could integrate and survive in the rabbit eye. Thanks, **Helder**, for sharing your master skills in Western blotting. Thanks, **Hammurabi**, for all those subretinal injections you performed and for inviting me to learn how they were done. **Monica**, thanks for taking good care of the rabbits and for explaining me how you collected the samples from them. Thanks to **Sophie** and **Emma**, for your valuable help with the rabbits and the tissue stainings. **Flavia**, I wish the best of lucks with your PhD.

Thanks to the super-skilled personnel of the Flow Cytometry and Live Imaging facilities at KI. **Iyadh**, your valuable input and hands-on experience was key for the successful results published in Paper III. Thanks, **Belinda**, for helping us with the FACS machine during the long Friday sorts. Thanks, **Sylvie and Gabriela**, for your extensive training sessions at the confocal microscope and for always being helpful and resourceful.

My sincere thanks also goes to the staff at **KFC**, Novum. Thanks, **Kathrin**, for being a proactive manager, stimulating social interaction and doing your best to improve the facilities and equipment at KFC. Gracias, **Nelson**, por nuestras pequeñas charlas en el cuarto de autoclave y por tu buen humor. Tack, **Isa**, för att du alltid var glad och effektiv.

To all the colleagues sitting at **Neo** building, thanks for making the long days at the flow cytometer and confocal microscope a bit more enjoyable. Thanks to **Maria Kasper** for being a great inspiration for many students. To **Tina**, for the endless projects we shared during our master studies and for trying to organize several events to keep the Biomedicine master 2014 crew reunited. **Lakshmi**, thanks for always helping out at the flow cytometer when we needed. Thanks, **Agus**, for sharing with me our Spanish passion of complaining about everything and for organizing and inviting us to many fun parties at Neo and also at your place. To **Marco**, for the countless afternoons at the confocal and the fun lunches we had together.

A la tribu de **españoles afincados en Estocolmo**, muchas gracias por hacer más soportables estos casi ocho años alejados de mi tierra. Gracias, **Lamberto y Patricia**, por las cenas y anécdotas que compartimos. **Gema y Luisma**, muchas gracias por vuestras fiestas y todas las risas que nos echamos juntos recordando a personajes de Córdoba y Andalucía en general. **Néstor**, gracias por los viajes y ratos que hemos compartido durante estos años. **Laia**, gracias por tu amistad, te deseo lo mejor ahora que por fin terminaste tu doctorado y puedes disfrutar de tu familia. **Sonia**, gracias por tus consejos y por incluirnos a Rafa y a mi en vuestra "mini-secta" de postdocs españoles (aún sin ser postdocs). **Lorena Marín**, gracias por tu espontaneidad y por apreciar mi trabajo con las lamininas. A ti **Jose**, muchas gracias por tu amistad, por las fiestas locas y compartir nuestros cortes de pelo aún más locos; te deseo lo mejor en Barcelona. **Lorena**, nos conocimos cuando éramos unos pipiolos yendo de congreso en congreso y el destino nos volvió a juntar en Salamanca y también en Estocolmo; mucha suerte con tu doctorado. A **Irene**, gracias por compartir tu pasión por el flamenco y quitarnos a Rafa y a mí un poquito la angustia de estar lejos de Andalucía.

A mi amiga **Ana**, muchísimas gracias por ser como eres. Te convertiste en un apoyo fundamental durante el máster y también en los momentos más duros del doctorado. Te quiero mucho y te deseo lo mejor! Thanks also to **Robin**, for the good moments we shared and for joining our craziness and endless complaints.

A los amigos que dejé en España, muchas gracias por vuestra amistad incondicional y por hacerme recordar cada una de las anécdotas y experiencias que vivimos juntos como si el tiempo no pasara. **Malu**, fuiste, eres y siempre serás un ejemplo de inteligencia y perseverancia para mi. Tu amistad es de las mejores cosas que me regaló mi paso por Sevilla. A mi amiga **Nane**, por compartir su (muy interesante) vida conmigo y por aportar ese punto de surrealismo y diversión que tanto me gusta. A **Reyes** por tu amistad y tu locura y por esos carnavales que disfrutamos juntos, y los que espero que estén por llegar. A **Mari**, porque nunca pude soñar con tener una compi de piso mejor que tú; por las fiestas, ferias y carnavales que pasamos juntos, nuestras evacuaciones de terremotos y nuestra pasión por Callejeros; ¡te quiero infinito! A ti, **Concha**, muchas gracias por confiar en mí como despertador personal, por los congresos

y eternas horas de estudio que pasamos juntos. A mi vecino **Pablo**, por ser mi compañero de Aikido y por meterme en el mundo de la Biotecnología. A mi amiga de la infancia, **Alejandra**, porque nuestra amistad no tiene fronteras y porque pase lo que pase siempre serás mi alma gemela. A mis Biotecs favoritos: **Clara**, **Pablo**, **Jose**, **Fran**, **Gina**, **Sara** y **Angie**; gracias por los momentos que compartimos en la carrera, por todas las reuniones navideñas y por las bodas, bautizos y comuniones que nos quedan por celebrar. ¡Os quiero compis!

Por supuesto, tengo que dar las gracias a mi familia, por su apoyo y su amor incondicional. A mi madre**, Teresa**, la persona que más quiero en este mundo y que además de madre ha ejercido en mi vida como profesora, psicóloga, enfermera, amiga, etc. Sabes que esta tesis no habría sido posible si no es gracias a ti…Te quiero infinito! A mi hermano**, Javi**, por todas las risas y peleas que hemos compartido; por los veranos y navidades que hemos disfrutado juntos y por todos los momentos que nos quedan por disfrutar...te quiero pishurra! A mi padre**, Álvaro**, por apoyarme económica y moralmente durante mis estudios y por luchar siempre por pasar más tiempo juntos. A mi prometido, **Rafa**, porque lo dejaste todo por compartir esta experiencia conmigo, porque haces pequeños los problemas por grandes que sean, por hacer de nuestra casa un hogar y demostrarme cada día tu amor incondicional…Te amo! A mi **abuela Ana** y a mi **abuelo Antonio**, gracias por vuestro amor y por enseñarme los valores que hoy día sigo practicando; ojalá estuvieras aquí abuelo para compartir mi alegría contigo; os quiero mucho! A mis tíos y tías: **Rosario**, **Chica**, **Miguel**, **Anita**, **Fernando**, **Ramón**, **Achim, Laura** y **Cristina**; muchas gracias por vuestro cariño. A mis primos y primas: **Patri**, **Antonio**, **Rubén**, **Andrés**, **Ana**, **Marta, Julia, Miguelito** y **Ana Corral**, gracias por las trastadas y travesuras que compartimos juntos y por vuestro cariño. A mi familia política, **la familia González Moriana**: Paqui, Rafa, Laura, Rubén, Encarni, Pili, Juan, la abuela Encarna, Rafa, José, Eva, Chema, Patri, Adri, Jesús, Juanjo y Marta; muchas gracias por acogerme como a uno más de la familia y compartir tantos buenos ratos juntos. A **Ana** y **Carmeli**, por los buenos ratos en los Caños y por las videollamadas que hicieron la cuarentena mucho más amena.

Finalmente, también quiero agradecer la labor de todos aquellos profesores que a lo largo de mi vida contribuyeron a mi formación y me motivaron e inspiraron a seguir el camino que me ha llevado hasta aquí. Especial reconocimiento a mi profesor de primaria, **Antonio Brenes**, por despertar mi pasión por las ciencias naturales. A mis profesores de Inglés, **Roman** y **TJ**, por conseguir hacer que aprender un idioma sea divertido. A mi profesor de bachillerato, **Jose María Gil**, gracias por transmitirme tu pasión por la Biología y hacerme decantar por la Biotecnología. Y a mi profesora de la carrera, **Menta Ballesteros**, gracias por ser toda una inspiración para todos los biotecnólogos que tuvimos la suerte de ser tus alumnos.

This work was financially supported by grants from Ming Wai Lau Centre for Reparative Medicine, Knut and Alice Wallenberg Foundation, Centre for Innovative Medicine (CIMED), Swedish Research Council, Ragnar Söderberg Foundation and Swedish Foundation for Strategic Research conceded to Fredrik Lanner. Support for travel was received from Edwin Jordans Foundation for Ophthalmological Research and Karolinska Institutet.

9 REFERENCES

1. Bruce, A. W. & Zernicka-Goetz, M. Developmental control of the early mammalian embryo: competition among heterogeneous cells that biases cell fate. *Curr. Opin. Genet. Dev.* **20**, 485–91 (2010).

2. Johnson, M. H. & Ziomek, C. A. The foundation of two distinct cell lineages within the mouse morula. *Cell* **24**, 71–80 (1981).

3. Cockburn, K. & Rossant, J. Making the blastocyst: Lessons from the mouse. *J. Clin. Invest.* **120**, 995–1003 (2010).

4. Gardner, R. L. & Rossant, J. Investigation of the fate of 4-5 day post-coitum mouse inner cell mass cells by blastocyst injection. *J. Embryol. Exp. Morphol.* **52**, 141–152 (1979).

5. Kwon, G. S., Viotti, M. & Hadjantonakis, A. K. The Endoderm of the Mouse Embryo Arises by Dynamic Widespread Intercalation of Embryonic and Extraembryonic Lineages. *Dev. Cell* **15**, 509–520 (2008).

6. Ortega, N. M., Winblad, N., Plaza Reyes, A. & Lanner, F. Functional genetics of early human development. *Curr. Opin. Genet. Dev.* **52**, 1–6 (2018).

7. Cummins, J. M. *et al.* A formula for scoring human embryo growth rates in in vitro fertilization: Its value in predicting pregnancy and in comparison with visual estimates of embryo quality. *J. Vitr. Fertil. Embryo Transf.* **3**, 284–295 (1986).

8. Edwards, R. G., Steptoe, P. C. & Purdy, J. M. Establishing full-term human pregnancies using cleaving embryos grown in vitro. *Br. J. Obstet. Gynaecol.* **87**, 737–756 (1980).

9. Mohr, L. R., Trounson, A. O., Leeton, J. F. & Wood, C. Evaluation of Normal and Abnormal Human Embryo Development During Procedures In Vitro. in *Fertilization of the Human Egg In Vitro: Biological Basis and Clinical Application* (eds. Beier, H. M. & Lindner, H. R.) 211–221 (Springer Berlin Heidelberg, 1983). doi:10.1007/978-3-642-68800-3_15

10. Kuijk, E. W. *et al.* Differences in early lineage segregation between mammals. *Dev. Dyn.* **237**, 918–927 (2008).

11. Kuijk, E. W. *et al.* The roles of FGF and MAP kinase signaling in the segregation of the epiblast and hypoblast cell lineages in bovine and human embryos. *Development* **139**, 871–882 (2012).

12. Niakan, K. K. & Eggan, K. Analysis of human embryos from zygote to blastocyst reveals distinct gene expression patterns relative to the mouse. *Dev. Biol.* **375**, 54–64 (2013).

13. Roode, M. *et al.* Human hypoblast formation is not dependent on FGF signalling. *Dev. Biol.* **361**, 358–363 (2012).

14. Van Den Berg, I. M., Galjaard, R. J., Laven, J. S. E. & Van Doorninck, J. H. XCI in preimplantation mouse and human embryos: First there is remodelling... *Hum. Genet.* **130**, 203–215 (2011).

15. Hirate, Y., Cockburn, K., Rossant, J. & Sasaki, H. Tead4 is constitutively nuclear,

while nuclear vs. cytoplasmic Yap distribution is regulated in preimplantation mouse embryos. *Proc. Natl. Acad. Sci. U. S. A.* **109**, E3389-90; author reply E3391-2 (2012).

16. Hirate, Y. *et al.* Polarity-dependent distribution of angiomotin localizes Hippo signaling in preimplantation embryos. *Curr. Biol.* **23**, 1181–94 (2013).

17. Nishioka, N. *et al.* Tead4 is required for specification of trophectoderm in pre-implantation mouse embryos. *Mech. Dev.* **125**, 270–283 (2008).

18. Rossant, J. & Tam, P. P. L. New Insights into Early Human Development: Lessons for Stem Cell Derivation and Differentiation. *Cell Stem Cell* **20**, 18–28 (2017).

19. Sasaki, H. Roles and regulations of Hippo signaling during preimplantation mouse development. *Dev. Growth Differ.* **59**, 12–20 (2017).

20. Yagi, R. *et al.* Transcription factor TEAD4 specifies the trophectoderm lineage at the beginning of mammalian development. *Development* **134**, 3827–3836 (2007).

21. Nishioka, N. *et al.* The Hippo signaling pathway components Lats and Yap pattern Tead4 activity to distinguish mouse trophectoderm from inner cell mass. *Dev. Cell* **16**, 398–410 (2009).

22. Nichols, J., Silva, J., Roode, M. & Smith, A. Suppression of Erk signalling promotes ground state pluripotency in the mouse embryo. *Development* **136**, 3215–22 (2009).

23. Yamanaka, Y., Lanner, F. & Rossant, J. FGF signal-dependent segregation of primitive endoderm and epiblast in the mouse blastocyst. *Development* **137**, 715–724 (2010).

24. Lanner, F. Lineage specification in the early mouse embryo. *Exp. Cell Res.* **321**, 32–39 (2014).

25. Finn, C. A. & McLaren, A. A study of the early stages of implantation in mice. *Reproduction* **13**, 259–267 (1967).

26. Hertig, A. T., Rock, J., Adams, E. C. & Menkin, M. C. Thirty-four fertilized human ova, good, bad and indifferent, recovered from 210 women of known fertility; a study of biologic wastage in early human pregnancy. *Pediatrics* **23**, 202–211 (1959).

27. Niakan, K. K., Han, J., Pedersen, R. A., Simon, C. & Pera, R. A. R. Human pre-implantation embryo development. *Development* **139**, 829–41 (2012).

28. Jedrusik, A. *et al.* Role of Cdx2 and cell polarity in cell allocation and specification of trophectoderm and inner cell mass in the mouse embryo. *Genes Dev.* **22**, 2692–2706 (2008).

29. Petropoulos, S. *et al.* Single-Cell RNA-Seq Reveals Lineage and X Chromosome Dynamics in Human Preimplantation Embryos. *Cell* **165**, 1012–1026 (2016).

30. R.R., S., E.J., S. & B.A.J., R. Usefulness of bovine and porcine IVM/IVF models for reproductive toxicology. *Reprod. Biol. Endocrinol.* **12**, 1–12 (2014).

31. Simmet, K. *et al.* OCT4/POU5F1 is required for NANOG expression in bovine blastocysts. *Proc. Natl. Acad. Sci.* 201718833 (2018). doi:10.1073/pnas.1718833115

32. Berg, D. K. *et al.* Trophectoderm Lineage Determination in Cattle. *Dev. Cell* **20**, 244–255 (2011).

33. Kobolak, J. *et al.* Promoter analysis of the rabbit POU5F1 gene and its expression in preimplantation stage embryos. *BMC Mol. Biol.* **10**, 88 (2009).

34. Cauffman, G., Van de Velde, H., Liebaers, I. & Van Steirteghem, A. Oct-4 mRNA and protein expression during human preimplantation development. *Mol. Hum. Reprod.* **11**, 173–181 (2005).

35. Piliszek, A., Madeja, Z. E. & Plusa, B. Suppression of ERK signalling abolishes primitive endoderm formation but does not promote pluripotency in rabbit embryo. *Dev.* **144**, 3719–3730 (2017).

36. Halder, G. & Johnson, R. L. Hippo signaling: growth control and beyond. *Development* **138**, 9–22 (2011).

37. Pocaterra, A., Romani, P. & Dupont, S. YAP/TAZ functions and their regulation at a glance. *J. Cell Sci.* **133**, 1–9 (2020).

38. Ma, S., Meng, Z., Chen, R. & Guan, K.-L. The Hippo Pathway: Biology and Pathophysiology. *Annu. Rev. Biochem.* **88**, 577–604 (2019).

39. Zheng, Y. & Pan, D. The Hippo Signaling Pathway in Development and Disease. *Dev. Cell* **50**, 264–282 (2019).

40. Handyside, a H. Time of commitment of inside cells isolated from preimplantation mouse embryos. *J. Embryol. Exp. Morphol.* **45**, 37–53 (1978).

41. Hillman, N., Sherman, M. I. & Graham, C. The effect of spatial arrangement on cell determination during mouse development. *Embryol. exp. Morph* **28**, 263–278 (1972).

42. Plusa, B. *et al.* Downregulation of Par3 and aPKC function directs cells towards the ICM in the preimplantation mouse embryo. *J. Cell Sci.* **118**, 505–15 (2005).

43. Hirate, Y. *et al.* Par-aPKC-dependent and -independent mechanisms cooperatively control cell polarity, Hippo signaling, and cell positioning in 16-cell stage mouse embryos. *Dev. Growth Differ.* **57**, 544–556 (2015).

44. Korotkevich, E. *et al.* The Apical Domain Is Required and Sufficient for the First Lineage Segregation in the Mouse Embryo. *Dev. Cell* **40**, 235-247.e7 (2017).

45. Cockburn, K., Biechele, S., Garner, J. & Rossant, J. The Hippo pathway member Nf2 is required for inner cell mass specification. *Curr. Biol.* **23**, 1195–201 (2013).

46. Leung, C. Y. & Zernicka-Goetz, M. Angiomotin prevents pluripotent lineage differentiation in mouse embryos via Hippo pathway-dependent and -independent mechanisms. *Nat. Commun.* **4**, 2251 (2013).

47. Brosens, I., Pijnenborg, R., Vercruysse, L. & Romero, R. The 'Great Obstetrical Syndromes' are associated with disorders of deep placentation. *Am. J. Obstet. Gynecol.* **204**, 193–201 (2011).

48. Silver, R. M. Examining the link between placental pathology, growth restriction, and stillbirth. *Best Pract. Res. Clin. Obstet. Gynaecol.* **49**, 89–102 (2018).

49. HERTIG, A. T., ROCK, J. & ADAMS, E. C. A description of 34 human ova within the first 17 days of development. *Am. J. Anat.* **98**, 435–493 (1956).

50. Carter, A. M., Enders, A. C. & Pijnenborg, R. The role of invasive trophoblast in

implantation and placentation of primates. *Philos. Trans. R. Soc. Lond. B. Biol. Sci.* **370**, 20140070 (2015).

51. Turco, M. Y. & Moffett, A. Development of the human placenta. *Dev.* **146**, 1–14 (2019).

52. Benirschke, K. The human placenta. J. D. Boyd and W. J. Hamilton. Heffer, Cambridge, 365 pp. 1970. *Teratology* **8**, 77–78 (1973).

53. Schlafke, S. & Enders, A. C. Cellular basis of interaction between trophoblast and uterus at implantation. *Biol. Reprod.* **12**, 41–65 (1975).

54. Aplin, J. D. Developmental cell biology of human villous trophoblast: current research problems. *Int. J. Dev. Biol.* **54**, 323–329 (2010).

55. Burton, G. J., Charnock-Jones, D. S. & Jauniaux, E. Regulation of vascular growth and function in the human placenta. *Reproduction* **138**, 895–902 (2009).

56. Kingdom, J. C. P. & Drewlo, S. Is heparin a placental anticoagulant in high-risk pregnancies? *Blood* **118**, 4780–4788 (2011).

57. Knöfler, M. *et al.* Human placenta and trophoblast development: key molecular mechanisms and model systems. *Cell. Mol. Life Sci.* **76**, 3479–3496 (2019).

58. Evain-Brion, D. & Malassine, A. Human placenta as an endocrine organ. *Growth Horm. IGF Res.* **13 Suppl A**, S34-7 (2003).

59. Moffett, A. & Loke, C. Immunology of placentation in eutherian mammals. *Nat. Rev. Immunol.* **6**, 584–594 (2006).

60. Pijnenborg, R., Dixon, G., Robertson, W. B. & Brosens, I. Trophoblastic invasion of human decidua from 8 to 18 weeks of pregnancy. *Placenta* **1**, 3–19 (1980).

61. Hammer, A., Hutter, H. & Dohr, G. HLA class I expression on the materno-fetal interface. *Am. J. Reprod. Immunol.* **38**, 150–157 (1997).

62. King, A. *et al.* HLA-E is expressed on trophoblast and interacts with CD94/NKG2 receptors on decidual NK cells. *Eur. J. Immunol.* **30**, 1623–1631 (2000).

63. McMaster, M. T. *et al.* Human placental HLA-G expression is restricted to differentiated cytotrophoblasts. *J. Immunol.* **154**, 3771–8 (1995).

64. Kaufmann, P., Stark, J. & Stegner, H. E. The villous stroma of the human placenta. I. The ultrastructure of fixed connective tissue cells. *Cell Tissue Res.* **177**, 105–121 (1977).

65. Castellucci, M., Kosanke, G., Verdenelli, F., Huppertz, B. & Kaufmann, P. Villous sprouting: fundamental mechanisms of human placental development. *Hum. Reprod. Update* **6**, 485–494 (2000).

66. Boss, A. L., Chamley, L. W. & James, J. L. Placental formation in early pregnancy: How is the centre of the placenta made? *Hum. Reprod. Update* **24**, 750–760 (2018).

67. Carter, A. M. & Enders, A. C. Comparative aspects of trophoblast development and placentation. *Reprod. Biol. Endocrinol.* **2**, 1–15 (2004).

68. Bode, C. J. *et al.* In vitro models for studying trophoblast transcellular transport.

Methods Mol. Med. **122**, 225–239 (2006).

69. King, A., Thomas, L. & Bischof, P. Cell culture models of trophoblast II: Trophoblast cell lines - A workshop report. *Placenta* **21**, 113–119 (2000).

70. Shiverick, K. T. *et al.* Cell culture models of human trophoblast II: Trophoblast cell lines - A workshop report. *Placenta* **22**, 104–106 (2001).

71. Tanaka, S., Kunath, T., Hadjantonakis, A.-K., Nagy, A. & Rossant, J. Promotion of Trophoblast Stem Cell Proliferation by FGF4. *Science (80-.).* **282**, 2072 LP – 2075 (1998).

72. Okae, H. *et al.* Derivation of Human Trophoblast Stem Cells. *Cell Stem Cell* **22**, 50-63.e6 (2018).

73. Turco, M. Y. *et al.* Trophoblast organoids as a model for maternal–fetal interactions during human placentation. *Nature* **564**, 263–281 (2018).

74. Haider, S. *et al.* Self-Renewing Trophoblast Organoids Recapitulate the Developmental Program of the Early Human Placenta. *Stem Cell Reports* **11**, 537–551 (2018).

75. Harrison, S. E., Sozen, B., Christodoulou, N., Kyprianou, C. & Zernicka-Goetz, M. Assembly of embryonic and extraembryonic stem cells to mimic embryogenesis in vitro. *Science (80-.).* **356**, (2017).

76. Rivron, N. C. *et al.* Blastocyst-like structures generated solely from stem cells. *Nature* **557**, 106–111 (2018).

77. Xu, R. H. *et al.* BMP4 initiates human embryonic stem cell differentiation to trophoblast. *Nat. Biotechnol.* **20**, 1261–1264 (2002).

78. Horii, M. *et al.* Human pluripotent stem cells as a model of trophoblast differentiation in both normal development and disease. *Proc. Natl. Acad. Sci. U. S. A.* **113**, E3882–E3891 (2016).

79. Thomson, J. A. Embryonic stem cell lines derived from human blastocysts. *Science (80-.).* **282**, 1145–1147 (1998).

80. Roberts, R. M., Ezashi, T., Sheridan, M. A. & Yang, Y. Specification of trophoblast from embryonic stem cells exposed to BMP4. *Biol. Reprod.* **99**, 212–224 (2018).

81. Bernardo, A. S. *et al.* BRACHYURY and CDX2 mediate BMP-induced differentiation of human and mouse pluripotent stem cells into embryonic and extraembryonic lineages. *Cell Stem Cell* **9**, 144–155 (2011).

82. Guo, G. *et al.* Trophectoderm Potency is Retained Exclusively in Human Naïve Cells. *bioRxiv* 2020.02.04.933812 (2020). doi:10.1101/2020.02.04.933812

83. Amita, M. *et al.* Complete and unidirectional conversion of human embryonic stem cells to trophoblast by BMP4. *Proc. Natl. Acad. Sci. U. S. A.* **110**, (2013).

84. Krendl, C. *et al.* GATA2/3-TFAP2A/C transcription factor network couples human pluripotent stem cell differentiation to trophectoderm with repression of pluripotency. *Proc. Natl. Acad. Sci.* **114**, E9579–E9588 (2017).

85. Dong, C. *et al.* Derivation of trophoblast stem cells from naïve human pluripotent stem

cells. *Elife* **9**, 1–26 (2020).

86. Cong, L. *et al.* Multiplex Genome Engineering Using CRISPR/Cas Systems. *Science (80-.).* **339**, 819–823 (2013).

87. Mali, P. *et al.* CAS9 transcriptional activators for target specificity screening and paired nickases for cooperative genome engineering. *Nat. Biotechnol.* **31**, 833–8 (2013).

88. Mali, P. *et al.* RNA-guided human genome engineering via Cas9. 823–827 (2013). doi:10.1126/science.1232033

89. Mojica, F. J., Juez, G. & Rodriguez-Valera, F. Transcription at different salinities of Haloferax mediterranei sequences adjacent to partially modified PstI sites. *Mol. Microbiol.* **9**, 613–621 (1993).

90. Mojica, F. J., Ferrer, C., Juez, G. & Rodriguez-Valera, F. Long stretches of short tandem repeats are present in the largest replicons of the Archaea Haloferax mediterranei and Haloferax volcanii and could be involved in replicon partitioning. *Mol. Microbiol.* **17**, 85–93 (1995).

91. Barrangou, R. *et al.* CRISPR provides acquired resistance against viruses in prokaryotes. *Science* **315**, 1709–1712 (2007).

92. Komor, A. C., Badran, A. H. & Liu, D. R. CRISPR-Based Technologies for the Manipulation of Eukaryotic Genomes. *Cell* **168**, 20–36 (2017).

93. Sargent, R. G., Brenneman, M. a & Wilson, J. H. Repair of site-specific double-strand breaks in a mammalian chromosome by homologous and illegitimate recombination. *Mol. Cell. Biol.* **17**, 267–277 (1997).

94. Plaza Reyes, A. & Lanner, F. Towards a CRISPR view of early human development: applications, limitations and ethical concerns of genome editing in human embryos. *Development* **144**, 3–7 (2017).

95. Donoho, G., Jasin, M. & Berg, P. Analysis of gene targeting and intrachromosomal homologous recombination stimulated by genomic double-strand breaks in mouse embryonic stem cells. *Mol. Cell. Biol.* **18**, 4070–8 (1998).

96. Jinek, M. *et al.* A programmable dual-RNA-guided DNA endonuclease in adaptive bacterial immunity. *Science* **337**, 816–821 (2012).

97. Sapranauskas, R. *et al.* The Streptococcus thermophilus CRISPR/Cas system provides immunity in Escherichia coli. *Nucleic Acids Res.* **39**, 9275–9282 (2011).

98. Baltimore, D. *et al.* A prudent path forward for genomic engineering and germline gene modification. *Science (80-.).* **348**, 36 (2015).

99. Lundberg, A. S. & Novak, R. CRISPR-Cas Gene Editing to Cure Serious Diseases: Treat the Patient, Not the Germ Line. *Am. J. Bioeth.* **15**, 38–40 (2015).

100. Kang, X. *et al.* Introducing precise genetic modifications into human 3PN embryos by CRISPR/Cas-mediated genome editing. *J. Assist. Reprod. Genet.* 1–8 (2016). doi:10.1007/s10815-016-0710-8

101. Liang, P. *et al.* CRISPR/Cas9-mediated gene editing in human tripronuclear zygotes. *Protein Cell* **6**, 363–372 (2015).

102. Sciences, N. A. of, Medicine, N. A. of & National Academies of Sciences and Medicine, E. *Human Genome Editing: Science, Ethics, and Governance*. (The National Academies Press, 2017). doi:10.17226/24623

103. Greely, H. T. CRISPR'd babies: Human germline genome editing in the 'He Jiankui affair'. *J. Law Biosci.* **6**, 111–183 (2019).

104. Blakeley, P. *et al.* Defining the three cell lineages of the human blastocyst by single-cell RNA-seq. *Dev.* **142**, 3151–3165 (2015).

105. Durruthy-Durruthy, J. *et al.* Spatiotemporal Reconstruction of the Human Blastocyst by Single-Cell Gene-Expression Analysis Informs Induction of Naive Pluripotency. *Dev. Cell* **38**, 100–115 (2016).

106. Töhönen, V. *et al.* Novel PRD-like homeodomain transcription factors and retrotransposon elements in early human development. *Nat. Commun.* **6**, 8207 (2015).

107. Xue, Z. *et al.* Genetic programs in human and mouse early embryos revealed by single-cell RNA sequencing. *Nature* **500**, 593–597 (2013).

108. Yan, L. *et al.* Single-cell RNA-Seq profiling of human preimplantation embryos and embryonic stem cells. *Nat. Struct. Mol. Biol.* **20**, 1131–1139 (2013).

109. Purves D, Augustine GJ, Fitzpatrick D, et al. Functional Specialization of the Rod and Cone Systems. in *Neuroscience. 2nd edition* (Sunderland (MA): Sinauer Associates, 2001).

110. Coleman, H. R., Chan, C., Iii, F. L. F. & Chew, E. Y. Age-related macular degeneration. *Lancet* **372**, 1835–1845 (2009).

111. Gehrs, K. M., Anderson, D. H., Johnson, L. V & Hageman, G. S. Age-related macular degeneration--emerging pathogenetic and therapeutic concepts. *Ann. Med.* **38**, 450–471 (2006).

112. Sparrow, J. R., Hicks, D. & Hamel, C. P. The retinal pigment epithelium in health and disease. *Curr. Mol. Med.* **10**, 802–23 (2010).

113. Chen, Y., Bedell, M. & Zhang, K. Age-related macular degeneration: genetic and environmental factors of disease. *Mol. Interv.* **10**, 271–81 (2010).

114. Bhutto, I. & Lutty, G. Understanding age-related macular degeneration (AMD): relationships between the photoreceptor/retinal pigment epithelium/Bruch's membrane/choriocapillaris complex. *Mol. Aspects Med.* **33**, 295–317 (2012).

115. Gregory S. Hageman, Karen Gehrs, Lincoln V. Johnson, and D. A. Age-Related Macular Degeneration (AMD). in *Webvision: The Organization of the Retina and Visual System* (ed. Kolb H, Fernandez E, N. R. (Salt L. C. (UT): U. of U. H. S. C.) (2008).

116. Ambati, J., Ambati, B. K., Yoo, S. H., Ianchulev, S. & Adamis, A. P. Age-related macular degeneration: Etiology, pathogenesis, and therapeutic strategies. *Surv. Ophthalmol.* **48**, 257–293 (2003).

117. Sunness, J. S. The natural history of geographic atrophy, the advanced atrophic form of age-related macular degeneration. *Mol Vis* **5**, 25 (1999).

118. Homayouni, M. Vascular endothelial growth factors and their inhibitors in ocular

neovascular disorders. *J. Ophthalmic Vis. Res.* **4**, 105–14 (2009).

119. Hobbs, R. P. & Bernstein, P. S. Nutrient supplementation for age-related macular degeneration, cataract, and dry eye. *J. Ophthalmic Vis. Res.* **9**, 487–493 (2014).

120. Radtke, N. D., Aramant, R. B., Seiler, M. J., Petry, H. M. & Pidwell, D. Vision change after sheet transplant of fetal retina with retinal pigment epithelium to a patient with retinitis pigmentosa. *Arch. Ophthalmol.* **122**, 1159–65 (2004).

121. Radtke, N. D. *et al.* Vision Improvement in Retinal Degeneration Patients by Implantation of Retina Together with Retinal Pigment Epithelium. *Am. J. Ophthalmol.* **146**, (2008).

122. Strauss, O. The retinal pigment epithelium in visual function. *Physiol. Rev.* **85**, 845–881 (2005).

123. Campbell, M. & Humphries, P. The blood-retina barrier: tight junctions and barrier modulation. *Adv. Exp. Med. Biol.* **763**, 70–84 (2012).

124. Zamiri, P., Masli, S., Streilein, J. W. & Taylor, A. W. Pigment epithelial growth factor suppresses inflammation by modulating macrophage activation. *Investig. Ophthalmol. Vis. Sci.* **47**, 3912–3918 (2006).

125. Zhu, D. *et al.* Polarized secretion of PEDF from human embryonic stem cell-derived RPE promotes retinal progenitor cell survival. *Invest. Ophthalmol. Vis. Sci.* **52**, 1573–85 (2011).

126. Tang, P. H., Kono, M., Koutalos, Y., Ablonczy, Z. & Crouch, R. K. New insights into retinoid metabolism and cycling within the retina. *Prog. Retin. Eye Res.* **32**, 48–63 (2013).

127. Clegg, D. O. *et al.* Retinal Pigment Epithelial Cells: Development In Vivo and Derivation from Human Embryonic Stem Cells In Vitro for Treatment of Age-Related Macular Degeneration BT - Stem Cell Research and Therapeutics. in (eds. Shi, Y. & Clegg, D. O.) 1–24 (Springer Netherlands, 2008). doi:10.1007/978-1-4020-8502-4_1

128. Mellough, C. B. *et al.* An integrated transcriptional analysis of the developing human retina. *Dev.* **146**, (2019).

129. Zuber, M. E., Gestri, G., Viczian, A. S., Barsacchi, G. & Harris, W. A. Specification of the vertebrate eye by a network of eye field transcription factors. *Development* **130**, 5155–5167 (2003).

130. Steinfeld, J. *et al.* RPE specification in the chick is mediated by surface ectoderm-derived BMP and Wnt signalling. *Dev.* **140**, 4959–4969 (2013).

131. Zhao, C., Wang, Q. & Temple, S. Stem cell therapies for retinal diseases: Recapitulating development to replace degenerated cells. *Dev.* **144**, 1368–1381 (2017).

132. Binder, S. *et al.* Outcome of transplantation of autologous retinal pigment epithelium in age-related macular degeneration: a prospective trial. *Invest Ophthalmol Vis Sci* **45**, 4151–4160 (2004).

133. van Meurs, J. C. *et al.* Autologous peripheral retinal pigment epithelium translocation in patients with subfoveal neovascular membranes. *Br. J. Ophthalmol.* **88**, 110–113 (2004).

134. Lund, R. D. *et al.* Subretinal transplantation of genetically modified human cell lines attenuates loss of visual function in dystrophic rats. *Proc. Natl. Acad. Sci. U. S. A.* **98**, 9942–9947 (2001).

135. Algvere, P. V, Berglin, L., Gouras, P. & Sheng, Y. Transplantation of fetal retinal pigment epithelium in age-related macular degeneration with subfoveal neovascularization. *Graefes Arch. Clin. Exp. Ophthalmol.* **232**, 707–716 (1994).

136. Weisz, J. M. *et al.* Allogenic fetal retinal pigment epithelial cell transplantin a patient with geographic atrophy. *Retina* **19**, 540–545 (1999).

137. Kvanta, A. & Grudzinska, M. K. Stem cell-based treatment in geographic atrophy: Promises and pitfalls. *Acta Ophthalmol.* **92**, 21–26 (2014).

138. Mooney, I. & Lamotte, J. Emerging options for the management of age-related macular degeneration with stem cells. *Stem Cells Cloning* **4**, 1–10 (2010).

139. Drukker, M. *et al.* Human embryonic stem cells and their differentiated derivatives are less susceptible to immune rejection than adult cells. *Stem Cells* **24**, 221–229 (2006).

140. Hirano, M. *et al.* Generation of Structures Formed by Lens and Retinal Cells Differentiating from Embryonic Stem Cells. *Dev. Dyn.* **228**, 664–671 (2003).

141. Klimanskaya, I. *et al.* Derivation and comparative assessment of retinal pigment epithelium from human embryonic stem cells using transcriptomics. *Cloning Stem Cells* **6**, 217–245 (2004).

142. Lund, R. D. *et al.* Human embryonic stem cell-derived cells rescue visual function in dystrophic RCS rats. *Cloning Stem Cells* **8**, 189–199 (2006).

143. Rowland, T. J. *et al.* Differentiation of human pluripotent stem cells to retinal pigmented epithelium in de fi ned conditions using puri fi ed extracellular matrix proteins. (2012). doi:10.1002/term

144. Idelson, M. *et al.* Directed differentiation of human embryonic stem cells into functional retinal pigment epithelium cells. *Cell Stem Cell* **5**, 396–408 (2009).

145. Lane, A. *et al.* Engineering efficient retinal pigment epithelium differentiation from human pluripotent stem cells. *Stem Cells Transl. Med.* **3**, 1295–1304 (2014).

146. Osakada, F. *et al.* In vitro differentiation of retinal cells from human pluripotent stem cells by small-molecule induction. *J. Cell Sci.* **122**, 3169–79 (2009).

147. Plaza Reyes, A. *et al.* Xeno-Free and Defined Human Embryonic Stem Cell-Derived Retinal Pigment Epithelial Cells Functionally Integrate in a Large-Eyed Preclinical Model. *Stem Cell Reports* **6**, 9–17 (2016).

148. Pennington, B. O., Clegg, D. O., Melkoumian, Z. K. & Hikita, S. T. Defined culture of human embryonic stem cells and xeno-free derivation of retinal pigmented epithelial cells on a novel, synthetic substrate. *Stem Cells Transl. Med.* **4**, 165–177 (2015).

149. Vaajasaari, H. *et al.* Toward the defined and xeno-free differentiation of functional human pluripotent stem cell-derived retinal pigment epithelial cells. *Mol Vis* **17**, 558–575 (2011).

150. Sharma, R. *et al.* Clinical-grade stem cell-derived retinal pigment epithelium patch rescues retinal degeneration in rodents and pigs. *Sci. Transl. Med.* **11**, 1–14 (2019).

151. Choudhary, P. *et al.* Directing Differentiation of Pluripotent Stem Cells Toward Retinal Pigment Epithelium Lineage. *Stem Cells Transl. Med.* **6**, 490–501 (2017).

152. Maruotti, J. *et al.* A simple and scalable process for the differentiation of retinal pigment epithelium from human pluripotent stem cells. *Stem Cells Transl. Med.* **2**, 341–54 (2013).

153. Tang, C. *et al.* An antibody against SSEA-5 glycan on human pluripotent stem cells enables removal of teratoma-forming cells. *Nat. Biotechnol.* **29**, 829–834 (2011).

154. Dubois, N. C. *et al.* SIRPA is a specific cell-surface marker for isolating cardiomyocytes derived from human pluripotent stem cells. *Nat Biotech* **29**, 1011–1018 (2011).

155. Cogger, K. F. *et al.* Glycoprotein 2 is a specific cell surface marker of human pancreatic progenitors. *Nat. Commun.* **8**, 331 (2017).

156. Lehnen, D. *et al.* IAP-Based Cell Sorting Results in Homogeneous Transplantable Dopaminergic Precursor Cells Derived from Human Pluripotent Stem Cells. *Stem Cell Reports* **9**, 1207–1220 (2017).

157. D'Cruz, P. M. *et al.* Mutation of the receptor tyrosine kinase gene Mertk in the retinal dystrophic RCS rat. *Hum. Mol. Genet.* **9**, 645–651 (2000).

158. Gal, A. *et al.* Mutations in MERTK, the human orthologue of the RCS rat retinal dystrophy gene, cause retinitis pigmentosa. *Nat. Genet.* **26**, 270–271 (2000).

159. Zeiss, C. J. Animals as models of age-related macular degeneration: an imperfect measure of the truth. *Vet. Pathol.* **47**, 396–413 (2010).

160. Petrus-Reurer, S. *et al.* Integration of subretinal suspension transplants of human embryonic stem cell-derived retinal pigment epithelial cells in a large-eyed model of geographic atrophy. *Investig. Ophthalmol. Vis. Sci.* **58**, 1314–1322 (2017).

161. Petrus-Reurer, S. *et al.* Subretinal Transplantation of Human Embryonic Stem Cell Derived-retinal Pigment Epithelial Cells into a Large-eyed Model of Geographic Atrophy. *J. Vis. Exp.* (2018). doi:10.3791/56702

162. Petters, R. M. *et al.* Genetically engineered large anin1al n1odel and degeneration in retinitis pign1entosa. **47**, (1997).

163. Vugler, A. *et al.* Elucidating the phenomenon of HESC-derived RPE: anatomy of cell genesis, expansion and retinal transplantation. *Exp. Neurol.* **214**, 347–361 (2008).

164. Diniz, B. *et al.* Subretinal implantation of retinal pigment epithelial cells derived from human embryonic stem cells: improved survival when implanted as a monolayer. *Invest. Ophthalmol. Vis. Sci.* **54**, 5087–5096 (2013).

165. Kamao, H. *et al.* Characterization of human induced pluripotent stem cell-derived retinal pigment epithelium cell sheets aiming for clinical application. *Stem Cell Reports* **2**, 205–218 (2014).

166. Stanzel, B. V. *et al.* Human RPE stem cells grown into polarized RPE monolayers on a polyester matrix are maintained after grafting into rabbit subretinal space. *Stem Cell Reports* **2**, 64–77 (2014).

167. Kearns, V. *et al.* Plasma polymer coatings to aid retinal pigment epithelial growth for

transplantation in the treatment of age related macular degeneration. *J. Mater. Sci. Mater. Med.* **23**, 2013–2021 (2012).

168. Subrizi, A. *et al.* Generation of hESC-derived retinal pigment epithelium on biopolymer coated polyimide membranes. *Biomaterials* **33**, 8047–8054 (2012).

169. Stern, J. H. *et al.* Regenerating Eye Tissues to Preserve and Restore Vision. *Cell Stem Cell* **22**, 834–849 (2018).

170. Schwartz, S. D. *et al.* Embryonic stem cell trials for macular degeneration: a preliminary report. *Lancet* **379**, 713–20 (2012).

171. Schwartz, S. D. *et al.* Human embryonic stem cell-derived retinal pigment epithelium in patients with age-related macular degeneration and Stargardt's macular dystrophy: follow-up of two open-label phase 1/2 studies. *Lancet (London, England)* **385**, 509–516 (2015).

172. Liu, Y. *et al.* The Application of Hyaluronic Acid Hydrogels to Retinal Progenitor Cell Transplantation. *Tissue Eng. Part A* **19**, 121012095712003 (2012).

173. Ballios, B. G., Cooke, M. J., van der Kooy, D. & Shoichet, M. S. A hydrogel-based stem cell delivery system to treat retinal degenerative diseases. *Biomaterials* **31**, 2555–2564 (2010).

174. Ballios, B. G. *et al.* A Hyaluronan-Based Injectable Hydrogel Improves the Survival and Integration of Stem Cell Progeny following Transplantation. *Stem cell reports* **4**, 1031–1045 (2015).

175. Song, W. K. *et al.* Treatment of macular degeneration using embryonic stem cell-derived retinal pigment epithelium: preliminary results in Asian patients. *Stem cell reports* **4**, 860–872 (2015).

176. Schwartz, S. D., Tan, G., Hosseini, H. & Nagiel, A. Subretinal Transplantation of Embryonic Stem Cell-Derived Retinal Pigment Epithelium for the Treatment of Macular Degeneration: An Assessment at 4 Years. *Invest. Ophthalmol. Vis. Sci.* **57**, ORSFc1-9 (2016).

177. Mandai, M. *et al.* Autologous Induced Stem-Cell–Derived Retinal Cells for Macular Degeneration. *N. Engl. J. Med.* **376**, 1038–1046 (2017).

178. da Cruz, L. *et al.* Phase 1 clinical study of an embryonic stem cell-derived retinal pigment epithelium patch in age-related macular degeneration. *Nat. Biotechnol.* **36**, 328–337 (2018).

179. Kashani, A. H. *et al.* A bioengineered retinal pigment epithelial monolayer for advanced, dry age-related macular degeneration. *Sci. Transl. Med.* **10**, (2018).

180. Rising, A. *et al.* Efficacy of clinical-grade iPSC-RPE cells and patch in rodent and swine models of retinal degeneration. *Invest. Ophthalmol. Vis. Sci.* **59**, 546 (2018).

181. Ben M'Barek, K. *et al.* Clinical-grade production and safe delivery of human ESC derived RPE sheets in primates and rodents. *Biomaterials* **230**, 119603 (2020).

182. Leach, L. L. *et al.* Induced Pluripotent Stem Cell-Derived Retinal Pigmented Epithelium: A Comparative Study Between Cell Lines and Differentiation Methods. *J. Ocul. Pharmacol. Ther.* **32**, 317–330 (2016).

183. Ganat, Y. M. *et al.* Identification of embryonic stem cell-derived midbrain dopaminergic neurons for engraftment. *J. Clin. Invest.* **122**, 2928–2939 (2012).

184. Xian, B. & Huang, B. The immune response of stem cells in subretinal transplantation. *Stem Cell Res. Ther.* **6**, 1–7 (2015).

185. Streilein, J. W., Ma, N., Wenkel, H., Fong Ng, T. & Zamiri, P. Immunobiology and privilege of neuronal retina and pigment epithelium transplants. *Vision Res.* **42**, 487–495 (2002).

186. Mandai, M., Kurimoto, Y. & Takahashi, M. Autologous Induced Stem-Cell–Derived Retinal Cells for Macular Degeneration. *N. Engl. J. Med.* **377**, 792–793 (2017).

187. Taylor, C. J., Peacock, S., Chaudhry, A. N., Bradley, J. A. & Bolton, E. M. Generating an iPSC bank for HLA-matched tissue transplantation based on known donor and recipient HLA types. *Cell Stem Cell* **11**, 147–152 (2012).

188. Umekage, M., Sato, Y. & Takasu, N. Overview: an iPS cell stock at CiRA. *Inflamm. Regen.* **39**, 1–5 (2019).

189. Jang, Y. *et al.* Development of immunocompatible pluripotent stem cells via CRISPR-based human leukocyte antigen engineering. *Exp. Mol. Med.* **51**, (2019).

190. Petrus-Reurer, S. *et al.* Generation of Retinal Pigment Epithelial Cells Derived from Human Embryonic Stem Cells Lacking Human Leukocyte Antigen Class I and II. *Stem Cell Reports* (2020). doi:10.1016/j.stemcr.2020.02.006

191. Kaempf, S., Walter, P., Salz, A. K. & Thumann, G. Novel organotypic culture model of adult mammalian neurosensory retina in co-culture with retinal pigment epithelium. *J. Neurosci. Methods* **173**, 47–58 (2008).

192. Reidel, B., Orisme, W., Goldmann, T., Smith, W. C. & Wolfrum, U. Photoreceptor vitality in organotypic cultures of mature vertebrate retinas validated by light-dependent molecular movements. *Vision Res.* **46**, 4464–4471 (2006).

193. Rodin, S. *et al.* Clonal culturing of human embryonic stem cells on laminin-521/E-cadherin matrix in defined and xeno-free environment. *Nat. Commun.* **5**, 3195 (2014).

194. Rodin, S., Antonsson, L., Hovatta, O. & Tryggvason, K. Monolayer culturing and cloning of human pluripotent stem cells on laminin-521-based matrices under xeno-free and chemically defined conditions. *Nat. Protoc.* **9**, 2354–2368 (2014).

195. Rayon, T. *et al.* Notch and Hippo Converge on Cdx2 to Specify the Trophectoderm Lineage in the Mouse Blastocyst. *Dev. Cell* **30**, 410–422 (2014).

196. Menchero, S. *et al.* Transitions in cell potency during early mouse development are driven by notch. *Elife* **8**, (2019).

197. Plaza Reyes, A. *et al.* Identification of cell surface markers and establishment of monolayer differentiation to retinal pigment epithelial cells. *Nat. Commun.* **11**, 1609 (2020).

198. De Sousa, P. A. *et al.* Development and production of good manufacturing practice grade human embryonic stem cell lines as source material for clinical application. *Stem Cell Res.* **17**, 379–390 (2016).

199. Petit, L. & Punzo, C. Gene therapy approaches for the treatment of retinal disorders.

Discov. Med. **22**, 221–229 (2016).

200. MacLaren, R. E., Bennett, J. & Schwartz, S. D. Gene Therapy and Stem Cell Transplantation in Retinal Disease: The New Frontier. *Ophthalmology* **123**, S98–S106 (2016).